



TECHNISCHE
UNIVERSITÄT
WIEN



Diploma Thesis

Novel nucleoside analogues for diagnosis and treatment of infectious diseases

Conducted at the

Department of Chemistry, Technical University of Denmark

Under supervision of

Assoc. Prof. Dr. Kira Astakhova

and

Prof. Dr. Marko D. Mihovilovic

submitted at the University of Technology Vienna

Faculty of Technical Chemistry

from

Bernhard Jandl, BSc

Mollardgasse 29/12, 1060 Wien

Wien, 14.01.2020



Die approbierte gedruckte Originalversion dieser Diplomarbeit ist an der TU Wien Bibliothek verfügbar.
The approved original version of this thesis is available in print at TU Wien Bibliothek.

Front Matter

TABLE OF CONTENTS

FRONT MATTER	III
Acknowledgments	VII
Abstract	VIII
Kurzfassung	IX
List of abbreviation	XI
1 INTRODUCTION	13
1.1 Chemical biology	13
1.2 Synthetic biomolecules	14
1.2.1 Synthetic oligonucleotides	14
1.2.2 Synthetic peptides.....	16
1.2.3 Bioconjugation and “click” chemistry	17
1.2.3.1 Azide-alkyne “click” reaction	18
1.2.3.2 Azide and alkyne installation on biomolecules.....	19
1.3 Diagnosis of nucleic acid mutations by synthetic probes	21
1.3.1 Hybridization assays.....	21
1.3.2 Flow cytometry and single cell studies.....	22
1.3.2.1 Fluorescence activated cell sorting.....	22
1.3.2.2 Mass cytometry	23
1.3.2.3 Why single cell studies?	23
1.3.2.4 Single cell analysis.....	24
1.3.2.5 Polymerase chain reaction.....	24
1.3.2.6 RNA/DNA sequencing	26
1.3.2.7 Single cell genome studies.....	26
1.3.3 Optical detection.....	27
1.3.3.1 Fluorescence resonance energy transfer.....	27
1.3.3.2 Molecular beacon	28
1.3.4 Clinical diagnostics of oncogenes and viruses.....	30
1.3.4.1 Liquid biopsy and non-invasive genetic diagnosis techniques.....	30
1.3.4.2 <i>EGFR</i> receptor mutation tracking	31

1.3.4.3	Fluorescent <i>in situ</i> hybridization.....	32
1.3.4.4	Comparative genome hybridization and single nucleotide polymorphism arrays	32
1.4	Bioconjugates as therapeutics: Delivery challenge	34
1.4.1	Nanocarriers.....	34
1.4.2	Smart drug delivery system.....	35
1.4.3	Liposomes and functionalization.....	36
1.4.4	Active cellular targeting strategies.....	37
1.4.5	Delivery of therapeutic RNA.....	38
1.5	Problem, study objectives and rationale	39
2	RESULTS AND DISCUSSION	40
2.1	Bioconjugate precursors and bioconjugation methodologies.....	40
2.1.1	Bioconjugate precursors: Modification and labeling	40
2.1.2	Bioconjugation methodologies	43
2.2	Design of synthetic biomolecules and synthetic approaches	45
2.2.1	Cell sorting.....	45
2.2.2	Mutation detection	48
2.2.3	Therapeutic conjugates.....	49
2.3	Synthesis and characterization	54
2.3.1	Cell sorting.....	54
2.3.1.1	Oligonucleotide synthesis and characterization	54
2.3.1.1.1	ON1 and ON2	54
2.3.1.1.2	ON3	54
2.3.1.2	Bioconjugate synthesis and characterization	55
2.3.1.2.1	SC1	55
2.3.1.2.2	SC2	56
2.3.1.2.3	SC3 (a-e).....	57
2.3.1.2.4	SC4 and SC5.....	58
2.3.2	Actin and gelsolin	59
2.3.3	Mutation detection	61
2.3.3.1	Peptide candidate screening	61
2.3.3.2	Oligonucleotide synthesis and characterization.....	65
2.3.3.2.1	ON4	65
2.3.3.2.2	ON5	66
2.3.3.2.3	ON5'	66
2.3.3.3	Bioconjugate synthesis and characterization	67

2.3.3.3.1	PEG	67
2.3.3.3.2	POC.....	69
2.3.3.3.3	Synthesis of control probe CP	70
2.3.4	Therapeutic conjugates.....	72
2.3.4.1	Linear peptides	72
2.3.4.1.1	Synthesis of mP6 and mP7.....	72
2.3.4.1.2	Lipid anchor.....	74
2.3.4.2	Cyclic peptides	76
2.3.4.2.1	Synthesis of mcP8 and mcP9.....	76
2.3.4.2.2	Orthogonal CBZ deprotection	80
2.3.4.2.3	Orthogonal Alloc-deprotection.....	81
2.3.4.2.4	Installation of the lipid anchor.....	83
3	CONCLUSION AND PERSPECTIVE.....	87
4	EXPERIMENTAL PART.....	89
4.1	General.....	89
4.1.1	General procedure of oligonucleotide Synthesis (GP1)	90
4.1.1.1	Automated synthesis and Hand coupling procedure.....	90
4.1.1.2	Cleavage, washing and solvent removal.....	90
4.1.1.3	DMT deprotection	90
4.1.2	General procedure of peptide synthesis.....	91
4.1.2.1	General procedure of SPPS on 2-chlorotrityl resin (GP2)	91
4.1.2.1.1	Coupling of the first amino acid.....	91
4.1.2.1.2	Elongations of the peptide sequence.....	91
4.1.2.1.3	Cleavage of the peptide from the resin	91
4.1.2.1.4	Global deprotection in solution	92
4.1.2.2	General procedure of SPPS on Rink resin (GP3)	92
4.1.2.2.1	Coupling of the first amino acid.....	92
4.1.2.2.2	Elongations of the peptide sequence.....	93
4.1.2.2.3	Cleavage of the peptide from the resin	93
4.2	Cell sorting.....	94
4.2.1	Oligonucleotide synthesis	94
4.2.1.1	ON1 and ON2.....	94
4.2.1.2	Synthesis of oligonucleotide ON3.....	94
4.2.1.3	SC1	95
4.2.1.4	SC2	95
4.2.2	Bioconjugations.....	96

4.2.2.1	SC4	96
4.2.2.2	SC5	96
4.3	Mutation detection	97
4.3.1	Oligonucleotide precursors	97
4.3.1.1	ON4	97
4.3.1.2	ON5'	98
4.3.2	Bioconjugations	99
4.3.2.1	PEG	99
4.3.2.2	POC	100
4.3.2.3	Control probe CP	101
4.4	Peptide synthesis	102
4.4.1	Synthesis of linear peptides	102
4.4.1.1	mP6	102
4.4.1.2	mP7	103
4.4.1.3	Lipid anchor LA	104
4.4.2	Synthesis of cyclic peptides	105
4.4.2.1	P8	105
4.4.2.2	cP8	107
4.4.2.3	cP8'	108
4.4.2.4	P9	109
4.4.2.5	cP9	111
4.4.2.6	cP9'	112
4.4.2.7	mP10	113
4.4.2.8	mcP10	114
5	APPENDIX	115
5.1	Analytical data	115
5.2	Curriculum Vitae	139
5.3	Publications resulting from this thesis	141
5.4	References	142

Acknowledgments

Dear Kira, thank you for your excellent supervision and for giving me the opportunity to work on this interesting and versatile project. It gave me insight into diverse techniques, approaches and strategies. It was a pleasure to collaborate with you and from now on I will always “keep an eye on the aesthetics”. Thank you!

Thank you Makro, for the supervision of the thesis, your steady interest in the progress of my work and your helpful input.

Furthermore, I would like to thank everybody from the group for the warm welcome that I received, the friendly atmosphere you created and the steady support. Thank you, Anders, Annika, Camilla, Esmira, Ivana, Jesper, Jonas, Lisa, Maria, Mikkel, Nikita, Nikolaos, Petya, Sangita and Sofie. To outline a few occasions - thank you Sofie, for being the best Pétanque teammate one could imagine; thank you Sangita, for sharing your poetry/rap skills with us (you really got brain in your...); thank you Maria, for the establishment of the cake club; thank you Jesper, for introducing me to the Danish party culture; thank you Esmira, for bringing some reggaeton and opera vibes to the lab and thank you Anders, for your worldly wisdoms and for extending the life expectancy of my computer. Thank you all, for the many unforgettable moments inside and outside the lab.

Dear Jonas, I am very thankful for your scientific support during this thesis and all the helpful advices that you gave me regarding any problem I was facing. Thank you for all the great conversations we had and for providing the office with WAY (!!!) too big speakers. I don't want to miss any of those music sessions.

Finally, I would like to express my deepest gratitude to my family, my better half and my friends for the support during my student time. My dear Birgit, thank you for your uncountable motivating words, support and patience during this time - you really kept me going.

Abstract

Infectious disease is one of the major global health threats that the world's population is facing. The potential of exponential transmission requires early, rapid, robust and affordable diagnostic techniques to prevent rapid propagation of infection and allow adequate and prompt treatment. The developments over the last decades in the areas of clinical diagnostics and therapeutics have been remarkable. However, current techniques still often suffer from compromises regarding accuracy, time consumption and cost efficiency. Bioconjugates in particular are appealing and have much to offer for applications in research, diagnostics and therapy. However, the synthesis is challenging, often lead to low yields, purification can be inconvenient and the process lacks in scalability.

In this thesis, it was investigated if potent diagnostic probes and therapeutics with high specificity and sensitivity could be developed by specific conjugation using rationally designed peptides and oligonucleotides. A pilot study was performed in order to evaluate the design and synthetic path of a model system that is capable of revealing if oligonucleotide adaptors can reach cellular proximity. Therefore, a detection element was used that utilizes fluorescence resonance energy transfer. On another topic, an oligonucleotide hybridization platform for detection of human cancer DNA was established. A hydrogel forming peptide attached to a specific hybridization detection probe (POC) as well as an eight-arm-PEG conjugated to a hybridization capture probe (PEG) were synthesized. POC and PEG were used to investigate the sensitivity and swiftness of detecting *EGFR* oncogene and to evaluate the potential as an amplification-free diagnostic system. As a final topic, the synthesis of modified transferrin targeting linear (mP6 and mP7) and cyclic peptides (mcP10) were successfully carried out with the purpose of enhancing blood brain barrier crossing of therapeutic lipid nanoparticles. The modified peptides aim to serve as a surface modifier of lipid nanoparticles to improve sensitivity and selectivity.

Kurzfassung

Eine der größten globalen Gesundheitsgefährdungen stellen Infektionserkrankungen dar. Mitunter trägt ihre exponentielle Übertragungsrate zu dem Gesundheitsrisiko bei. Um diesem Potential der raschen Ausbreitung entgegenzusteuern, ist es notwendig, schnelle, einfache, robuste und leistbare Wege der Diagnose zu entwickeln und bereitzustellen. Darüber hinaus trägt eine frühzeitige Diagnose der Krankheiten dazu bei, rechtzeitig eine adäquate Therapie einzuleiten. Die Entwicklung klinischer Diagnosemethoden und Therapien waren in den letzten Jahrzehnten bemerkenswert rasant, jedoch ist das Potential aktueller Techniken im Hinblick auf Genauigkeit, Kosteneffizienz und Zeitaufwand noch nicht ausgeschöpft. Diesbezüglich sind Biokonjugate sehr vielversprechend für Forschung, Diagnose und Therapie. Allerdings sind die synthetische Herstellung und Aufreinigung oft herausfordernd und unbequem und darüber hinaus ist der Herstellungsprozess nur eingeschränkt skalierbar und häufig mit geringen Ausbeuten verbunden.

In dieser Diplomarbeit werden spezifische Biokonjugate von rational designten Peptiden und Oligonukleotiden auf ihr Potential untersucht, Anwendung in der Diagnose oder der Therapie zu finden. Mittels diverser Techniken der Biokonjugation wurde an der Etablierung eines Modellsystems gearbeitet, welches als Pilotstudie zur Entwicklung einer neuen Methode der fluoreszenz-basierenden Durchflusszytometrie dienen soll. Das dafür entwickelte Modellsystem beinhaltet ein Detektionselement, welches auf Fluoreszenz markierten Oligonucleotiden basiert. Dieses Detektionselement macht sich den Förster-Resonanzenergietransfer zu Nutzen. Darüber hinaus wurde eine Hybridisierungs-Plattform basierend auf Oligonukleotiden entwickelt, welche es ohne Signalverstärkung ermöglicht, menschliche Krebs-DNA zu detektieren. Dafür wurde ein Hydrogel formendes Peptid mit einer Oligonukleotid-Nachweissonde (POC) konjugiert, sowie eine acht-armige-PEG Verbindung mit einer Oligonukleotid-Fängersonde (PEG). Dieses Detektionssystem wurde anschließend auf die Empfindlichkeit und Schnelligkeit der *EGFR*-Oncogen-Detektion untersucht. Des Weiteren wurden modifizierte lineare (mP6 und mP7) und cyclische Peptide (mcP10) synthetisiert, welche den Transferrin Rezeptor anzielen. Diese Peptide dienen dazu, die Oberfläche von therapeutischen Lipid Nanoparticles zu modifizieren. Die Modifizierung der Oberfläche

erleichtert den Lipid Nanoparticles das Passieren der Bluthirnschranke und verbessert somit die Sensitivität und Selektivität der Wirkstoffübertragung.

List of abbreviation

AAC	Azide-Alkyne Cycloaddition	<i>EGFR</i>	Epidermal Growth Factor Receptor
AC	Anthracene	ELISA	Enzyme Linked Immunsorbent Assay
ACN	Acetonitrile	EPR	Enhanced Permeability and Retention
Alexa547	AlexaFluor545	equiv.	Molecular Equivalent
Alloc	Allyloxycarbonyl	FA	Formic Acid
BBB	Blood Brain Barrier	FACS	Fluorescence Activated Cell Sorting
BSA	Bovine Serum Albumin	FDA	Food and Drug Administration
Calcd.	Calculated	FISH	Fluorescence in Situ Hybridization
cat	Catalyst	Fmoc	Fluorenyl- methyloxycarbonyl- chloride
CBZ	Benzyl Chloroformate	FRET	Fluorescence Resonance Energy Transfer
cfDNA	Cell-Free DNA	h	Hour
CGH	Comparative Genome Hybridization	HATU	Hexafluoro-phosphate Azabenzotriazole Tetramethyl Uronium
CISH	Chromogenic in Situ Hybridization	HFIP	Hexafluoro-2-propanol
CMV	Cytomegalovirus	IE-HPLC	Ion Exchange High Performance Liquid Chromatography
CNS	Central Nervous System	LCM	Laser Capture Microdissection
CTC	Circulating Tumor Cell	LNA	Locked Nucleic Acid
CuAAC	Copper(I)-Catalyzed Azide-Alkyne Cycloaddition	LNP	Lipid Nanoparticle
Cy3.5	Cyanine 3.5	MALDI-TOF	Matrix Assisted Laser Desorption Ionization- Time of Flight
DAP	Diaminopropionic Acid	MB	Molecular Beacon
DCC	N,N'-Dicyclohexyl- carbodiimide	MeOH	Methanol
DCM	Dichloromethane	MQ-water	Milli-Q Water
ddPCR	Digital Droplet Polymerase Chain Reaction	MS	Mass Spectrometry
DHB	2,5-Dihydroxybenzoic Acid	NC	Nanocarrier
DIPEA	N,N-Diisopropyl- ethylamine	NGS	Next Generation Sequencing
DMF	Dimethylformamide		
DMSO	Dimethyl Sulfoxide		
DMT	N,N-Dimethoxytrityl		
DNA	Deoxyribonucleic Acid		

NHS	N-Hydroxy-succinimide	TLC	Thin Layer Chromatography
NMR	Nuclear Magnetic Resonance	Tris	Tris(hydroxymethyl) aminomethane
PAGE	Polyacrylamide Gel Electrophoresis		
PBS	Phosphate-Buffered Saline		
PCR	Polymerase Chain Reaction		
PdAc ₂	Palladium(II)-acetate		
PdCl ₂	Palladium(II)-chloride		
PEG	Polyethylene Glycol		
POC	Peptide Oligonucleotide Conjugate		
POC	Point-of-care		
PS	Polystyrene		
qPCR	Quantitative Polymerase Chain Reaction		
RNA	Ribonucleic Acid		
RP-HPLC	Reverse Phase High Performance Liquid Chromatography		
RT	Retention Time		
rt	Room Temperature		
RT-PCR	Real Time Polymerase Chain Reaction		
RuAAC	Ruthenium-Catalyzed Azide-Alkyne Cycloaddition		
SDS	Sodium Dodecyl Sulfate		
SNP	Single Nucleotide Polymorphism		
SPAAC	Strain Promoted Azide- Alkyne Cycloaddition		
SPE	Solid Phase Extraction		
SPPS	Solid Phase Peptide Synthesis		
STP	4-Sulfo-2,3,5,6- tetrafluorophenol		
TFA	Trifluoroacetic Acid		
THF	Tetrahydrofuran		
TIPS	Triisopropylsilane		

1 Introduction

1.1 Chemical biology

Chemical biology is a rather new research field that is located at the interface of chemistry and biology. Over the past decade, investigations on a molecular level, especially the interactions between small molecules and biomolecules, have become more and more the center of interest among researchers. This occurrence is not only based on the promising techniques that have been offered for studying and manipulating complex biological systems and processes. It is also based on the highly potent output of applications that have been established within that field, particularly in research and healthcare. Especially, the remarkable progress in the development of highly efficient, reliable and convenient synthetic strategies provided the necessary tools for chemical biologists to perform and design their investigations.

These synthetic strategies include robust ways for establishing synthetic biomolecules such as peptides and oligonucleotides. In particular, the development towards solid supports led to highly appealing applications that are commonly used today. Moreover, the exceptional progress within synthetic chemistry enables diverse conjugation techniques to tune and modify the properties of biological probes. Notably, the development of “click” chemistry and other biorthogonal reactions strongly contributed to that progress.^{1,2}

Applications that come from the field of chemical biology include highly potent diagnostics and therapeutics for infectious disease, cardiovascular disease and cancer.^{3,4} Furthermore, the field also offers promising approaches with regards to the development of advanced analytical methodologies. More specific, single cell studies are highly appealing to overcome the problems of reduced information gain when it comes to the analysis of bulk populations of cells via e.g. western plotting or microarraying. Therefore, analysis on a single cell level would provide a solution to this problem.⁵⁻⁷ Single cell studies are appealing due to their greater accuracy and resolution. The avoidance of information loss is of particular importance for genomics, transcriptomics, proteomics and metabolomics.

1.2 Synthetic biomolecules

Synthetic biomolecules have a large potential for applications in research, diagnostics and therapy. Bioconjugates have demonstrated promising results with regards to specificity and efficacy with their full potential still to be revealed. Conveniently, oligonucleotide and peptide synthesis became less time and labor consuming due to the establishment of solid phase strategies and the implementation of automatization techniques. However, the synthesis of their more appealing bioconjugates often leads to low yields; purification can be inconvenient and the process lacks in scalability.^{3,8}

1.2.1 Synthetic oligonucleotides

The development of phosphoramidite chemistry paved the way for modern nucleic acid synthesis. With the development towards solid phase supports⁹ and the implementations of automation techniques¹⁰, it is still considered as the method of choice for oligonucleotide synthesis amongst researchers.¹¹ A commonly used strategy utilizes DMT-protected nucleoside phosphoramidites to synthesize the desired oligonucleotide sequence in 3' to 5' direction. Starting from the 3'-terminus of the nucleoside attached to a solid support (typically controlled pore glass or polystyrene) via a cleavable linker, a stepwise addition of nucleoside residues at the 5'-termini is performed to build up the desired sequence. Each nucleoside coupling follows a four-step cycle (**Figure 1**), resulting in the elongation of the oligonucleotide backbone.

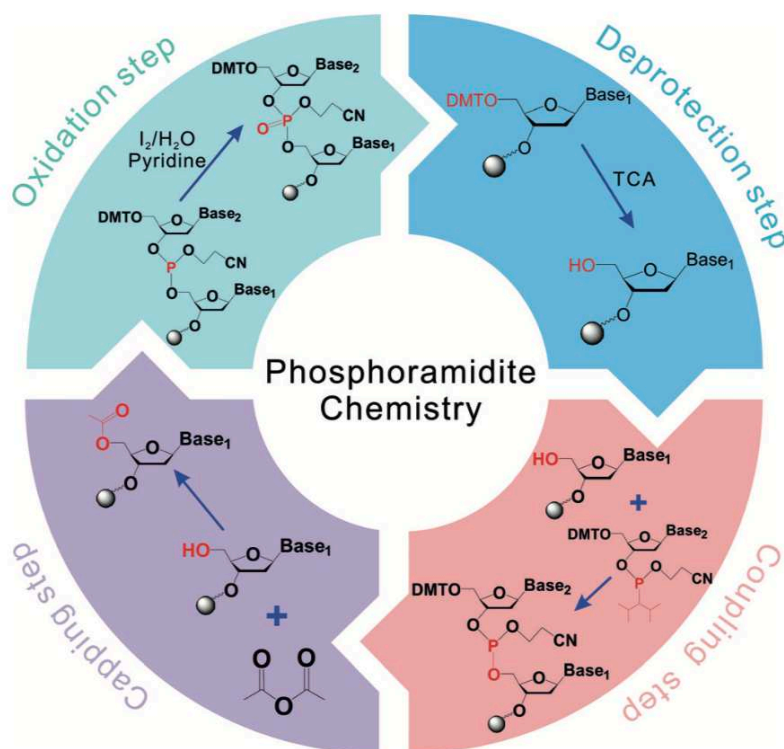


Figure 1¹²: Synthesis of oligonucleotides based on phosphoramidite chemistry. Synthesis starts with the 3'-terminus of the desired nucleotide and elongation proceeds through a series of cycles. Each cycle involves four steps: Deprotection, coupling, capping and oxidation.

In the initial step, DMT-deprotection (or detritylation) is performed using trichloroacetic acid. Afterwards, coupling of the follow-up base of the designed sequence (DMT-protected nucleoside phosphoramidite monomer) is allowed to take place at the 5'-hydroxy group. A phosphite triester linkage is formed leading to the third step, the capping. This capping step covers the acylation of unreacted 5'-hydroxy groups which prevents any interaction during upcoming steps. In the fourth step an oxidation is performed resulting in a closure of the chain-elongation cycle. This step enables the stabilization of the reaction product by converting the phosphite triester into a cyanoethyl protected phosphate triester, using an iodine solution. This synthetic cycle is designed to be repeated for as many couplings as needed to receive the required oligonucleotide sequence.¹³ Nowadays, the average coupling efficiency of one cycle reaches up to 99.5%, which leads to a full length recovery rate of e.g. 88.6% for a 25-mer.¹⁴ Afterwards, the synthesized oligonucleotide is cleaved from the solid support. Next, the removal of the protecting groups from the backbone and the bases follows. Common approaches for oligonucleotide purification are high-performance liquid

chromatography (HPLC) or polyacrylamide gel electrophoresis (PAGE). Errors, such as side reactions, incomplete couplings and misincorporations, during the synthesis may occur but it was shown that phosphoramidite chemistry can be optimized to an efficiency up to 99% or higher.^{11,15}

1.2.2 Synthetic peptides

Peptides and proteins play an essential role in every living organism due to the enormous number of physiological and biological processes they are involved in. Processes, such as intercellular communication, biocatalysis and inter- and intracellular transportation, are just a few examples of the integral parts in the design of life. The growing functional and structural understanding led to the development of many different pharmaceutical and biological applications. There are many different approaches to prepare peptides and proteins. The approach most commonly used for synthetically making peptides is solid phase peptide synthesis (SPPS)¹⁶ (**Figure 2**). In particular the so-called “Fmoc strategy”, which follows a repetitive cycle to gradually establish the desired peptide sequence.

The initial loading step covers the coupling of the first amino acid to the linker (attached on solid support). Next, the elongation of the sequence is performed via a repetitive cycle of deprotections and amino acid couplings. As soon as the synthesis of the desired sequence is completed, cleavage of the peptide from the resin is performed as a terminal step. Depending on the cleavage mixture used, side chain protecting groups can be remained or removed.

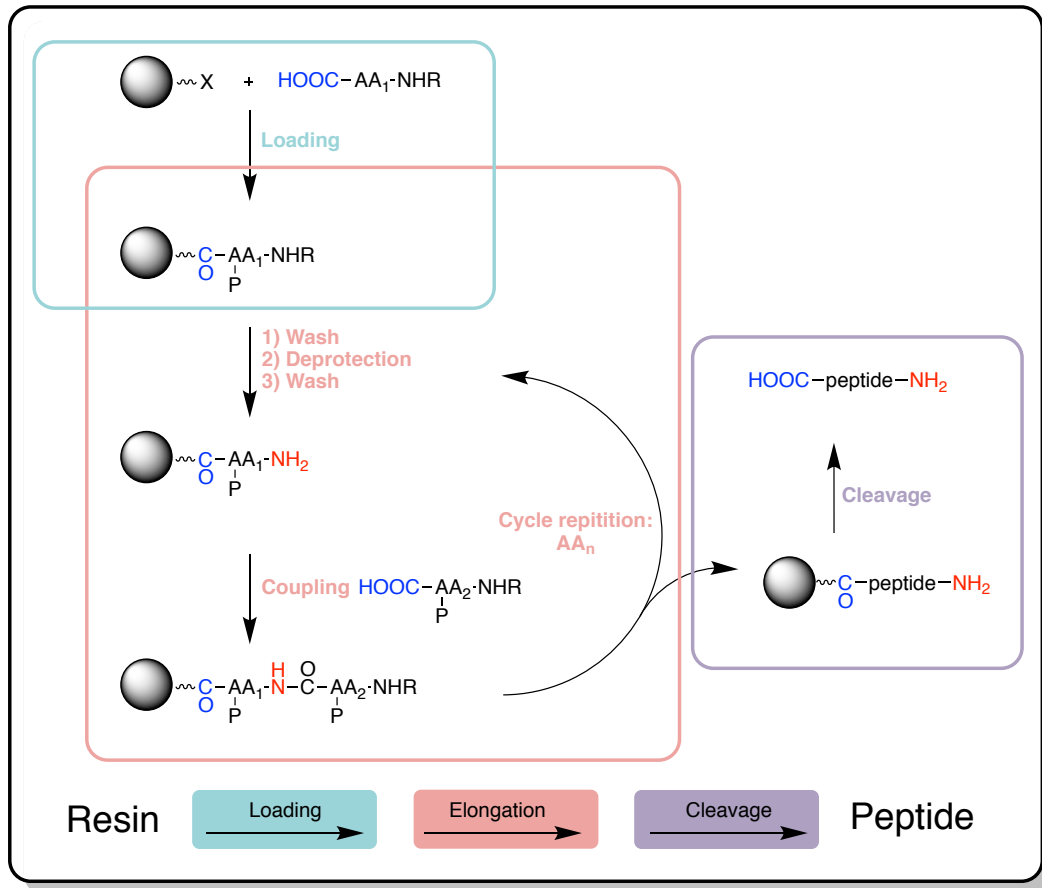


Figure 2: Schematic overview of solid phase peptide synthesis (SPPS), covering the elementary steps of the synthesis strategy: Loading, elongation and cleavage. (Modified figure from reference.¹⁷)

1.2.3 Bioconjugation and “click” chemistry

Bioconjugate chemistry is a rather modern research field that focuses on discovering efficient strategies to form stable covalent linkages between two molecules of different origin, where at least one of them is a biomolecule. Once a covalent linkage is formed, the received bioconjugate is commonly used to investigate certain effects in biological systems to gain information about them. On that account, “click” chemistry² is a frequently used approach that enables an efficient and convenient way of making a high variety of bioconjugates (**Figure 3**).^{18–20}

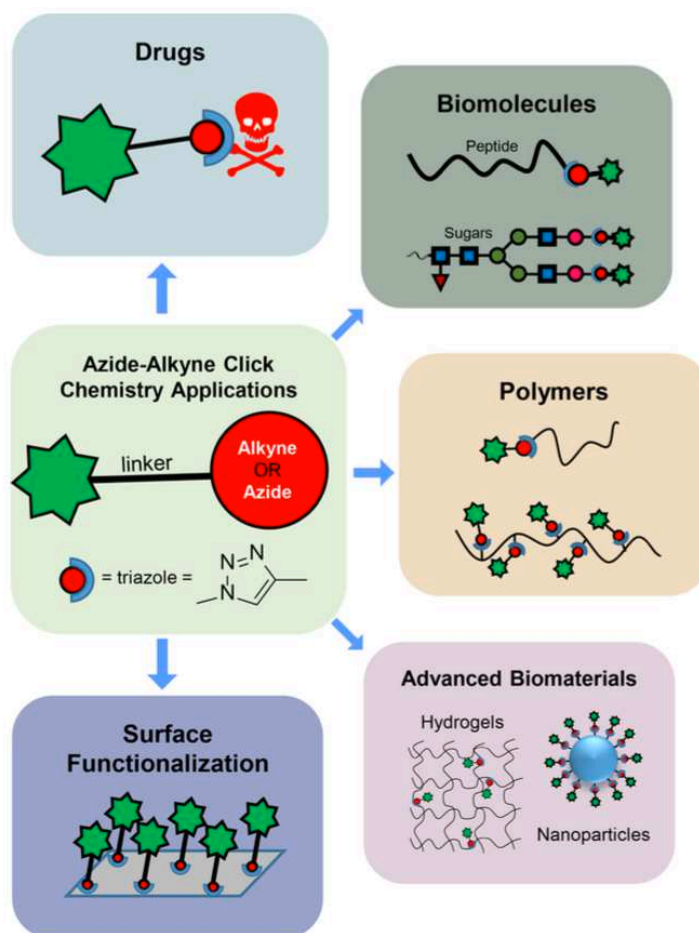


Figure 3²⁰: Toolbox of azide-alkyne “click” chemistry showing the variety of applications.

1.2.3.1 Azide-alkyne “click” reaction

One of the most commonly used “click” reaction is the bioorthogonal copper-catalyzed azide-alkyne cycloaddition (CuAAC). The reason for the popularity is the high practicability, efficiency and capability to access conjugates with various architecture and functionalities. This reaction exploits the active catalytic species Cu^+ , which is produced via reduction of the more stable Cu^{2+} *in situ*. Typically this reduction is achieved by sodium ascorbate²¹, hydrazine²² or hydroxylamine²³. The presence of Cu^+ and sodium ascorbate can promote the oxidation of certain amino acid residues. Therefore, Cu-stabilizing ligands (**Figure 4**) were introduced to limit amino acid degradation and to increase the reaction rate.^{24,25}

In order to avoid usage of copper, reducing agents and accelerating ligands, strain promoted azide-alkyne cycloaddition (SPAAC) was developed.¹³ Beneficially, SPAAC can be used under

mild reaction conditions but the approach faces a drawback due to a lack of regioselectivity. An overview of diverse azide-alkyne cycloadditions (AAC) and their limitations is shown in

Table 1.

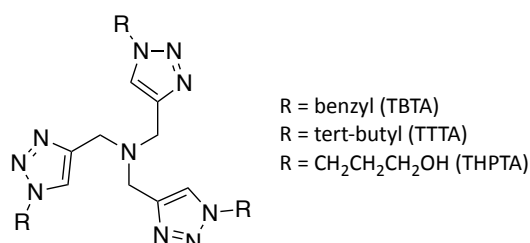


Figure 4²⁰: Structures of commonly used Cu-stabilizing ligands.

Table 1: Various types of azide-alkyne cycloadditions (AAC) and their limitations. (Modified figure from reference.²⁰)

Reaction Type	Reagent 1	Reagent 2	Catalyst	Product	Limitations
Huisgen AAC	R ₁ -N ₃	R ₂ -C≡C-R ₃ Internal or terminal alkyne	Δ	R ₁ -N ₃ -C(R ₂)=C(R ₃) + R ₁ -N ₃ -C(R ₃)=C(R ₂)	not regioselective days-weeks >100 °C
CuAAC	R ₁ -N ₃	C≡C-R ₂	Cu ¹⁺	R ₁ -N ₃ -C(R ₂)=C	catalyst required reducing agent stabilizing agent
RuAAC	R ₁ -N ₃	R ₂ -C≡C-R ₃ Internal or terminal alkyne	Ru ²⁺	R ₁ -N ₃ -C(R ₂)=C(R ₃)	catalyst required 1,5 regioisomer formed
SPAAC	R ₁ -N ₃	Cyclooctyne-R ₂	→	R ₁ -N ₃ -Cyclooctyne-R ₂	not regioselective cyclooctyne more expensive (reagents)

1.2.3.2 Azide and alkyne installation on biomolecules

There are two common strategies to install azide or alkyne functionalities on intact biomolecules. One is the utilization of N-hydroxysuccinimide (NHS) mediated amide bond formation. The other one is the coupling of a maleimide labeled molecule to a sulfhydryl

group.²⁰ The labeling of biomolecules via NHS activated compounds is widely used due to their aqueous compatibility, commercial availability and selectivity towards primary amine (e.g. lysine residues or N-termini). Mostly, the reaction is performed at room temperature in aqueous buffers with slightly basic pH (pH 7-9). An elevated pH value tends to boost the efficiency of the reaction due to the higher degree of amine deprotonation. In contrast, the reaction simultaneously suffers from a higher hydrolysis rate of the activated ester. At neutral pH, the opposite occurs. Besides primary amines, NHS activation can also be performed *in situ* on carboxylic acids functionalities. In order to achieve this, appropriate coupling reagents are essential (e.g. 1-ethyl-3-(3-(dimethylamino)propyl)carbodiimide (EDC) and N,N'-dicyclohexylcarbodiimide (DCC). As mentioned before, another strategy commonly used is the coupling of a maleimide labeled molecule to a sulfhydryl group in order to form a thioether linkage via Michael-Addition. Common side reactions of the thioether formed are thiol exchange reactions as well as the reverse reaction.²⁶ The reaction mechanism for the maleimide coupling is strongly depending on the solvent, initiator (base) and sulfhydryl group used.²⁷

1.3 Diagnosis of nucleic acid mutations by synthetic probes

Rapid, reliable and inexpensive detection of nucleic acid mutations is highly desired in research and clinical applications. Therefore, detection strategies that utilize synthetic probes to perform hybridization assays are appealing with clear advantages regarding high specificity and sensitivity. In addition, single cell FACS studies are appealing as high performance diagnostic tools. FACS studies and other fluorescent-based detection applications are depended on effective fluorescent signal reporting strategies. In particular, taking advantage of the fluorescence resonance energy transfer enables attractive strategies including the use of molecular beacons.

1.3.1 Hybridization assays

The structure of DNA, two helical chains coiled around the same axis and held together via hydrogen bonds, is forming the foundation of hybridization assays.^{28–30} DNA-DNA or DNA-RNA hybrids, constructed by the complementary pairing of single strands, can be formed in solution as well as on solid support (e.g. 96-well plates, labeled beads).³¹ The use of hybridization assays is widely applied in research and diagnostic applications. These assays are commonly based on labeled probes, which enable detection and quantification of nucleic acids of interest.³¹ Various different strategies are used and can be classified into amplification (e.g. RT-PCR^{32,33}, rolling-circle amplification³² and ddPCR³⁴) and amplification-free methods (e.g. Northern Plot³³, Microarray³², UPT-LF³⁵ and time-gated FRET ligation³⁶). Starting from radioisotope labeling as a reporting technique, today the scientific spotlight is more centered towards various kinds of fluorescent labeling, such as fluorophores, quantum dots or rare metal complexes.³⁷ Regarding real-time amplification techniques, unselective intercalating dyes and target-specific fluorescently labeled oligonucleotides are increasingly used in routine methods.³⁸ Besides that, the use of dual-labeled target-specific oligonucleotides as reporting tools (e.g. hydrolysis probes, molecular beacons) is a widespread approach that is based on fluorescence resonance energy transfer (FRET) between two fluorescent moieties.³⁹

1.3.2 Flow cytometry and single cell studies

Fluorescent activated cell sorting (FACS) was invented in the late 1960s by researchers who worked in the field of flow cytometry and cell sorting of viable cells.⁴⁰ Over the last years this technique has developed to a traditional tool in the field of cell sorting and recently regained attention for the ability among various types of flow cytometers to isolate single cells.⁴¹ Alternatively, common techniques are magnetic-activated cell sorting, laser-capture microdissection⁴², manual cell picking/micromanipulation and microfluidics.⁴³

1.3.2.1 Fluorescence activated cell sorting

Fluorescence activated cell sorting is a technique which allows the characterization and differentiation of diverse cell types in a heterogeneous cell population. The sorting is typically based on granularity, size and fluorescence of the cells. A common approach to perform fluorescence surface labeling of target cells is utilizing fluorophore-conjugated monoclonal antibodies.

For conducting FACS-studies a cell sample suspension is passed through the cytometer. Meanwhile, each cell is exposed to a laser and internally installed fluorescent detectors enable the identification of the labeled cells. Right after this process the suspension reaches a valve, which allows the suspension to form fluid droplets. Those droplets, which contain cells of interest, are electorally charged and subsequently exposed to an electrical field. Differently charged droplets can be collected due to different deflection (**Figure 5**).

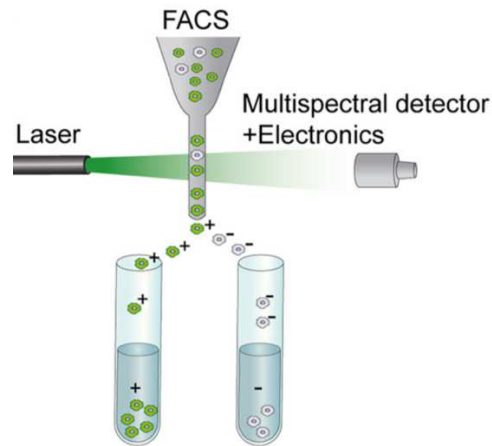


Figure 5⁴⁴: Principle of fluorescent activated cell sorting (FACS).

1.3.2.2 Mass cytometry

Fluorophore emission spectra in FACS studies often suffer from a lack of resolution due to overlapping emission signals. The problem with such experiments is, that the informational output is limited. A promising modern attempt to overcome this problem is mass cytometry.⁴⁵ The method is a fusion of flow cytometry and elemental mass spectrometry. Single cell experiments with simultaneous detection of more than 40 cellular parameters make this instrument to a powerful tool that enables the quantification of multiple cellular features at a single cell resolution.⁴⁶

1.3.2.3 Why single cell studies?

Conventional analytical techniques are generating information from a population of cells. Typically, the result of these measurements is given as an average response. However, recent studies have shown that even the same cell line can differ in genome, transcriptome and epigenome during division and differentiation of cells.⁴⁷ If individual cells within a population are not homogeneous as once thought and rather show unique features, an average value can completely suppress potentially relevant information about subpopulations. With that in mind, considering the complex heterogeneous system of a tumor microenvironment, highly

important information can get lost due to interaction between tumor cells and non-cancerous neighbor cells. Therefore, it is necessary to develop new technologies to isolate and analyze single cells.

1.3.2.4 Single cell analysis

Due to cell to cell variation within a cell population, single cell analysis can give a far more detailed understanding of cells than we currently have.⁶ Technologies for single cell genome, transcriptome and proteome analysis will help to further study diseases and stem cells and to improve drug development.^{6,48} To achieve that, a simultaneous demand on amplification methodologies emerges, due to an extremely small amount of template oligonucleotides recovered from a single cell. Common techniques for amplifying and analyzing nucleic acids include qPCR, RT-qPCR and RNA/DNA sequencing. Especially the recent development of RNA sequencing towards a cost effective and high throughput technique brought increased attention to that field over the last years.^{49,50} Moreover, immunohistochemistry and quantitative mass spectrometry (MS) are typically in use for protein analysis.^{49,51,52}

1.3.2.5 Polymerase chain reaction

Polymerase chain reaction (PCR) is a very efficient and commonly used amplification tool for specific DNA fragments.^{53,54} This highly sensitive technique is capable of generating an enormous amount of copies of a preselected DNA fragment in a reasonable amount of time. The presence of nucleotides, primers, DNA polymerase and template DNA are required to perform PCR. Furthermore, a thermal cycler is essential to perform the process. The thermal cycler repeatedly follows a predefined temperature program to which the sample is exposed to, leading to the amplification of the desired DNA fragment. Each cycle is divided into three steps. The initial step, called Denaturation, covers the separation of complementary DNA strands of the target DNA. This is achieved by heating above the melting point of the DNA (94 – 98 °C). The follow-up step is called Annealing and includes the hybridization of the primers to the target DNA. Primers are short DNA strands (usually around 18-25 base pairs) that are

designed to be recognized from the DNA polymerase and to mark the DNA fragment of interest for the enzyme via specific hybridization to the template strand. Both processes occur at a temperature between 55 - 70 °C. After the hybridization and the binding of the DNA polymerase to the primer had occurred, the temperature is increased between 68 - 72 °C to allow the DNA polymerase to build up the complementary DNA strand. This step closes the cycle and is called Elongation. An overview of the main steps in PCR is given in **Figure 6**.

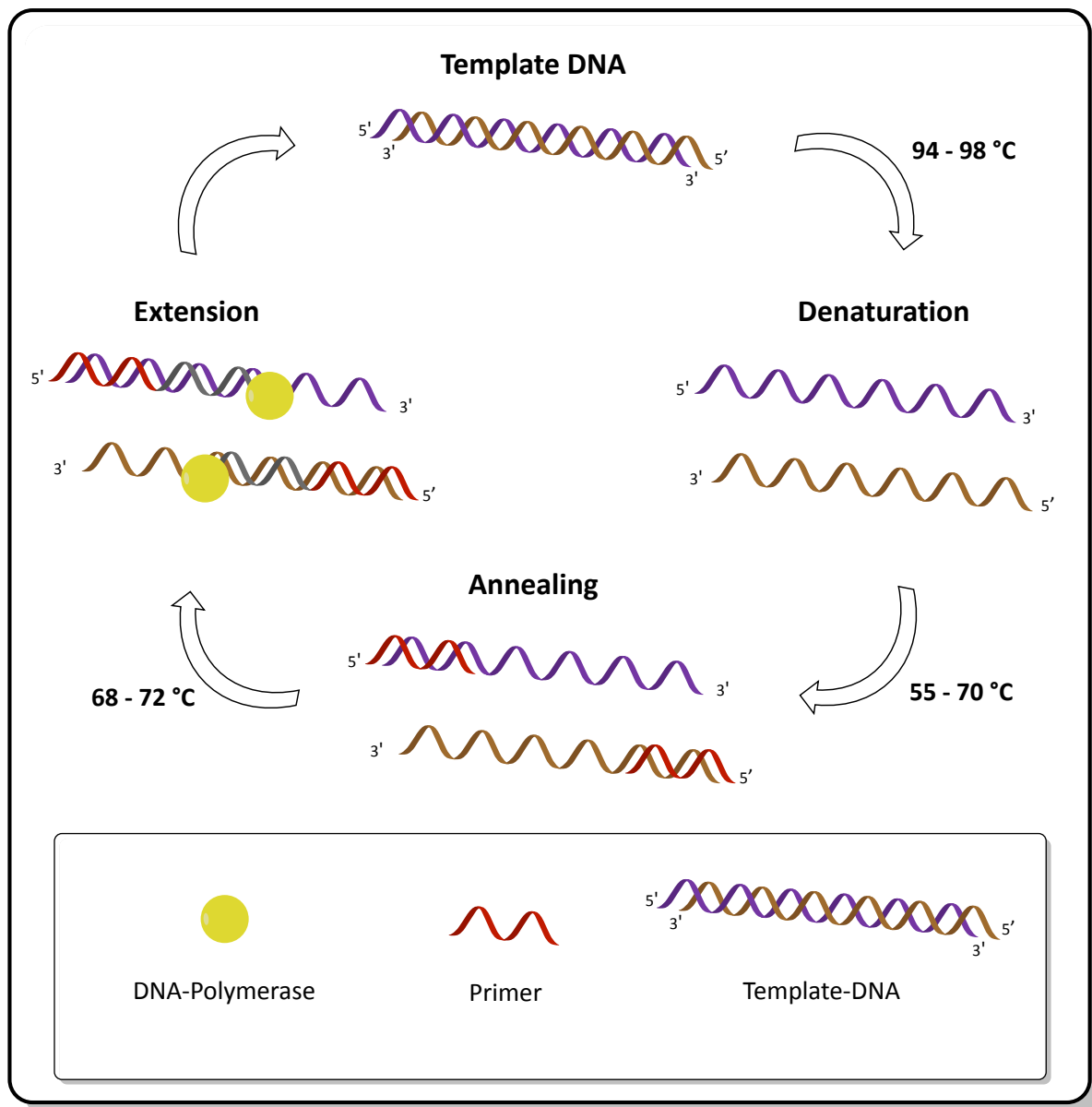


Figure 6: Overview of the main steps in PCR for target sequence amplification using a template DNA.

Once the cycle is completed, two copies of each DNA template are received. With this exponential growth given, the amount of copies rises rapidly after a reasonable number of cycles applied. PCR products can be analyzed and separated via agarose gel electrophoresis, which requires subsequent visualization of the gel received. Two common techniques for visualizing PCR products are chemical dyes (e.g. ethidium bromide) and the use of fluorescent labeled PCR primers. A more advanced approach is quantitative real-time PCR. This technique allows simultaneous detection and quantification of PCR products. This real time PCR is often combined with reverse transcription (RT-qPCR). That allows the conversion of mRNA into cDNA and a subsequent quantification. This technique is sufficiently sensitive to measure a single mRNA molecule.

1.3.2.6 RNA/DNA sequencing

DNA and RNA sequencing has been a challenging topic in research for more than 40 years.⁵⁵ Besides, the technique has led to some breakthrough discoveries including the result of the Human Genome Project. While the first analysis of a RNA sequence covered the work of five people for three years, techniques progressed to “massively parallel sequencing” and furthermore to real time single-molecule sequencing.^{7,55,56}

A promising approach of real time single-molecule sequencing was introduced by Pacific Biosciences. The company established a device that utilizes an optical method that allows the observation of the polymerase-mediated synthesis in real time.^{57,58} That is realized by the help of a zero-mode waveguide. This waveguide enables fluorescent excitation of a tiny volume and leading to an excitation of a single polymerase. To receive a sufficient signal on the detector side, fluorescently labeled nucleotides are essential.

1.3.2.7 Single cell genome studies

Single cell genomics help to increase the understanding of the basic unit of biological structure. Typically, studies in that field allow characterization of cell identity and function. More advanced techniques are utilizing PCR and have obtained significant progress over the

last years. Degenerated oligonucleotide-primed PCR is a method that is used for whole and single cell genome amplification.⁵⁹ The use of hybrid oligonucleotides with partially degenerated bases allows a dense priming of the template. This process is typically divided into two stages. First, the primer extension and second, the amplicon replication.

A challenging key step in the whole genome amplification is to suppress contamination. Only an extremely small amount of templates is received from a single cell. Therefore, contamination from the sample, the lab, the processing instruments and the reagents used, needs to be avoided.⁶⁰ Alternative whole-genome amplifications techniques are isothermal. These amplification techniques include multiple displacement amplification⁶⁰ and several hybrid methods (e.g. multiple annealing and looping based amplification cycles⁶¹ and displacement DOP-PCR (PicoPlex)).⁶² Since PCR-based methods often suffer from low coverage and isothermal approaches from a lack of uniformity, hybrid methods are a promising development to overcome these problems.⁵²

1.3.3 Optical detection

1.3.3.1 Fluorescence resonance energy transfer

Fluorescence resonance energy transfer (FRET) is a non-invasive phenomenon that can be utilized to carry out short distance studies, particularly for interactions on the lower nanometer scale.^{63,64} This concept is used in biomolecular research to study heterogeneous systems, dynamic processes or transient conformational changes. First biological applications started in the field of protein research. Later on FRET-based DNA applications appeared.^{65,66}

FRET is a quantum phenomenon that appears between two fluorophore molecules. In the presence of a donor and acceptor fluorophore, an excitation can be transferred from donor to acceptor fluorophore via dipole-dipole coulomb interaction. This energy transfer occurs without photon emission and results in a shift of the excitation state towards the acceptor molecule. This phenomenon only occurs when the distance between these two fluorophores is less than 10 nm and particularly has a high dynamic range for distances in the range of 3-9 nm.^{65,66}

1.3.3.2 Molecular beacon

Nucleic acids and their features provide a suitable framework for molecular modifications, making them highly appealing for plenty of applications in bioanalysis including biosensing and bioimaging.⁶⁷ The modification of nucleic acids can be achieved via diverse engineering strategies.⁶⁸ That modification can vary in the design and helps to target nucleic acids, proteins or small molecules with high sensitivity and specificity.⁶⁷ The concept of molecular beacons (MB) as a reporting tool was first published in 1996 by Tyagi and Kramer⁶⁹. They showed that oligonucleotide hybridization probes are capable of specifically targeting nucleic acids in homogenous solutions. Typically, molecular beacons are composed of a short oligonucleotide chain forming a single-stranded loop, a hybridized stem structure and a signal reporter. The stem part typically consists of five to seven complementary nucleotides. One strategy that enables monitoring of the stem hybridization state is achieved via fluorophore and quencher attachment to the particular ends. (**Figure 7a**).⁷⁰ An example of a FRET system utilizing EDNAS (5-(2'-aminoethyl) aminonaphthalene-1-sulfonic acid) as fluorophore and DABCYL as quencher is illustrated in **Figure 7b**. If the stem is hybridized and the fluorophore is in close proximity to the quencher, fluorescence is quenched by FRET. In contrary, if binding to the complementary sequence takes place, quenching is suppressed and fluorescent emission occurs (**Figure 7c**).⁷¹ Additionally, a typical fluorescence emission spectra resulting from a molecular beacon is illustrated in **Figure 7d**.

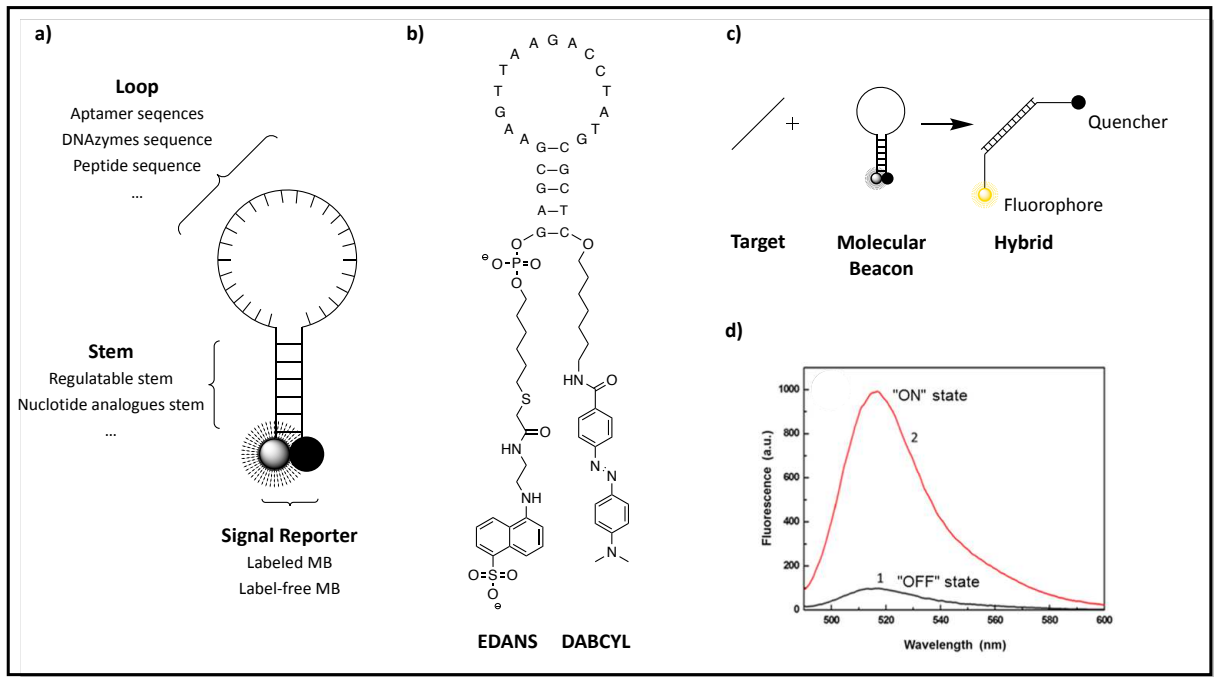


Figure 7: **a):** General structure of a molecular beacon and various rationally designed strategies for different parts. **b):** Exemplary design and structure of a molecular beacon. A 15-nucleotide-long-probe with two complementary 5-nucleotide-long arm sequences. EDANS (fluorophore) is attached to the 5'-terminal via a $-(\text{CH}_2)_5\text{-S-CH}_2\text{-CO-}$ linker; DABCYL (quencher), attached to 3'-terminal via a $-(\text{CH}_2)_7\text{-NH-}$ linker. **c):** Operation principle of molecular beacons. The hairpin stem occurs if complementary sequences bind together and a hybrid is formed if hybridization to target sequences takes place. **d):** Resulting fluorescence emission spectra in open "OFF" state (1) and closed "ON" state (2) form of the molecular beacon. (Modified figure from references.^{67,69,70})

Assays based on molecular beacons are popular among the scientific community due to their fast, simple and inexpensive application. Especially for real-time monitoring used *in vivo* as well as *in vitro*, molecular beacons are a highly employed approach.

1.3.4 Clinical diagnostics of oncogenes and viruses

Diagnostics of viruses has undergone a huge development in the second half of the last century. Important milestones have been reached since diagnostic tools, such as transmission electron microscopy and diverse serological methods, got well established. The major breakthrough came as enzyme-linked immunosorbent assay and monoclonal antibodies were implemented in diagnostic strategies. Furthermore, the development of polymerase chain reaction and nucleic acid based amplification technologies enabled the detection of microbial and host genetic sequences in a very sensitive and specific manner. Both techniques are increasingly used to detect and quantify viruses such as human immunodeficiency virus, hepatitis B virus, hepatitis C virus and cytomegalovirus.⁷² The Human Genome Project and The Cancer Genome Atlas not only revealed that cancer is a genome disease but also that genomic analysis can be used to identify mutations.^{73–75} It is expected that next generation sequencing (NGS) will bring a paradigm-shift towards genetic signature-based diagnoses⁷⁶ and specific molecular-targeted therapy.^{77,78}

1.3.4.1 Liquid biopsy and non-invasive genetic diagnosis techniques

The typical DNA source for screening single oncogene loci is a tumor tissue, that is commonly taken by surgery or core needle biopsy.⁷⁹ Individual variables and failures in sampling and processing of the tumor tissue are factors that can weaken the quality of the sample.⁸⁰ Therefore, the sample lacks in representativity. The dynamic behavior of the mutational profile can be used to trace the progression of the disease. Vice versa, the response to the treatment can be monitored.²⁷ Histological data is useful at any stage of the disease, but testing tends to non-invasive genetic diagnosis.⁷⁹

Disseminating tumor cells and circulating tumor cells (CTCs), frequently released from the surface of malignant tumors, can be sampled by peripheral blood. For gaining more local information, spinal, pleural or peritoneal fluid and urine can be used. To enhance the number of target cells, different cell sorting techniques, such as immunological, magnetic or flow sorting, can be applied.^{82,83}

Cell-free DNA (cfDNA), also isolated from peripheral blood, is commonly used as a representative sample for non-invasive monitoring of the malignant process.^{79,84} Cell-free DNA has received a lot of attention in cancer monitoring and diagnostics due to next generation sequencing tools. This approach is attractive especially when tumor tissue testing fails in regard of anatomical, technical or sampling problems.⁷⁹ Cross-validation of mutations, enabled via analysis of CTCs and cfDNA together, leads to an even greater blood-based tumor profiling.⁸⁴

1.3.4.2 *EGFR* receptor mutation tracking

Screening and targeting are commonly used methods for epidermal growth factor receptor (*EGFR*) mutation testing.⁸⁵ Screening methods, such as denaturing high-performance liquid chromatography (dHPLC)⁸⁶ and high-resolution melting analysis⁸⁷, are promising alternatives to widely used direct sequencing. HPLC has shown 100% analytical sensitivity and HRMA exhibited 100% sensitivity and 90% specificity, compared to direct sequencing.^{87,88} Besides that, various targeting methods include PCR-based screening. Reviewing 24 studies, Ellison *et al.*⁸⁵ concluded that PCR-based screening methods (to specifically detect exon 19 deletions and exon L858R point mutation) are able to virtually detect all mutations which were also tested positive by direct sequencing. Furthermore, targeting methods were able to detect mutations in samples, which were tested negative via direct sequencing, without giving a false-positive result.⁸⁵ Some studies show, that amplification refractory mutation system, fragment length analysis and pyrosequencing, have a higher sensitivity than direct sequencing.⁸⁹⁻⁹¹ A more modern technique adapted for PCR-based mutation detection is cationic conjugated polymer based fluorescence resonance energy transfer.⁹²

The *EGFR* oncogene is associated with multiple types of cancer including lung cancer, breast cancer and melanoma. That makes mutation monitoring highly important for early diagnosis and successful therapy. Besides that, the oncogene has been recently linked to immunotherapy with regards to its effectiveness and role in hyperactivation of cancer progression.^{93,94}

1.3.4.3 Fluorescent *in situ* hybridization

After the structure of DNA and the base pairing was revealed³⁰, it soon became widespread in scientific communities to use the unique coding for analytical purposes. First radioactive labeled⁹⁵ and later on fluorescent labeled RNA and DNA probes⁹⁶ were used to track specific sequences in a biological sample. Fluorescent *in situ* hybridization (FISH) is today an essential tool in cytogenetics. Previously it was a commonly used technique for gene mapping (e.g. Human Genome Project⁷³). Today, this technique has become an appealing tool for clinical diagnosis due to the useful ability to localize the position of the gene of interest via fluorescent microscopy.^{97,98}

The principle of the technique is based on the specific interaction between nucleotides. Complementary sequences can be chemically modified via active or passive fluorophore labeling. Once the labeled probe and the natural DNA are mixed, both biopolymers undergo a denaturing process. After denaturation, the modified probe anneals with the natural DNA and can be analyzed via fluorescent microscopy.

1.3.4.4 Comparative genome hybridization and single nucleotide polymorphism arrays

Comparative genome hybridization (CGH) offers the possibility to gain information about alternation of certain chromosomal regions and their correlating genetic information. That enables the screening for copy number variations.⁹⁹ Using this technique, researchers were able to discover the amplification of a gene, which encodes a catalytic subunit of phosphatidylinositol 3-kinase that is responsible for ovarian cancer.^{100,101} This method was further developed into a microarray based set-up, which provides two main advantages: Simultaneous detection, duplications and deletions of aneuploidies as well as the independency of the usage of metaphase chromosomes.⁹⁶ Microarrays additionally offer the possibility to collect transcriptomic data in parallel and therefore allow analysis of dynamics in gene expression.¹⁰⁴

Single nucleotide polymorphisms (SNPs) describe the variation of a single nucleotide at a certain position in the genome. These occurrences can be located in noncoding or coding regions in DNA sequence. The latter could affect the encoding of the amino acid sequence leading to the conclusion that SNPs are associated with cancer development.^{105,106}

CGH and SNP are used in clinical environment for evaluation of patients with developmental delay/intellectual disability, multiple congenital anomalies¹⁰⁷ and neuropsychiatric disorders.^{108,109} Recent studies show that copy number variations are linked to different diseases including Alzheimer disease¹¹⁰, Parkinson disease¹¹¹, Chron's disease¹¹² and autism¹¹³.

1.4 Bioconjugates as therapeutics: Delivery challenge

Besides diagnostic applications, synthetic biopolymers and their conjugates find growing appeal in biological therapies. The advantages of biological therapies include high specificity, low dose and low to no side effects. However, the delivery of biological therapeutics and their stabilization *in vivo* are important obstacles to be overcome. Therefore, the concept of smart drug delivery systems had been established and some resulting delivery carriers have already found the way into clinical praxis. Approaches on the development of a smart drug delivery system include the utilization of diverse nanocarriers. Nanocarriers, such as liposomes, micelles, gold nanoparticles and carbon nanotubes, are currently under investigation and show promising behavior with regards to *in vivo* stabilization.

1.4.1 Nanocarriers

A widely used modern strategy for targeted delivery of therapeutics involves nanocarriers (NCs). These nanocarriers can be used for systemic administration of therapeutics or localized therapeutics delivery to target tissues.¹¹⁴ Improved solubility, higher bioavailability, altered bio-distribution and facilitation of entering diseased cells are observed passive effects of nanocarriers. These effects can be utilized through encapsulation of therapeutic molecules.¹¹⁴ Although this strategy improves permeability and additionally shows an enhanced permeability and retention effect¹¹⁵ (EPR-effect), the major proportion of NCs are still cleared by the mononuclear phagocytic system and the reticuloendothelial system, get stuck physically in sinusoids of the liver or are taken up by hepatocytes and Kupffer cells.^{116,117} Both, the increased permeability of tumor blood vessels and the compression of the lymphatic vessels (responsible for cell waste elimination) are responsible for the EPR-effect.¹¹⁸ This occurrence is due to accelerated growth of tumor mass. However, the EPR-effect depends on the type of tumor and actual state of the disease progression and is not as universal as originally assumed.¹¹⁹ Even if a high EPR-effect is occurring, there are several different challenging barriers such as the elevated interstitial fluid pressure¹²⁰ or the dense extracellular matrix¹²¹. To overcome the latter barrier, diverse alternatives have been proposed. One example is using pH-sensitive polymeric nanocapsules.¹²² These nanocapsules are carrying

collagenase and are capable to release the enzyme when they are exposed to mild acidic conditions. Exactly these conditions are found in tumor tissues and as a result it was possible to show an enhanced penetration in three-dimensional tumor tissue models.¹²²

1.4.2 Smart drug delivery system

Conventional drug delivery often suffers from nonspecific distribution and uncontrollable drug release. This limitation led to the development of smart nanocarrier-based drug delivery systems (Smart Drug Delivery System) with the aim of overcoming these problems.^{123–125} The eight most reported nanocarriers are liposomes, micelles, dendrimers, meso-porous silica nanoparticles, gold nanoparticles, super paramagnetic iron oxide nanoparticles, carbon nanotubes and quantum dots.¹²⁵ **Figure 8** shows the essential steps to establish a liposome-based smart drug delivery system for cancer therapy.

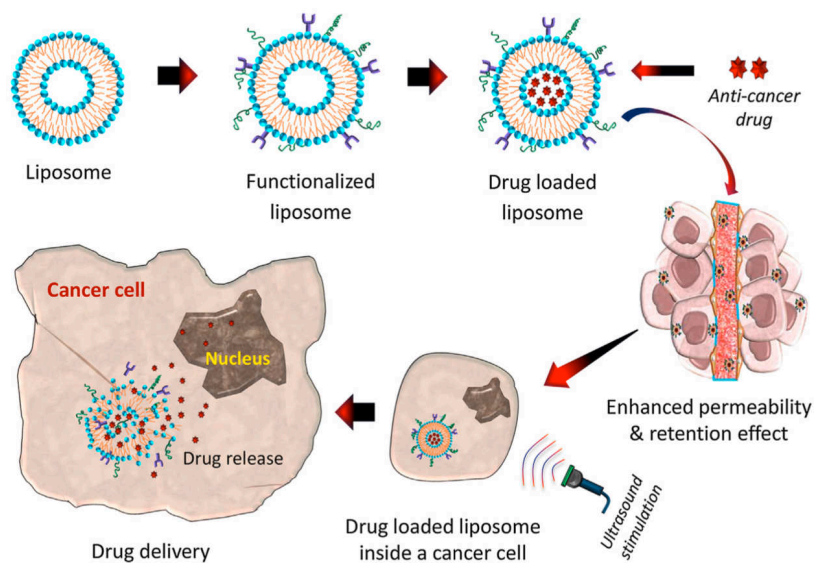


Figure 8¹²⁵: Illustration of the essential steps of liposome-based smart drug delivery system for cancer therapy.

1.4.3 Liposomes and functionalization

Liposomes are usually phospholipid-based amphipathic self-assembling bi-layered vesicles.¹²⁵ They were long considered to be both pharmacologically inactive and minimally toxic, but recent studies show that they are less immunologically inert as expected.^{126,127} This naturally occurring bi-layered phenomenon can be used to capture water-soluble drugs in the core of the nanocarrier.¹²⁸ Traditionally, the Bangham method¹²⁹, reverse phase evaporation¹³⁰ and detergent dialysis¹³¹ were used to prepare liposomes. More state-of-the-art techniques include supercritical reverse phase evaporation¹³² and supercritical anti-solvent method¹³³. Pure liposomes suffer from insufficient drug loading, fast drug release, short circulation time in blood and instability.¹²⁵ Functionalization can help to overcome these problems. Therefore, peptides, proteins, PEG, monoclonal antibodies and glycoproteins are used to decorate the liposome. With this decorations applied, the modified liposome gives access to a smart delivery systems.^{134,135} Liposomes can be used for diagnosis as well as therapy. Additionally, they show promising behavior as co-delivery systems¹²⁵ (e.g. delivering two chemotherapeutic drugs, gene agents¹³⁶ or chemotherapeutics with anticancer metals¹³⁷). A schematic illustration of different types of drug delivery systems based on liposomes is shown in **Figure 9**.

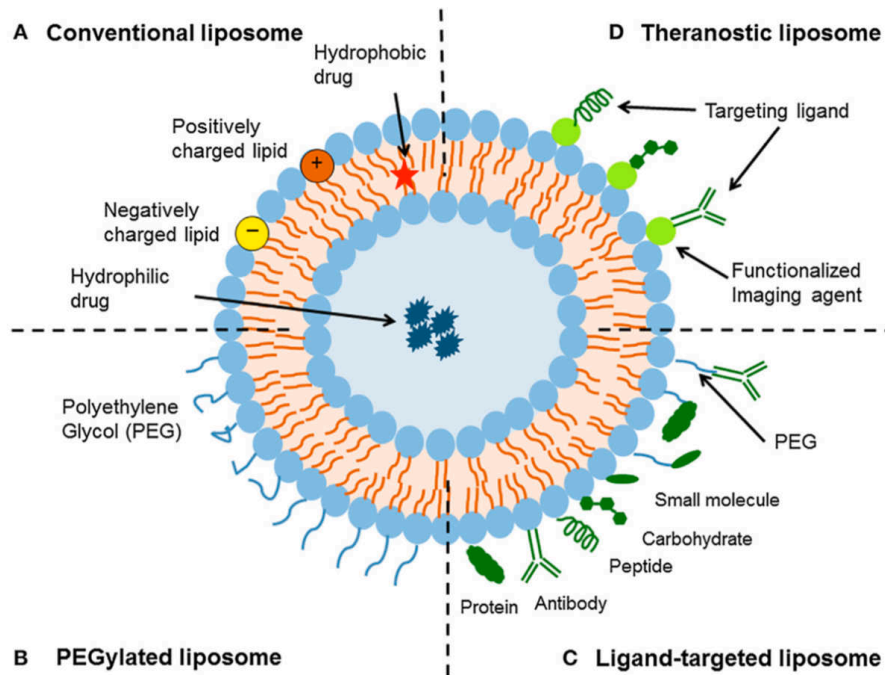


Figure 9¹³⁸: Schematic illustration of different types of drug delivery systems based on liposomes. **a):** Conventional liposome; a lipid bilayer that is typically composed of cationic, anionic or neutral (phosphor)lipids and cholesterol and which encloses an aqueous core. The lipid bilayer and the aqueous core respectively can be used to incorporate hydrophobic or hydrophilic compounds. **b):** PEGylated liposome; surface coating with polyethylene glycol (PEG) leads to steric stabilization. **c):** Ligand-targeted liposome; diverse ligands (e.g. antibodies, peptides and carbohydrates) can be attached to the surface to achieve specific targeting. **d):** theranostic liposome; composed of a nanoparticle, a targeting ligand, an imaging component and a therapeutic component.

1.4.4 Active cellular targeting strategies

Active cellular targeting can be achieved via surface modification of nanocarriers, using various functional ligands.¹³⁹ These strategies involve the utilization of affinity ligands for specific homing, increased uptake by target cells and increased retention at the target site.¹⁴⁰ For combatting cancer, ligands are chosen that bind to overexpressed or clustered receptors on diseased tissues and diseased cell surfaces. Furthermore, for tackling both neurological diseases, such as Parkinson's and Alzheimer's, brain neoplasm transferrin receptor-mediated delivery is a widely used strategy to overcome the blood brain barrier.¹⁴¹

1.4.5 Delivery of therapeutic RNA

Recent developments in RNA-based gene therapy show high potential for both scientific and therapeutic tasks. Applications include RNA oligonucleotides and polymers that knock down, insert and replace disease associated RNA. The main potential of these therapeutics lies in the highly variable design, which can be used to interact and manipulate an enormous variety of biological processes. Antisense oligonucleotides (ASOs), RNA interference oligonucleotides, messenger RNAs and single guide RNA systems are just a few examples and some have already been approved by the Food and Drug Administration (FDA) (e.g. Mipomersen, Exondyn 51 and Patisiran).¹⁴² Main challenges that have to be addressed include RNA stability, intracellular delivery and off-target effects *in vivo*.¹⁴³ Patisiran is based on a lipid nanoparticle (LNP) formulation and is the first FDA-approved siRNA therapeutic. It tackles hereditary transthyretin amyloidosis, which is a disease caused by mutation of the gene encoding for transthyretin.¹⁴⁴ The formulation includes pH-sensitive fusogenic amino lipid, phosphatidylcholine, cholesterol and dimyristolglycerol-PEG.^{143,145} Especially in phase III clinical trial, the intravenous administration of Patisiran showed high therapeutic activity without apparent side effects.¹⁴⁶

1.5 Problem, study objectives and rationale

Overall, bioconjugates have a large potential for applications in research, diagnostics and therapy. However, there is a lack of robust and reliable strategies for the design of bioconjugates that would demonstrate high performance as diagnostic and therapeutic tools. In particular, single cell studies put very high demands on bioconjugate reagents in terms of efficacy and specificity. In spite of a recent progress, synthesis of bioconjugates remains being challenging, often leading to low yields; purification of bioconjugates can be inconvenient and the process lacks in scalability. Main objectives of this work have been to develop a series of novel potent bioconjugates for appealing single cell FACS studies, detection of oncogenes and gene therapy.

The key hypothesis in this work has been that by applying rationally designed peptides, oligonucleotides and their conjugated products, it is possible to develop potent diagnostic probes and therapeutics with high specificity and sensitivity. The methods that were used in this thesis to test this hypothesis include solid phase oligonucleotide and peptide synthesis, conjugation techniques, such as “click” chemistry and diverse coupling methods, and appropriate purification techniques in this field. More specifically, three different approaches were tested.

The first approach was the development of a novel methodology for fluorescence-based cell sorting that is capable of narrowing down the biomolecular population for applications such as FACS and single cell sequencing. Therefore, a model system was designed, where oligonucleotide adaptors are used to establish a detection element via FRET, to initially test if these adaptors are capable of revealing cellular proximity. The second approach was a point-of-care detection for human *EGFR* oncogene, using a peptide–fluorophore signal boosting approach. This approach contains a hydrogel forming peptide conjugated to a specific hybridization probe to test the capability of detecting human cancer DNA in very low abundance. The third approach includes the synthesis of modified peptides serving as surface ligands for therapeutic LNPs. These ligands aim to enhance the blood brain barrier crossing of LNPs, which leads to an increased uptake in the central nervous system (CNS) and therefore enhances the therapeutic efficacy.

2 Results and Discussion

2.1 Bioconjugate precursors and bioconjugation methodologies

2.1.1 Bioconjugate precursors: Modification and labeling

The synthesis was performed using various modifiers with diverse functionalities to obtain desired products. **Figure 10** shows oligonucleotide modifiers used throughout the synthesis to ensure oligonucleotide precursors with appropriate functionalities for desired reactions.

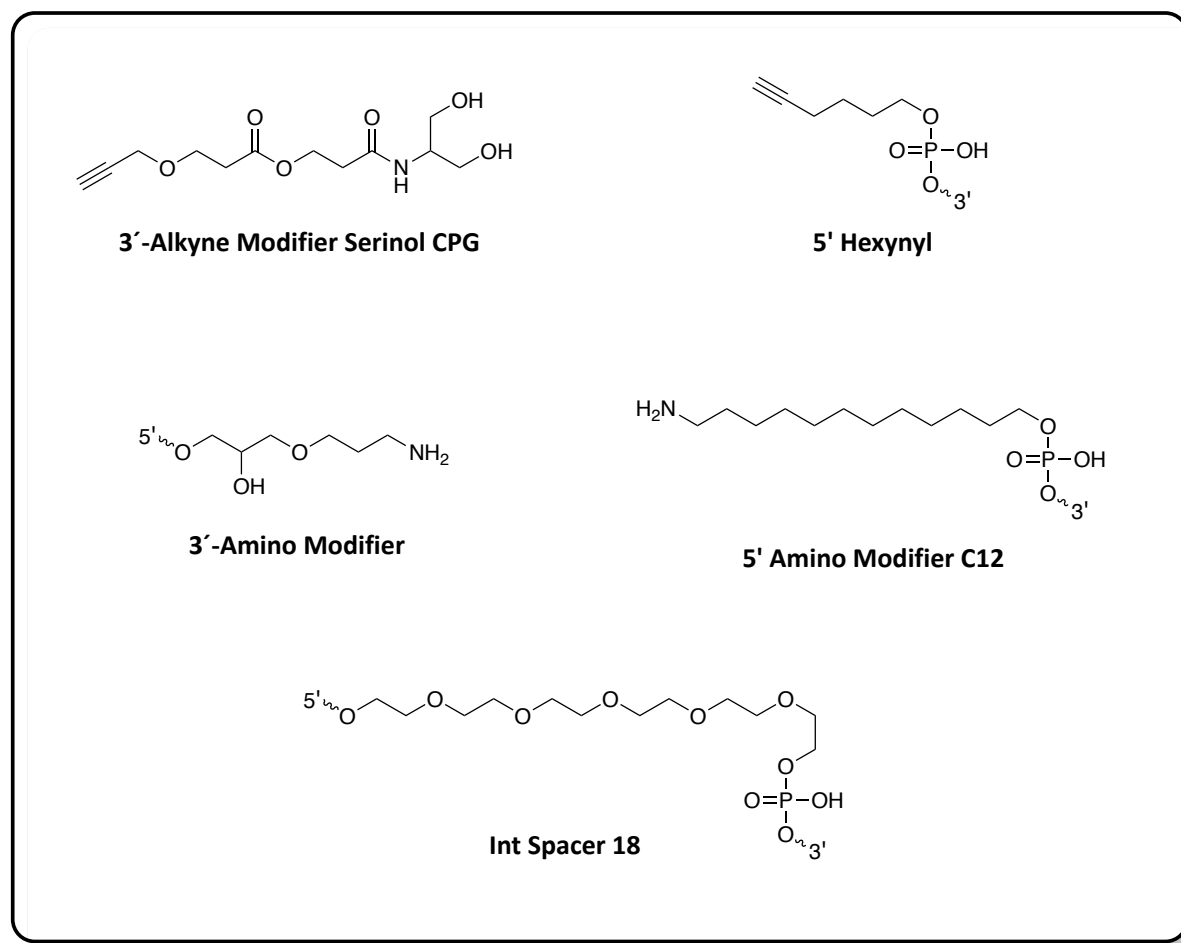


Figure 10: Structures of modifiers used for synthetic oligonucleotides.

Azide- and alkyne-modifiers were utilized for making “clickable” oligonucleotides accessible and internal linkers were attached to oligonucleotide probes to receive modified oligonucleotides with less sterically hindered reactive sites. Especially the use of the CuAAC reaction is favorable due to its optimization for biological molecules in aqueous buffers, the formation of little or no by-products as well as the potential of giving near quantitative yields.^{1,147} Moreover, succinimidyl-ester were used for acylation of primary amines in proteins to receive desired modification. Primary amines as targets are attractive due to the high abundance of lysine in the human proteome. That said, it is important to keep in mind that these sorts of modifications could potentially affect the protein/peptides functionality.^{148,149} Additionally, amino modifiers were incorporated to serve as attachment points for succinimidyl-ester conjugations.

Besides that, heterobifunctional linkers were used to perform linkages between proteins and oligonucleotides as well as between proteins and proteins. These heterobifunctional linkers consist of terminal maleimide and succinimidyl-esters functionalities. The succinimidyl-ester functionality was used to attach the linker to oligonucleotides or proteins. That paves the way to perform subsequent maleimide conjugation to sulfhydryl group containing biomolecules. Similar to that, STP-azide and STP alkyne labeling of biomolecules was performed to make “clickable” synthetic probes accessible. The structure of the two linkers maleimide-PEG2-succinimidyl ester and sulfo-SMCC as well as the STP labeling reagents used during the synthesis course are shown in **Figure 11**.

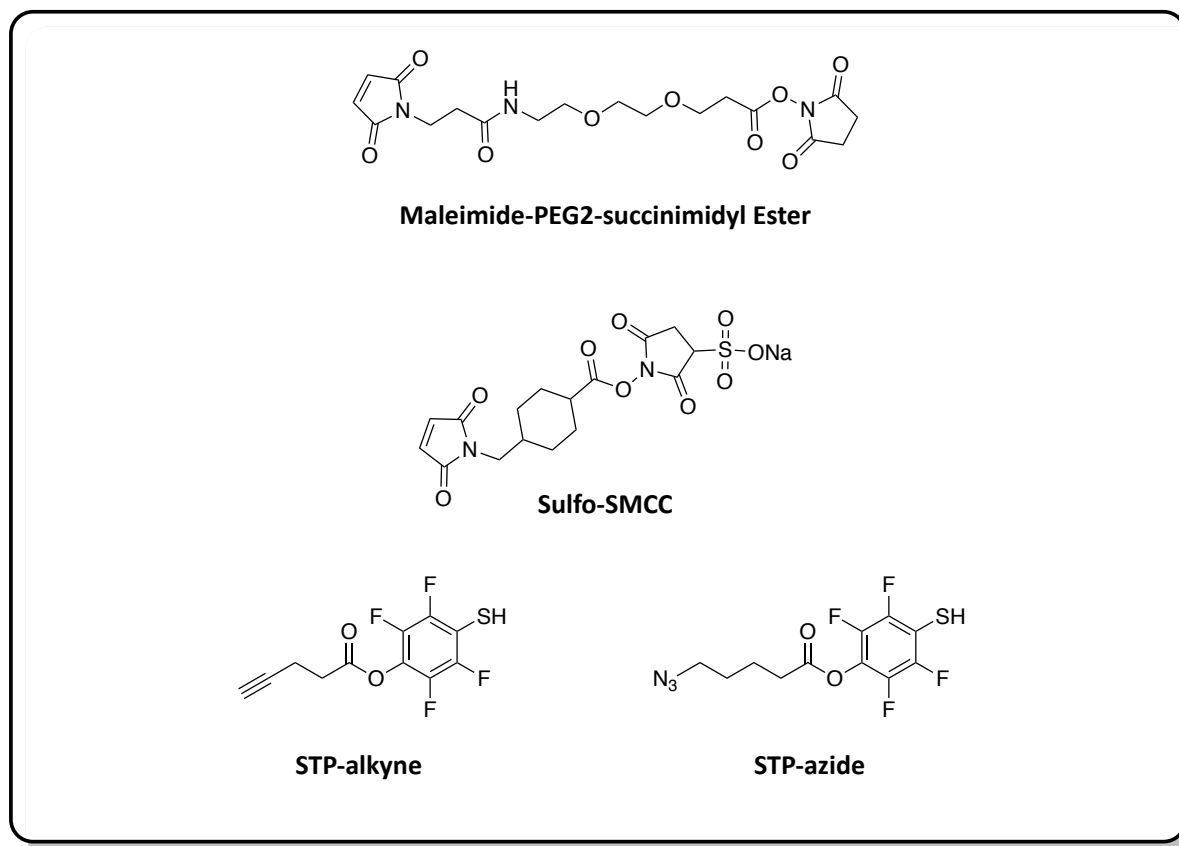


Figure 11: Structures of linkers and labeling reagents used.

2.1.2 Bioconjugation methodologies

Diverse bioconjugation methodologies were performed to establish desired synthetic probes. Methodologies used include CuAAC, maleimide coupling, amide coupling and labeling strategies via STP or NHS activated compounds. “Click” chemistry was applied to make detection and capture molecules accessible to establish an amplification free detection assay. Therefore, a hydrogel forming peptide was conjugated with an oligonucleotide detection probe (PEG) to serve as a detection element. Besides that, an 8× PEG azide was “clicked” with an oligonucleotide capturing probe (POC). Additionally, the control probe CP was synthesized by CuAAC of an oligonucleotide detection probe with the fluorophore Cy3.5. STP azide or STP alkyne labeling of proteins was used to make the proteins ready for “click” reactions (SC1 and SC4). Azide-alkyne cycloaddition was used to perform a simultaneous conjugation (SC5) of an oligonucleotide reporter molecule with an oligonucleotide aptamer. Furthermore, heterobifunctional linker (e.g. sulfo-SMCC) were used to perform oligonucleotide-protein (SC2) and protein-protein (SC3) crosslinking via succinimidyl-ester labeling and maleimide coupling. Amide couplings were applied to make peptide sequences accessible and to conjugate them with fatty acids (mP6, mP7 and mP8-mP10). A schematic overview of the bioconjugation methodology used in the three projects is shown in **Figure 12**.

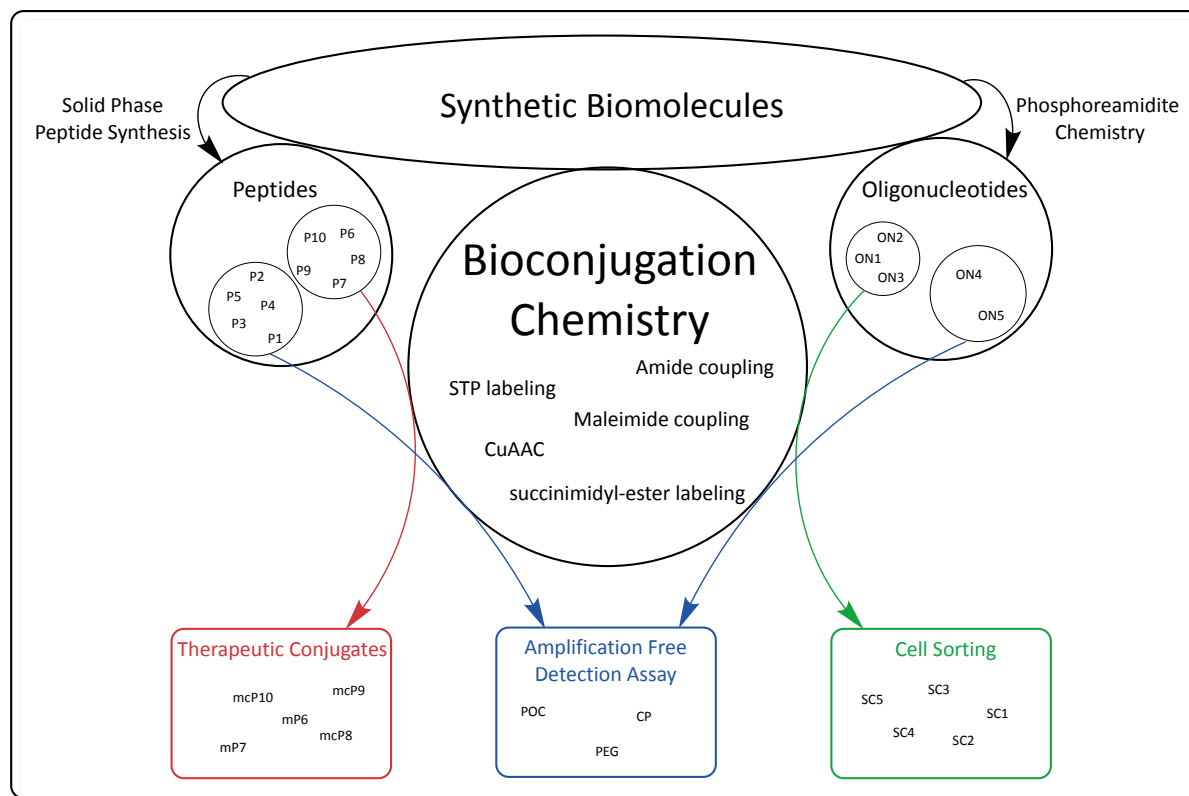


Figure 12: General overview of the synthetic pathway applied to the three projects “Therapeutic conjugates”, “Amplification free detection assay” and “Cell sorting”. Starting from rationally designed synthetic biomolecules (peptides and oligonucleotides), diverse bioconjugation techniques (maleimide coupling, amide coupling, STP labeling, succinimidyl-ester labeling and CuAAC) serve to develop potent diagnostic probes and therapeutics with high specificity and sensitivity.

2.2 Design of synthetic biomolecules and synthetic approaches

Oligonucleotides, peptides and their bioconjugates were designed to undergo specific hybridization, hydrogel formation and receptor targeting. That was achieved by the application of various bioconjugation methodologies. More specifically, oligonucleotides were designed to enable a reporting element based on FRET as well as to achieve specific hybridization of human cancer DNA. Moreover, rationally designed peptides were used to obtain hydrogel formation and to serve as transferrin receptor ligands on the surface of lipid nanoparticles.

2.2.1 Cell sorting

Oligonucleotide adaptors with attached fluorophores were designed to serve as a reporter element utilizing fluorescence resonance energy transfer. The fluorescent labeling acts as transducer that transforms the information of hybridization into a fluorescent signal. Therefore, two oligonucleotides (ON1 and ON2) were designed with complementary up- and downstream regions and terminally attached fluorescent reporter molecules. By hybridization of the complementary regions, terminally attached reporter fluorophores are allowed to reach proximity for fluorescence resonance energy transfer. For a pilot study the selected model system was composed of two parts named System A and System B. The key components of System A are BSA, CD63 and a fluorescently marked oligonucleotide (ON1). The composition of System A features a covalent linkage of CD63 and the oligonucleotide ON1 with BSA. Regarding System B, the key components are BSA, CD63 aptamer (ON3) and a fluorescently marked oligonucleotide (ON2). Covalent linkages are to be performed between BSA and both oligonucleotides ON2 and ON3. The use of surface protein CD63 is appealing due to reported applications as cell surface marker.^{150–152} The use of aptamers is appealing due to their high affinity target binding, which can be transformed into a highly specific detection tool. In contrast to widely used approach of antibodies, oligonucleotide aptamers have lower production costs and elicit no antigenic reactions. Although interesting approaches

in this field have already been taken^{147,153}, further investigation to disclose their full potential is still needed. The synthesis is carried out with the help of bioconjugation techniques. The final design of the model systems as well as the interaction mechanism to be tested are illustrated in **Figure 13**.

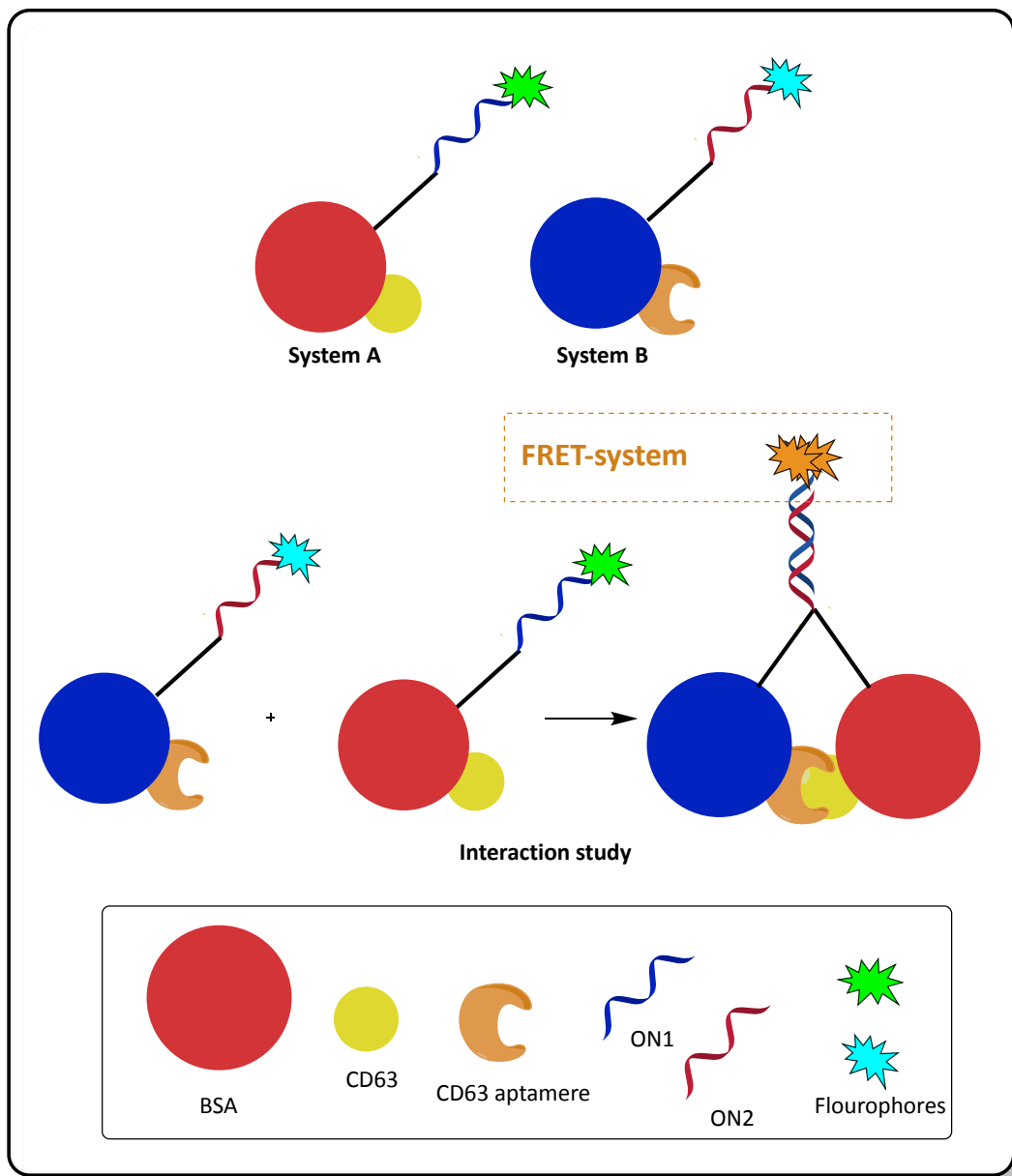


Figure 13: Overview of the synthetic approach to establish System A and System B for fluorescent based single cell studies.

The synthetic approach for System A initially includes labeling of oligonucleotide ON1 (SC1), using maleimide-PEG2-succinimidyl ester. Once the oligonucleotide labeling is performed, the product can be used for subsequent maleimide coupling with BSA (SC2). Next, the synthetic strategy includes a protein-protein crosslink reaction between the modified BSA (SC2) and CD63. Finally, fluorescent labeling of the modified oligonucleotide is attempted to make System A accessible for interaction studies. Regarding the synthetic approach for System B, it begins with STP-labeling of BSA (SC4). Next, a simultaneous “click” reaction of the two oligonucleotides ON1 and ON3 with the STP-labeled BSA (SC4) is attempted. The last step in the synthesis of System B includes fluorescent labeling of the oligonucleotide to make System B ready for interaction studies. An overview of the synthetic approach to establish System A and System B for the interaction study is shown in **Figure 14**.

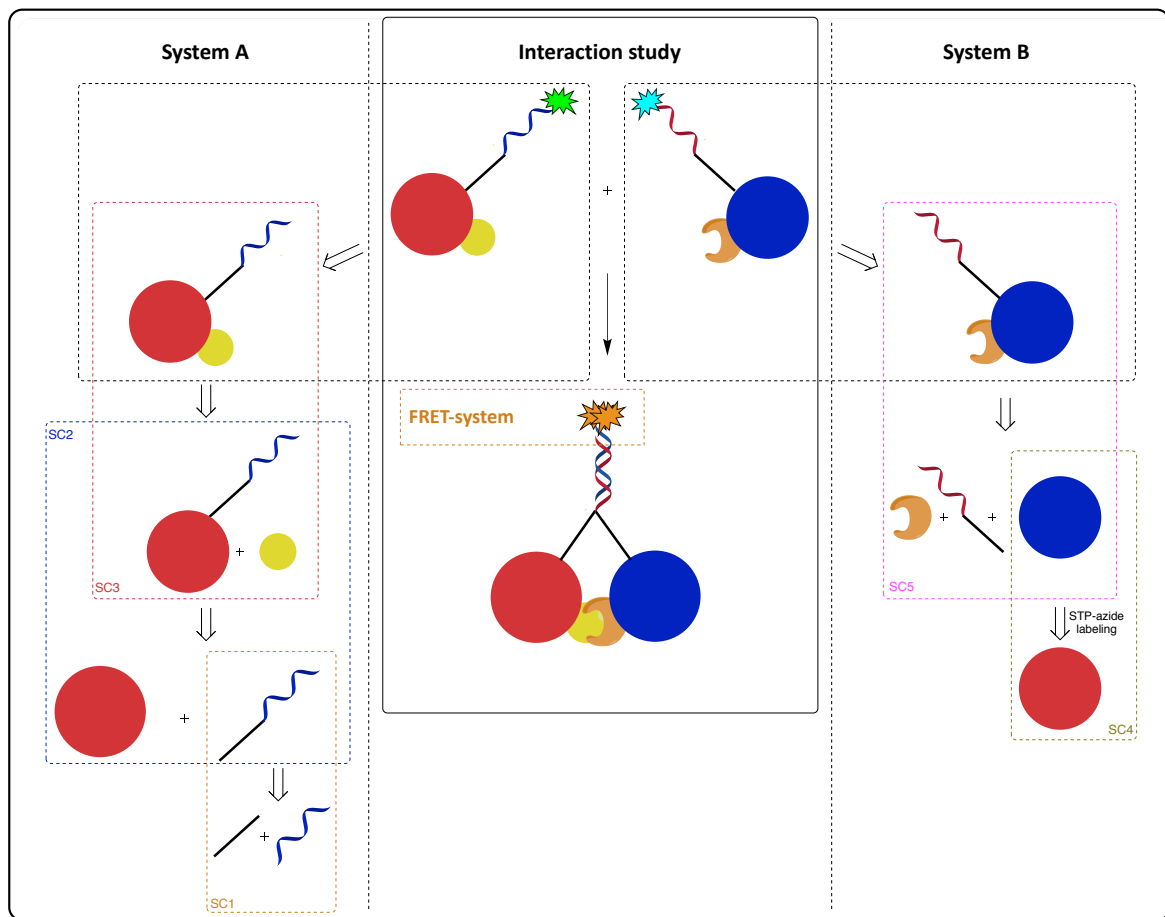


Figure 14: Composition of System A and System B and the proposed interaction.

2.2.2 Mutation detection

A detection methodology for cancer DNA was designed consisting of an oligonucleotide hybridization platform to perform amplification-free detection of human cancer DNA. The design is based on the selective binding of mutant versus wild type (unbound) DNA. Therefore, oligonucleotide capture and detection probes were utilized. The oligonucleotide capturing probe (ON4) is complementary to the downstream region and the oligonucleotide detection probe (ON5) is complementary to the upstream region of the selected cancer DNA. Moreover, ON4 was attached to 8× PEG and ON5 was attached to a hydrogel forming peptide (P1). The idea is that PEG-capture can form large size products with cancer DNA and the resulting separation task can conveniently be solved via size exclusion. The detection and capture probes (ON4 and ON5) were enriched by the incorporation of locked nucleic acids (LNPs) to enhance the affinity and specificity.¹⁵⁴ A schematic overview of the synthetic approach and the purposed detection strategy is shown in **Figure 15**.

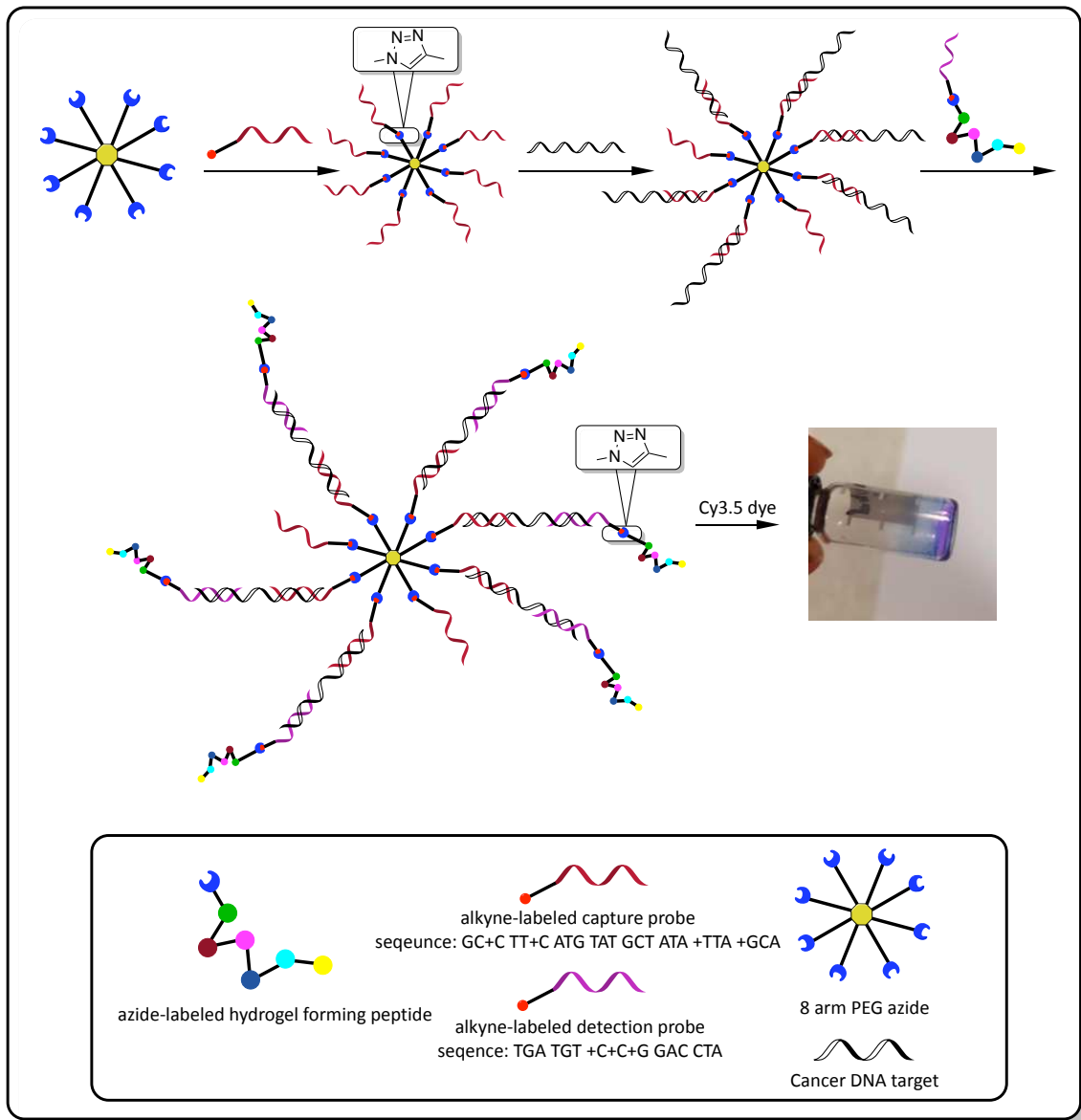


Figure 15: Schematic overview of the synthetic approach and the proposed detection strategy of hydrogel forming conjugates.

2.2.3 Therapeutic conjugates

Peptide sequences of interest were selected based on the requirements for binding the transferrin receptor. Overall, transferrin peptides should serve as a modification tool to decorate the surface of LNPs with the purpose of receptor-mediated transcytosis across the blood brain barrier.¹⁴¹ The transferrin receptor is an attractive target due to its exclusive expression on endothelial cells of the brain capillaries without being expressed on endothelia

cells lining the vessels in other tissues.¹⁵⁵ Transferrin receptor binding peptides as well as cell-penetrating peptides are widely used to enhance the therapeutic sensitivity of LNPs.^{141,156} Both sorts of peptides are included for biological evaluation, but the work in this thesis is focused on the establishment of peptides that serve as transferrin ligands and are modified for liposome attachment.

The peptide selection process was inspired by the literature.^{157,158} The selection is shown in **Table 2**. According to the literature the selected peptides were identified as transferrin receptor ligands via phage display.^{159,160} The target sequences consist of linear and cyclic peptides. An overview of the design for the modified target peptides is given in **Figure 16**.

Table 2: Target peptide selection: Codes and their corresponding sequences of selected peptides.

Code	Sequence (N->C)	Modification
P6	HAIYPRH	
P7	THRPPMWSPVWP	
P8	IGPSVKCRT	N -> C cyclization
P9	KGPSVCCRT	N -> C cyclization
P10	CRTIGPSVC	C -> C disulfide bridge

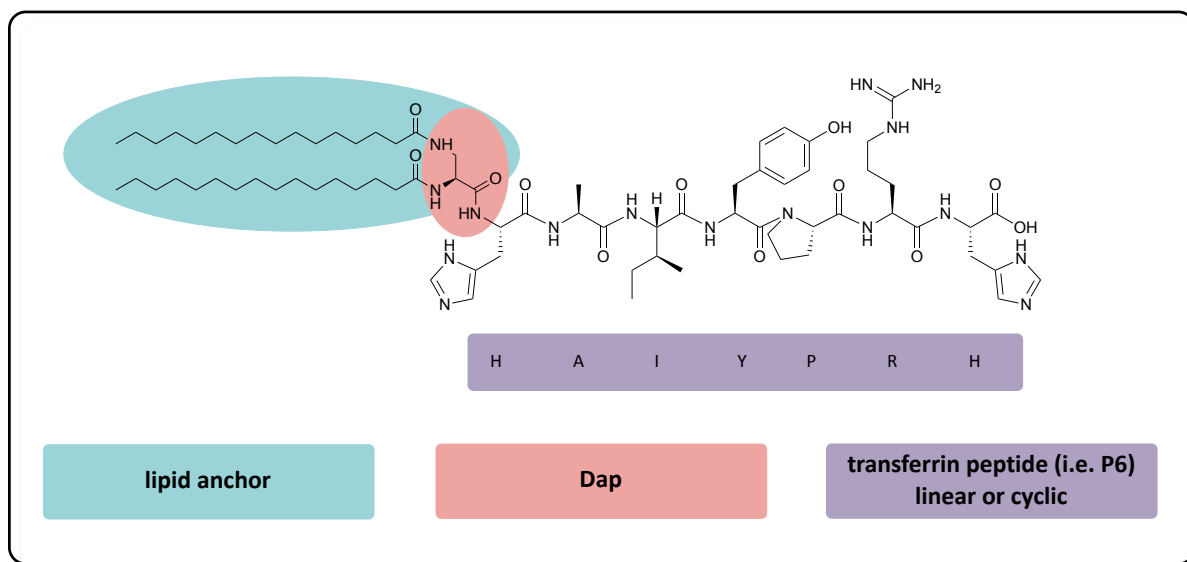


Figure 16: Schematic overview of the general design of target compounds.

The peptide sequences were modified via N-terminal lipidation to make each transferrin receptor targeting peptide ready for later LNP attachment. The design of the lipid anchor and the way of attachment varies from linear to cyclic constructs. This is due to the different synthetic strategy necessary for the installation of the lipid anchor in both types of peptide targets. The basic scaffold of the lipid anchor consists of Dap (diaminopropionic acid) and a palmitic acid (C_{16}) residue attached to each of the free amines introduced to the sequence by Dap. Palmitic acid was selected due to convenient installation via solid phase peptide synthesis and for economic reasons. The installation of the lipid anchor for the two linear peptides P6 and P7 was achieved via stepwise coupling of Dap and palmitic acid on resin. Differently, the installation strategy of the lipid anchor for cyclic peptides was attempted via a single coupling in solution. To achieve this, the synthesis of the lipid anchor LA was carried out separately on resin. Since the cyclization of the peptide was performed prior to the attachment of the lipid anchor, it seemed attractive to avoid two coupling steps in solution with subsequent purifications. The difference in the design of the lipid anchor LA used in the cyclic attempt is the addition of an extra glycine (2x palmitic acid-Dap-Gly-OH).

The design of the cyclic transferrin peptides P8 and P9 included the replacement of an amino acid from the original sequence by a lysine (**Figure 17**). In a pilot study a hydrophobic (isoleucine) and a hydrophilic (cysteine) amino acid were selected. In the following, the

resulting biological data from the pilot study can be used to make further adjustments regarding peptide design.

The free primary amine (ϵ -position) at the side chain of the lysine serves as an anchor point to facilitate installation of the lipid anchor LA. The spacing C_4 alkane chain allows the performance of a less sterically hindered coupling due to higher accessibility and flexibility of the free amine without peptide structure denaturation. Double lipidation was performed to achieve a stronger attachment of the modified peptides to the liposome.

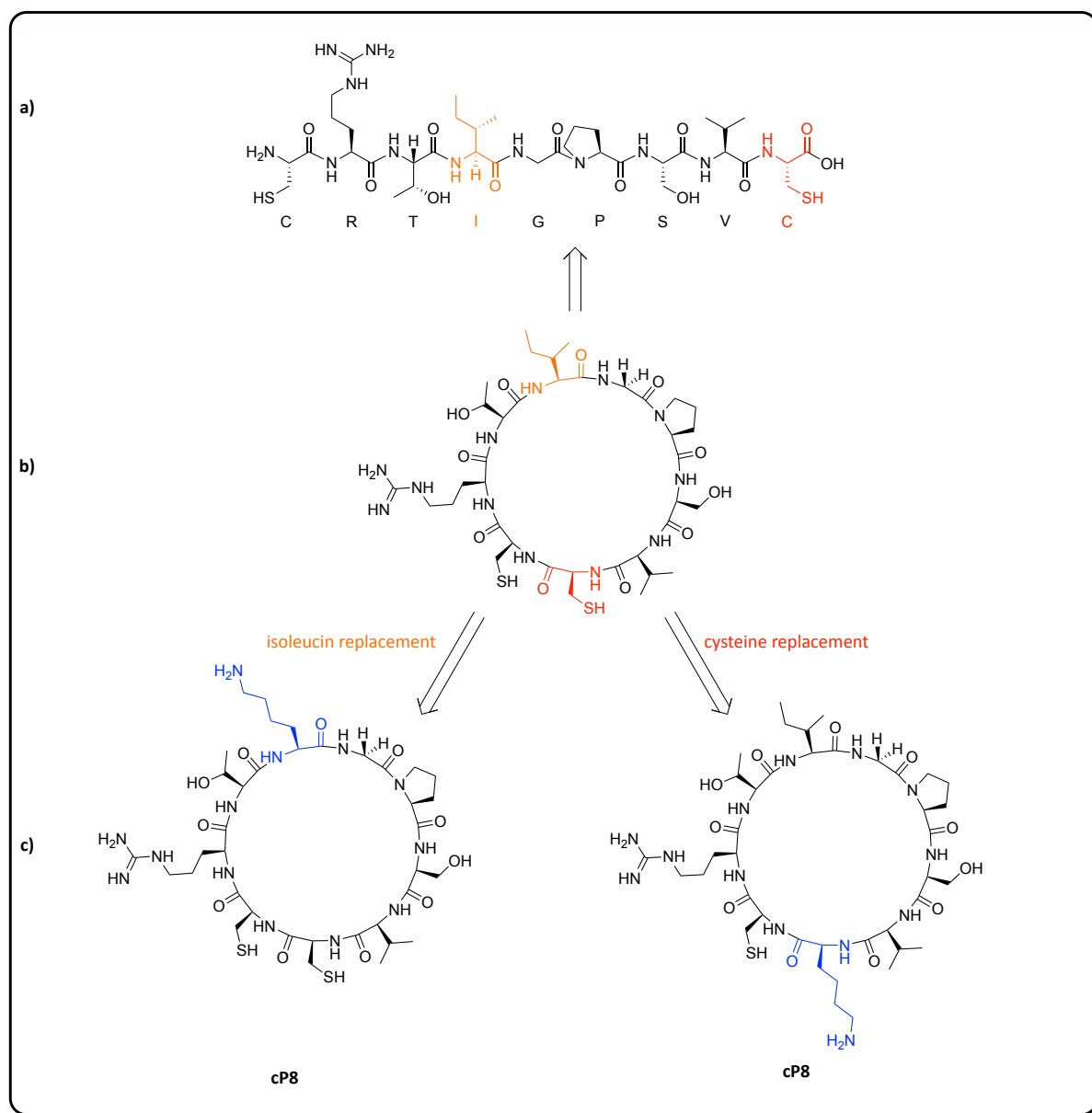


Figure 17: Replacement of a hydrophobic (Isoleucine - marked in orange) and a hydrophilic (cysteine - marked in red) amino acid by a lysine (marked in blue) to facilitate a lipid anchoring point. **a)** Linear template sequence/peptide; **b)** cyclic template peptide; **c)** cyclic target peptides cP8 and cP9.

Similar approaches to install a lipid anchor reported in the literature include the incorporation of lipid modified amino acids into the peptide sequence as well as the installation of terminal cysteines that serve as cyclization points via cysteine bridging. Cyclic peptides, in particular end-to-end cyclized peptides, are appealing due to reported high affinity receptor binding and higher metabolic stability by enhanced enzymatic degradation resistance.^{161,162}

2.3 Synthesis and characterization

2.3.1 Cell sorting

2.3.1.1 Oligonucleotide synthesis and characterization

2.3.1.1.1 ON1 and ON2

Both modified oligonucleotides ON1 and ON2 (**Table 3**) were purchased from Integrated DNA Technologies (IDT) and were used without further analysis or purification in the following synthetic step (ON1 in SC1 and ON2 SC5).

Table 3: Sequence and modification of oligonucleotides ON1 and ON2.

Code	Sequence	Modification
ON1	5' - TCC ACG TCT TC - 3'	3' - AmMO 5' - Hexynyl-iSp18
ON2	5' - AAG ACC TTC T - 3'	3' - AmMO 5' - Hexynyl

2.3.1.1.2 ON3

Oligonucleotide ON3 was synthesized on an automated DNA synthesizer PerSpective Bio-systems Expedite 8909 following a standard protocol in 1.0 μ M scale. Modification of the sequence was performed using a 3'-alkyne-modifier CPG (**Figure 10**). The received product was characterized via IE-HPLC and MALDI-TOF. The resulting IE-HPLC chromatogram showed one major peak with a retention time (RT) of 19.12 min (**Figure 29**). IE-HPLC additionally showed that the product was received in sufficient purity. To verify the identity of the received product, the corresponding eluent of the major peak was isolated and analyzed by MALDI-TOF mass spectrometry (**Figure 30**). The received mass spectra showed a broad peak that verified the identity of ON3. No further purification was conducted and the product was used directly

in the following synthetic step (SC5). The summarized analytical data are illustrated in **Table 4**.

Table 4: Analytical data of ON3: Sequence, modification, calculated and found mass (MALDI-TOF/MS), retention time (IE-HPLC) and purity.

Code	Sequence			Modification
	5' - CAC CCC ACC TCG CTC CCG TGA CAC TAA TGC TA - TTTT-3'			3' - alkyne
ON3	Calcd. mass [M+H] ⁺	Found mass [M+2H] ²⁺	RT [min]	Purity [%]
	11159	5579	19.12	89

2.3.1.2 Bioconjugate synthesis and characterization

2.3.1.2.1 SC1

A short PEG-spacer and a dual functionalized linker were introduced as an adaptor at the oligonucleotide precursor ON1 via NHS ester labeling.¹⁶³ Therefore, maleimide-PEG2-succinimidyl ester (**Figure 11**) was used to modify oligonucleotide ON1. The second terminus of the spacer provided the opportunity to perform the follow-up maleimide coupling (SC2) to establish a linkage between the oligonucleotide and the protein. The identity of the received product was characterized via MALDI-TOF mass spectrometry (**Figure 31**). The spectrum received shows a peak in high intensity that verifies the desired product SC1. The product was used without any further purification in the next reaction step (SC2). The summarized analytical data are illustrated in **Table 5**.

Table 5: Analytical data of SC1: Sequence, modification, calculated and found mass (MALDI-TOF/MS).

Code	Sequence	Modification
SC1	5'- AA GAC CTT CT - 3'	3' - maleimide-PEG2- amide 5' - alkyne
	Calcd. [M+H ⁺]	Found mass [M+H ⁺]
	3683	3683

2.3.1.2.2 SC2

To establish an oligonucleotide-protein linkage, maleimide coupling between modified oligonucleotide SC1 and BSA was performed. Therefore, the following work was performed according to the protocol from Lumiprobe¹⁶⁴. The received reaction product was analyzed via SDS-PAGE (**Figure 18**). Notably, the gel received showed some tailing especially for BSA. Furthermore, it clearly shows that the BSA used for the reaction contains impurities. The running time of the gel potentially could have been extended to receive a gel with higher resolution. However, the received gel confirmed the conversion of the starting material BSA (**Figure 18**, lane 2) by a clear shift of the reaction product SC2 (**Figure 18**, lane 3) towards a higher molecular mass. The product was used in the next reaction step (SC3) without any further purification.

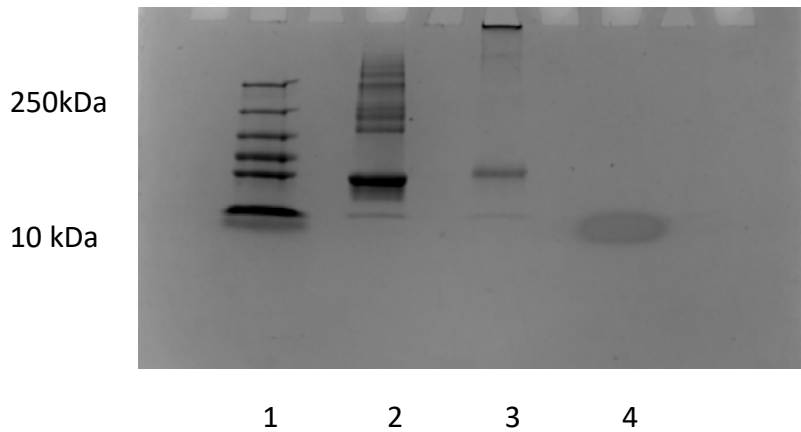


Figure 18: Denaturing (8 M urea) PAGE of ladder (lane 1), BSA (lane 2), SC2 (lane 3) and amicon 30K wash of SC2 (lane 4); stained with GelRed.

2.3.1.2.3 SC3 (a-e)

Protein-protein crosslinking reaction between SC2 and CD63 was performed utilizing sulfo-SMCC (4-(N-maleimidomethyl)cyclohexane-1-carboxylic acid 3-sulfo-N-hydroxysuccinimide ester sodium salt) (**Figure 11**) as a crosslinking reagent.¹⁶⁵ This heterobifunctional crosslinker consists of an amine reactive sulfo-NHS-ester group and a sulfhydryl reactive maleimide that allows for two sequential conjugations steps. The reagent consists of a cyclohexane spacer with a length of 8.3 Å between the two reactive functionalities.

Five different reaction conditions were screened to perform the protein-protein crosslink reaction. In all reactions a mixture of 1× bicarbonate buffer (pH 8.3), SC2 (dissolved in MQ-water), CD63 (dissolved in MW-water) sulfo-SMCC (dissolved in MQ-water) and MQ-water was used. Each reaction was performed at an equal reaction volume (40 µL). To achieve that, the amount of water used in the reaction mixture was adjusted. The amount of 1× bicarbonate buffer always corresponded to 10% of the reaction volume.

For SC3a an initial one-hour incubation step at 37 °C was applied to a mixture of SC2 (0.014 nmol), CD63 (0.007 nmol) and MQ-water. After the incubation step, the crosslinking reagent sulfo-SMCC (0.003 nmol) and the 1× bicarbonate buffer were added to the reaction mixture, mixing was applied and the mixture was kept for additional 35 min at 37 °C. Afterwards the reaction mixture was filtered using amicon 30K columns. For SC3b all starting materials were mixed together (same amounts as for SC3a), the resulting reaction mixture was kept at room

temperature for 40 min and an amicon 30K work-up was applied. Next, SC3a and SC3b were analyzed via SDS-PAGE and after visualization of the gel, no bands were received for all reaction mixtures. Afterwards, two more reactions (SC3c and SC3d) were performed where the amount of the sulfo-SMCC crosslinker was reduced by 50%. To SC3c the same conditions as for SC3a and to SC3d the same conditions as for SC3b were applied. SDS-PAGE analysis was applied to both reaction mixtures and again no bands were received. Finally, the fifth attempt SC3e was following the same conditions as were used in SC3d, but without the amicon 30K work-up. SDS-PAGE analysis of SC3e showed that both starting materials (SC2 and CD63) were still in the mixture and no conversion occurred. The amicon work-up seems not to be an appropriate work-up for these reaction conditions, most likely because of the low protein concentration used in this reaction. One possible explanation for the missing conversion of the starting materials can be an increased hydrolysis rate of the NHS ester due to an elevated pH value in the reaction mixture.¹⁶⁶ That results in inefficient crosslinking conditions because of the reduced half-life of the NHS ester. One attempt to counteract this problem would be the use of a non-amine containing conjugation buffer system (e.g. sodium phosphate, sodium chloride) adjusted to pH 7-7.5. Certainly, a possible side reaction can be a polymerization of the protein mixture leading to a distribution of various forms of heterogenic and homogenic polymerization products in a linear or a clustered form. However, as the SDS-PAGE analysis of SC3e (**Figure 32**) did not show any conversion of the starting materials this problem does not need to be considered further at this point. Another approach for making the crosslinking successful could be a sequential two step conjugation.¹⁶⁷ Alternatively, exchanging BSA as a model protein with glycoprotein TIMP1 could potentially ease up the protein-protein crosslinking due to the naturally occurring affinity of TIMP1 towards CD63.¹⁶⁸

2.3.1.2.4 SC4 and SC5

To establish System B, the initial reaction step included STP-azide (**Figure 11**) labeling of BSA to prepare BSA for the follow-up simultaneous “click” reaction. Therefore, the protocol “NHS ester labeling of amino biomolecules”, from Lumiprobe¹⁶³ was followed. Afterwards the received reaction mixture was filtered via an amicon 30K column. The received product was not further characterized or purified and directly used in the following reaction step (SC5).

The STP-labeled precursor SC4 was used for simultaneous “click” reaction with ON2 and ON3. The reaction was performed under standard CuAAC “click” conditions.¹⁶⁹ After the reaction was stopped, the reaction mixture was filtered via an amicon 30K column. The received reaction product was subsequently characterized via SDS-PAGE (**Figure 19**). The received gel notably showed significant tailing especially for sample SC5 and the precursor SC4. Furthermore, the running time of the gel could have potentially been extended to receive a gel with higher resolution. However, the received gel confirmed the conversion of the starting material SC4 (**Figure 19**, lane 2) due to a clear shift of the reaction product SC5 (**Figure 19**, lane 3) towards a higher molecular. Furthermore, no reaction product can be identified in the amicon 30K wash.

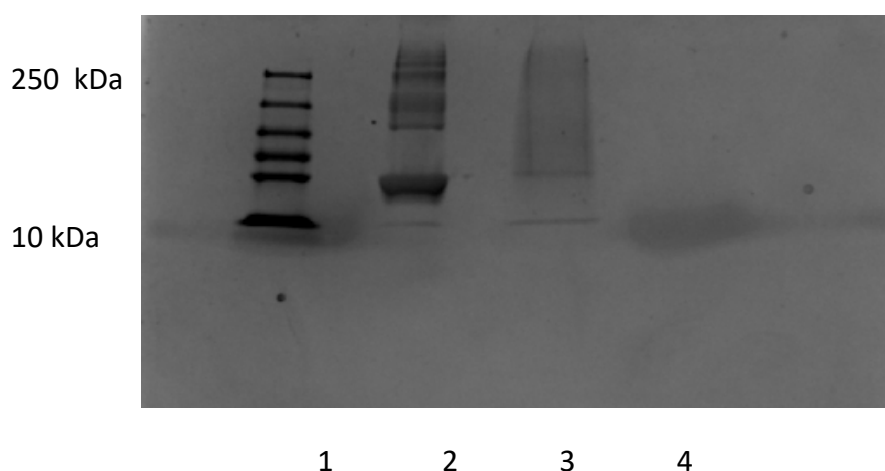


Figure 19: Denaturing (8 M urea) PAGE of ladder (lane 1), SC4 (lane 2), SC5 (lane 3), amicon wash SC5 (lane 4); stained with GelRed.

2.3.2 Actin and gelsolin

After the protein-protein crosslink attempts (SC3a-e) had not shown an immediate success, it was decided to rearrange the model system for a pilot study. The reason for that decision was predominantly the use of CD63, which is an expensive and precious resource to spend on early studies. It was decided to utilize actin and gelsolin as new backbones. A switch to a system based on actin and gelsolin is less expensive and would additionally overcome the necessity for establishing a protein-protein linkage.

Actin and gelsolin will be considered as new backbones to be modified with oligonucleotide adaptors as detection tools for future investigations. Therefore, actin and gelsolin will respectively exchange BSA from each System A and System B and due to the specific interaction between these proteins, no additional installation of a protein-aptamer interaction in the system will be needed.¹⁷⁰ It is believed, that this exchange would lead to a simplified and a less expensive system to perform pilot studies on.

2.3.3 Mutation detection

2.3.3.1 Peptide candidate screening

Initially, a screening of hydrogel forming peptide candidates was performed. The peptide should be able to form a hydrogel in aqueous media. According to the literature short peptides with aromatic groups¹⁷¹ as well as short charged peptides¹⁷² have a high tendency of self-assembly hydrogel formation. Furthermore, the fluorophores should be embedded into the hydrogel without getting quenched and the fluorescent signal should have a linear dependence according to the amount of peptides added. A pool of five different peptides (**Table 6**) combined with three different fluorophores (**Figure 20**) was analyzed. Simultaneously control experiments were conducted for each peptide and fluorophore. For the control experiments MQ-water was used instead of the fluorophore addition, leading to a final number of 23 samples. The hydrogel samples were prepared by mixing an aqueous solution of peptide with a solution of fluorophore in dimethylsulfoxide (DMSO). The resulting solutions were kept at room temperature for 1 – 48 h. The quality of each gel transition, if gel-formation occurred, was rated and each sample was categorized with one of three statuses. The categories were assigned based on the viscosity of the liquid/gel and the visible behavior of the sample when mechanical forces such as, spinning, tending and slight shaking were applied. If the sample kept liquid behavior, it was rated as “no gel”. If the gel could be categorized as highly viscous, but still showed liquid behavior when mechanical forces were applied, it was rated as “gelish”. If a gel showed no liquid behavior at all, including the application of mechanical forces, it was rated as a “gel”. The gel formation was monitored after 1, 2, 4, 12, 24 and 48 h. The results of the peptide/fluorophore gel formation screen and their resulting ratings are given in **Table 7**.

Table 6: Peptides and their sequences used for gel formation screening.

Peptide	Sequence	Modification
P1	H-GGKKRRQKGR-OH	P1 - P5: N-terminus: N ₃ (CH ₂) ₄ CO-
P2	H-KKKYGGFM-OH	
P3	H-RKKRRRRR-OH	
P4	H-GGAAGGAY-NH ₂	
P5	H-YGGAAGGK-NH ₂	

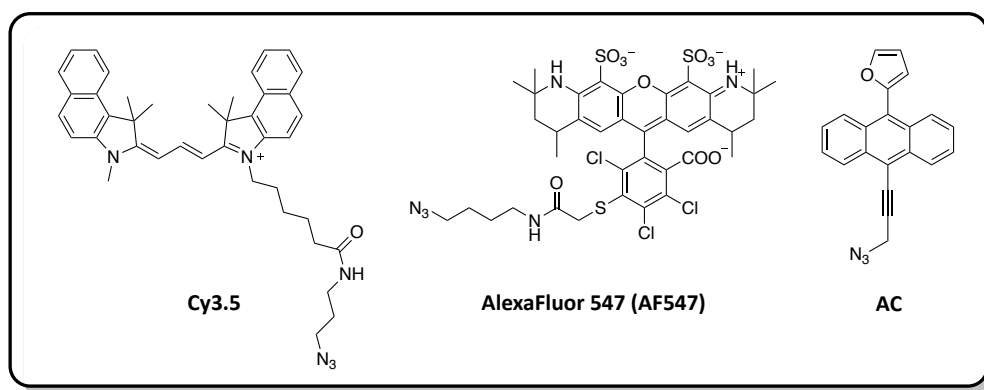


Figure 20: Structure of fluorescent dyes used.

Table 7: Results of the peptide/fluorophore gel formation screening at 2 h time point.*

Sample	P1 (Tat2a)	P2 (CSM 94A)	P3 (CSM 82A)	P4 (Neutral B)	P5 (Lyspep 4)
Peptide without dye (control)	1-2	x	2	1	2
Dye without peptide (control)	x (Cy3.5)	x (CB)	x (AF547)		
Cy 3.5	2	x	2	1	2
AC	x	x	2	1	1-2
Alexa 547	x	x	1-2	1	1-2

*Key/color: x/grey = no gel; 1/blue = gelish; 2/red = gel.

Except P2, all peptides formed a hydrogel in MQ-water. When fluorophores were added, P3 and P5 showed the best results. Notably, P1 formed a hydrogel only with the fluorophore Cy3.5. Furthermore, peptide P4 showed in all possible fluorophore combinations no hydrogel formation, most likely due to its hydrophobic properties. The gelation process of P1, P3 and P5 was slightly slowed by addition of fluorophores. **Figure 21** shows hydrogel formation by best performing candidates.

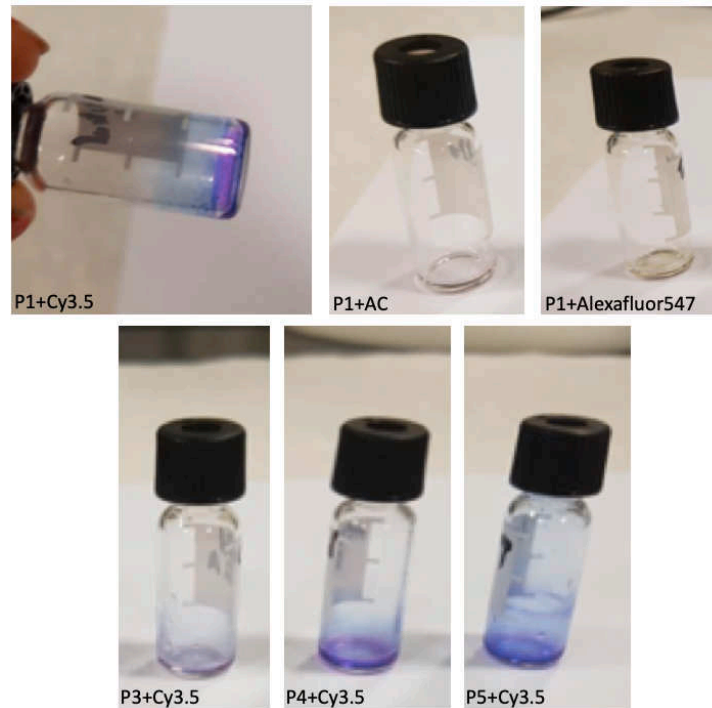


Figure 21: Hydrogel formation of five peptide/fluorophore combinations. Peptide sequences were as follows: Written in C to N direction: P1: GGKRRQKGR; P3: RKKRRRRR; P4: GGAAGGAY; P5: YGGAAGGK.

A key feature to perform successfully point-of-care diagnostics is the velocity of peptide hydrogel formation. Therefore, a selection of peptide/fluorophore combinations were made (**Table 8**) to further investigate the kinetics of hydrogel formation and optimize the conditions to secure a complete gel formation in 1.5 h. Furthermore, fluorescence studies to evaluate the effects of the hydrogel on the fluorophores as well as the dependency of the fluorescent signal on the amount of peptide added, were performed. The results were used as a criteria for the final selection of candidates for the biological assay.

Table 8: Final selection of peptide/fluorophore combinations used of the hybridization assay.

Selected peptide/fluorophore combinations
P1 + Cy3.5
P3 + AC
P5 + AC

2.3.3.2 Oligonucleotide synthesis and characterization

2.3.3.2.1 ON4

The DNA oligonucleotide ON4 was synthesized on a PerSpective Bio-systems Expedite 8909 system using a standard protocol on 1.0 μ M scale. Modification of the sequence was performed using a 3'-alkyne-modifier CPG (**Figure 10**). The received oligonucleotide was analyzed via IE-HPLC and the resulting chromatogram represented one major peak eluted in the center of the run with a retention time of 16.86 min (**Figure 33**). To verify the identity of the received product, the corresponding eluent of the major peak was isolated and analyzed by MALDI-TOF mass spectrometry (**Figure 34**). The spectra received showed a clear but broad peak that verified the identity of ON4. The summarized analytical data are illustrated in **Table 9**.

Table 9: Analytical data of ON4*: Sequence, modification, exact and found mass (MALDI-TOF), retention time (IE-HPLC) and purity.

Code	Sequence			Modification
	5' - TGA TGT +C+C+G GAC CTA - 3'			3' - alkyne
ON4	Calcd. mass [M+H] ⁺	Found mass	RT [min]	Purity [%]
	5012	5011	16.86	89

*LNA is indicated with a plus (+) in front of the corresponding nucleotide letter.

2.3.3.2.2 ON5

The oligonucleotide precursor (**Table 10**) was purchased from Integrated DNA Technologies (IDT) as a 5'-amino modified (**Figure 10**) oligonucleotide precursor. ON5 was used without further analysis or purification in the following synthetic step ON5'.

Table 10: Sequence and modification of oligonucleotide ON5*.

Code	Sequence	Modification
ON5	5' - GC+C TT+C ATG TAT GCT ATA +TTA +GCA - 3'	5' - amino, C12

*LNA is indicated as a plus (+) in front of the corresponding nucleotide letter.

2.3.3.2.3 ON5'

To make oligonucleotide ON5 ready for CuAAC “click” reaction, STP-alkyne (**Figure 11**) labeling was performed. Therefore, labeling procedure “NHS ester labeling of amino biomolecules” from Lumiprobe¹⁶³ was followed. The reaction mixture was worked up using Illustra NAP-5 columns. After work-up, the received product was analyzed via IE-HPLC (**Figure 35**) and MALDI-TOF mass spectrometry (**Figure 36**). The mass spectra received showed a broad peak in the range of 7700 – 8300 m/z. The found mass for ON5' given in **Table 11** illustrates the most intense point of the peak, which was automatically picked from the analysis software. That said, the deviation between the found and the calculated masses can be explained. Mass analysis verified the identity of the desired product and IE-HPLC confirmed that the product was received in high purity. Both spectra were received in low intensities. The summarized analytical data are illustrated in **Table 11**.

Table 11: Analytical data of ON5'*: Sequence, modification, calculated and found mass (MALDI-TOF/MS), retention time (RP-HPLC) and purity.

Code	Oligonucleotide sequence		Modification	
	5' - GC+C TT+C ATG TAT GCT ATA +TTA +GCA - 3'		5' - alkyne, STP	
ON5'	Calcd. mass [M+H] ⁺	Found mass	RT [min]	Purity [%]
	7787	7806	5.34	99

*LNA is indicated with a plus (+) in front of the corresponding nucleotide letter.

2.3.3.3 Bioconjugate synthesis and characterization

2.3.3.3.1 PEG

The “click” reaction between the alkyne modified oligonucleotide ON5' and 8× PEG azide was performed using standard CuAAC “click” conditions.¹⁶⁹ The structure of the 8× PEG azide, is shown in **Figure 22**.

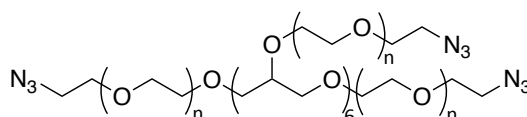


Figure 22: Structure of 8× PEG azide.

The molecular equivalents of oligonucleotide used in the reaction were selected in a manner to allow the formation of the eight-time “clicked” product. More specific, reaction PEG was set-up with a 25-fold excess (25 equiv.) of oligonucleotide ON5' relative to the 8× PEG azide (1 equiv). The reaction was performed overnight and the received crude reaction mixture was passed through an Illustra NAP-5 columns. Next, the received product was analyzed with RP-HPLC and compared to each of starting materials (8× PEG azide and ON5'). Additionally, a co-

injection, composed of both starting materials (8× PEG azide and ON5') plus the product, was analyzed. Detection of the UV signal was performed at 260 nm and 214 nm.

The recorded spectra (**Figure 37-44**) showed that a single product and not a distribution of diverse reaction products, due to a varying amount of attachments, were formed. Notably, the spectra of the reaction mixture showed that no starting oligonucleotide ON5' was left, concluding that all excess ON5' was removed by NAP-5 work-up. Furthermore, the product was received in sufficient purity. Next, the received reaction product was analyzed on MALDI-TOF mass spectrometry, but only signals coming from the matrix were recorded. To obtain information about the number of attachments to 8× PEG azide, denaturing PAGE analysis was performed utilizing SybrGreen as a staining solution (**Figure 23**). PAGE analysis confirmed that six 24mer DNA strands have been attached to 8× PEG azide. The summarized analytical data are illustrated in **Table 12**.

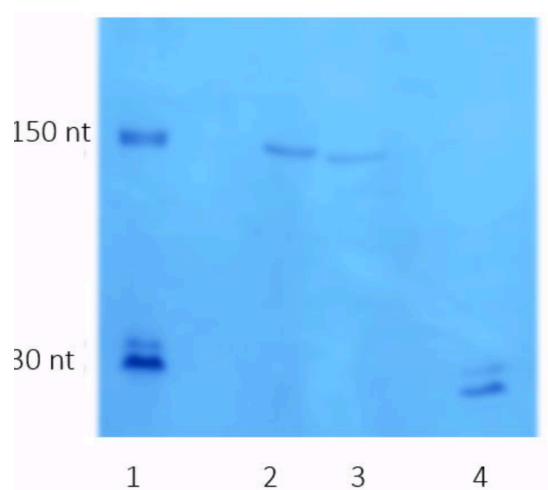


Figure 23: Denaturing (8 M urea) PAGE of ladder (lane 1), conjugate ON3 5 µg/lane 2, 1 µg/lane 3 and starting ON5' (lane 4); stained with SybrGreen.

Table 12: Analytical data of PEG: Sequence, modification, calculated and found mass (MALDI-TOF/MS), retention time (RP-HPLC) and purity.

Code	Oligonucleotide sequence		Modification	
	5' - GC+C TT+C ATG TAT GCT ATA +TTA +GCA - 3'		8× PEG azide	
PEG	Calcd. mass [M+H] ⁺	Found mass	RT [min]	Purity [%]
	56837	nd*	0.99	92

*nd = no data

2.3.3.3.2 POC

Peptide oligonucleotide conjugation between modified oligonucleotide precursor ON4 and azido modified peptide P1 (**Table 5**) was performed under standard CuAAC “click” conditions.¹⁷³ The reaction POC was performed with the molecular equivalent ratio 7.5/1 of peptide/oligonucleotide and the reaction mixture was worked up via Illustra NAP-5 columns. Analysis of the products was performed utilizing RP-HPLC (**Figure 45-52**) and MALDI TOF. RP-HPLC analytical runs of each starting material (P1 and ON4) and the received reaction mixture were performed. Additionally, a co-injection, composed of both starting materials (P1 and ON4) plus the received product, was analyzed. All four samples were analyzed by the same analytical method. Detection of the UV signal was performed at two different wavelengths, 214 nm and 260 nm. Furthermore, the reaction product was characterized via MALDI-TOF mass spectrometry.

The HPCL analysis of POC (**Figure 48**) showed one major peak with a retention time (RT) of 3.93 min. Notably, no peak with a retention time of the starting oligonucleotide ON4 can be identified, concluding that the starting material fully converted. Spectra recorded at 214 nm wavelength were used to identify peptide bonds and therefore peptide P1. P1 elutes at a retention time of 0.77 min and can clearly be distinguished from the injection peak in both, retention time and intensity (**Figure 51**). The 214 nm spectra recorded from the reaction mixture (**Figure 47**) did not show a peak of unconjugated P1, concluding that all excess peptide

was removed by NAP-5 work-up. Furthermore, the product was received in high purity. The summarized analytical data are illustrated in **Table 13**.

Table 13: Analytical data of POC: Sequence, modification, calculated and found mass (MALDI-TOF/MS), retention time (RP-HPLC) and purity.

Code	Oligonucleotide sequence		Modification	
	5' - TGA TGT +C+C+G GAC CTA - 3'		3' - conjugate with P1	
POC	Calcd. mass [M+Na] ⁺	Found mass [M+Na] ⁺	RT [min]	Purity [%]
	6332	6332	3.92	95

2.3.3.3.3 Synthesis of control probe CP

Bioconjugations of modified oligonucleotide **ON4** with Cy3.5 azide modified dye was performed using CuAAC “click” conditions to establish control probe **CP**.¹⁷⁴ The reaction mixture was worked up using Illustra NAP-5 columns and afterwards characterized by MALDI-TOF mass spectrometry (**Figure 53**) and RP-HPLC (**Figure 54**). The MALDI-TOF spectra was received in good intensity and verified the identity of the desired product. The RP-HPLC analysis showed that the product was received with sufficient purity. The summarized analytical data are illustrated in **Table 14**.

Table 14: Analytical data of CP: Sequence, modification, calculated and found mass (MALDI-TOF/MS), retention time (RP-HPLC) and purity.

Code	Oligonucleotide sequence		Modification	
	5' - TGA TGT +C+C+G GAC CTA - 3'		3' - conjugate with Cy3.5	
CP	Calcd. mass [M+K] ⁺	Found mass [M+K] ⁺	RT [min]	Purity [%]
	5694	5694	7.61	83

2.3.4 Therapeutic conjugates

2.3.4.1 Linear peptides

2.3.4.1.1 Synthesis of mP6 and mP7

Solid phase peptide synthesis (SPPS) was carried out to make target compounds mP6 and mP7 accessible. The structure of both linear target compounds is shown in **Figure 24**.

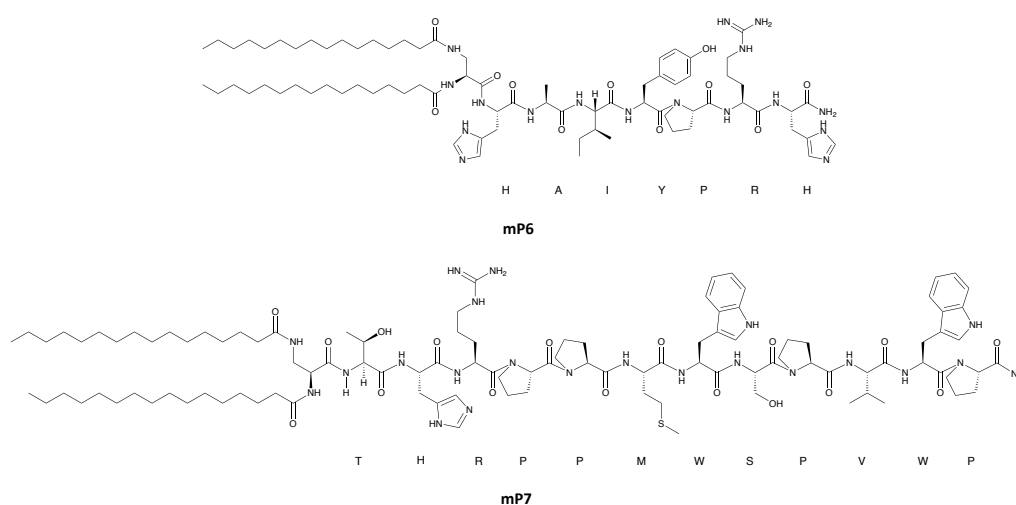


Figure 24: Linear target compounds: Modified linear transferrin receptor targeting peptides mP6 and mP7.

Initially, all reaction steps were performed at standard conditions on solid support. Due to the unsuccessful coupling of proline to proline (NH_2 -PPMWSPVWP-H), when standard conditions are applied, harsher reaction conditions were attempted. Therefore, a microwave reactor was utilized and heating at 80 °C for 15 min was applied. Under these reaction conditions the coupling succeeded. Most likely the coupling of proline to proline was challenging due to hindered accessibility of the nucleophilic amine of the proline (NH_2 -PPMWSPVWP-H). Hence, it seems that microwave treatment allowed the existing sequence on solid support a higher freedom of movement, resulting in a higher accessibility of the nucleophilic amine. That allowed the amide bond to be formed. After the synthesis of P6 was completed, 30 mg of the resin were cleaved using 95% TFA cleaving solution. Then the received peptide was purified via reverse phase preparative chromatography and characterized by MALDI-TOF mass spectrometry (**Figure 55**). The mass spectrum was received in good quality and verified the

mass of desired sequences in high intensity. Next, four NMR spectra (^1H , ^{13}C , COSY and HSQC) of the peptide sequence P6 were recorded (**Figure 56a-g**). The quality of the spectra received suffered from low intensity, most likely from a too low concentrated sample. That makes the received spectra diagnostically less conclusive. However, the presence of six crosspeaks (**Figure 56f**) in the fingerprint area of the COSY spectra, confirmed the presence of all expected alpha proton couplings with backbone amides and N-terminal protons. Concluding that the peak at 3.95 ppm, which has no crosspeak in the fingerprint area, corresponds to alpha proton of proline.

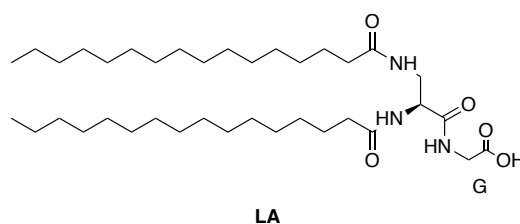
The lipid modification of each sequence was performed on solid support and the coupling of Dap and palmitic acid was archived via standard coupling procedure. After the final coupling on solid support, the target sequences were cleaved from the resin using a 95% TFA solution to perform simultaneous global deprotection of all side chains. After cleavage of mP6 and mP7 from solid support, both compounds were purified via chromatography. Normal phase chromatography was applied for purification of mP6 and the received colorless reaction product yielded 6%. The crude modified peptide mP7 was purified by reverse phase preparative chromatography and after lyophilization the received reaction product yielded 7%. The received products were subsequently characterized via MALDI-TOF mass spectrometry (**Figure 57** and **Figure 58**). The spectra were received in low intensity but verified the formation of the desired products. The yield of the received peptides is two to three times lower compared to experiments without lipidation.¹⁷⁵ This can be explained by less efficient coupling of the lipid anchor due to sterically hindrance. Notably, the coupling of the terminal fatty acid is less efficient due to the sterically hinderance of the carboxylic acid coming from the C_{16} alkyne chain. Moreover, the solubility of the received lipidated peptides strongly varied and were overall weak in most organic solvents. Most likely because of the combination of a hydrophobic fatty acid attached to a hydrophilic peptide sequence. That said, purification of the modified peptides by chromatographic techniques appeared to be challenging tasks. It is believed that the reduced coupling efficacy of the fatty acids as well as the challenging purification are the reasons for reduced yields. The summarized analytical data are of mP6 and mP7 illustrated in **Table 15**.

Table 15: Analytical data of mP6 and mP7: Sequence, modification, calculated and found mass (MALDI-TOF/MS).

Code	Peptide sequence N->C	Modification
mP6	HAIYPRH	N-terminal: palmitic acid (2x) - DAP
	Calcd. mass [M+H] ⁺	Found mass [M+H] ⁺
	1455.9	1455.5
Code	Peptide sequence N->C	Modification
mP7	THRPPMWSPVWP	N-terminal: palmitic acid (2x) - DAP
	Calcd. mass [M+H] ⁺	Found mass [M+H] ⁺
	2053.2	2053.7

2.3.4.1.2 Lipid anchor

The synthesis of the lipid anchor LA (**Figure 25**) was performed on solid support following a standard procedure for solid phase peptide synthesis (SPPS) on 2-chlorotrityl resin.

**Figure 25:** Molecular structure of the lipid anchor LA.

As mentioned before, in contrast to the lipidation performed in the linear attempt, the lipid anchor LA for the cyclic peptides includes a glycine at the C-terminal. This glycine serves as a spacer between the 2-chlorotrityl resin to improve the coupling efficiency when Dap is coupled. The decision was made based on previous experiments showing that the initial coupling of Fmoc-Dap(Fmoc)-OH to the resin suffers in coupling efficiency and leads to

reduced yields. It is believed that the reason for that is related to the two Fmoc groups attached to each N-terminals of Dap. These relative large groups cause the C-terminal of the Fmoc-Dap(Fmoc)-OH to be less accessible. Furthermore, sterically hindrance from the alkyne chains and the palmitic acids can negatively influence the coupling efficiency of the lipid anchor to the cyclic peptides. Both problems are minimized by improving accessibility of the electrophilic site. This is key to enhance the coupling efficiency and was realized by the addition of glycine.

After the synthesis was completed, the lipid anchor LA was cleaved from the resin, the received product was verified on MALDI-TOF mass spectrometry (**Figure 59**) and used without any further purification for following reactions. The summarized analytical data of the lipid anchor LA are illustrated in **Table 16**.

Table 16: Analytical data of lipid anchor LA: Sequence, modification, calculated and found mass (MALDI-TOF/MS).

Code	Peptide sequence N->C	Modification
LA	Dap-G	N-terminal: 2x palmitic acid
	Calcd. mass [M+Na] ⁺	Found mass [M+Na] ⁺
	660.6	660.7

2.3.4.2 Cyclic peptides

2.3.4.2.1 Synthesis of mcP8 and mcP9

The structures of the two end-to-end cyclized target compounds mcP8 and mcP9 as well as the cyclic precursors (prior to lipidation) are given in **Figure 26**. Moreover, an overview of the synthetic strategy followed to make the two modified cyclic transferrin peptides mcP8 and mcP9 accessible is shown in **Figure 27**.

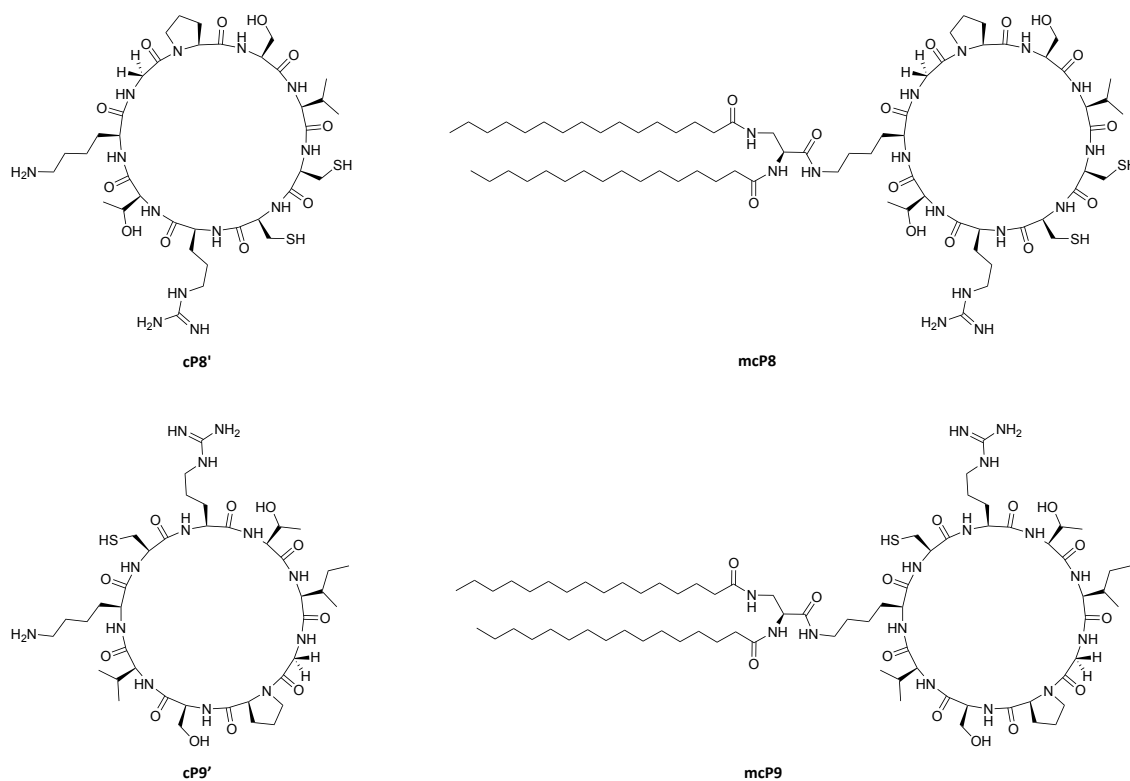


Figure 26: Modified and end-to end cyclized transferrin receptor targeting peptides (mcP8 and mcP9) and their precursors (cP8' and cP9').

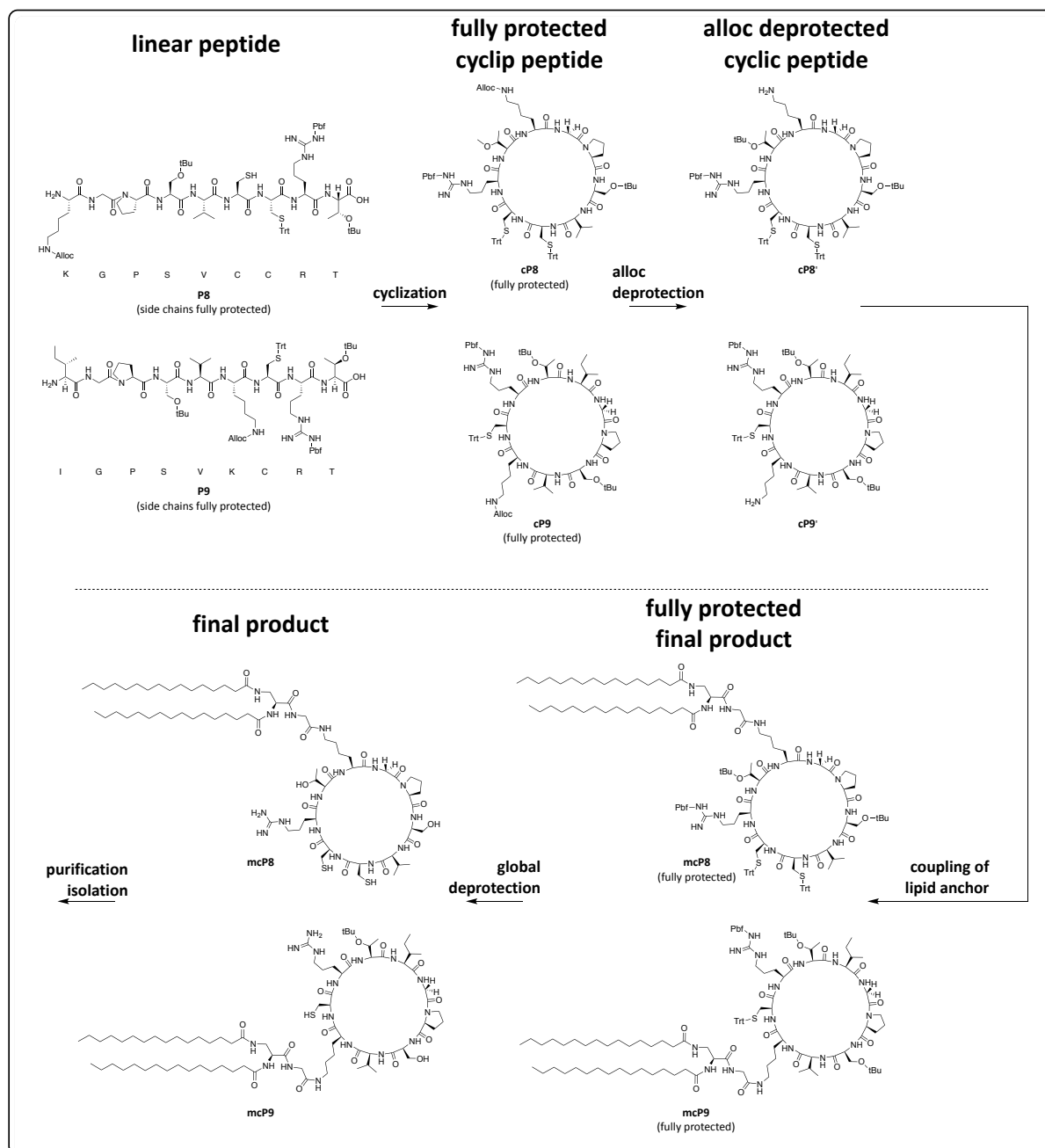


Figure 27: Synthetic strategy used to make cyclic transferrin peptides accessible.

All synthetic steps for making target sequences P8 and P9 accessible, were carried out via solid phase peptide synthesis (SPPS) utilizing standard Fmoc-strategy on a 2-chlorotrityl resin. After all couplings were performed, N-terminal Fmoc protecting groups were removed on both peptides, followed by the cleavage from the solid support using 20% HFIP. HFIP treatment was performed to keep side chain protecting groups. Furthermore, a small amount of each peptide

P8 and P9 was cleaved using 95% TFA to confirm the identity of the peptide sequence. The cleavage of all side chain protecting groups was performed for analytical purpose to simplify the identification process via MALDI-TOF analysis. During the ionization process with the high voltage laser some side chain protecting groups tend to fall off from peptides, which complicates the identification process. After TFA treatment the peptides were globally deprotected, except the Alloc (N-allyloxycarbonyl) protecting group on the side chain of the lysine. The remaining Alloc protecting group did not show any tendency to fall off during the ionization process and the mass of the peptide was found as expected by MALDI-TOF mass spectrometry (**Figure 60** and **Figure 61**). The summarized analytical data of P8 and P9 are illustrated in **Table 17**.

Table 17: Analytical data of P8 and P9: Sequence, modification, calculated and found mass (MALDI-TOF/MS).

Code	Peptide sequence N->C	Modification
P8	IGPSVKCRT	-
	Calcd. mass [M+H] ⁺	Found mass [M+H] ⁺
	1034.5	1034.6
Code	Peptide sequence N->C	Modification
P9	KGPSVCCRT	-
	Calcd. mass [M+H] ⁺	Found mass [M+H] ⁺
	1044.6	1044.7

The globally protected peptides after HFIP cleavage were purified via reverse phase preparative chromatography and the received reaction products yielded 24% for P8 and 21% for P9. Next, the peptides were used for follow-up end-to-end cyclization, performed in solution. To do this, the dissolved peptides were added dropwise to a solution containing a large excess of coupling reagents. This dropwise set-up was performed to favor the formation

of the cyclic product over intermolecular coupling/polymerization. Next, the reaction mixtures were purified by reverse phase preparative chromatography and analyzed by MALDI-TOF mass spectrometry to confirm the formation of the cyclized product. The received reaction products cP8 yielded 41% and cP9 yielded 42%. Successful formation of the cyclic product was observed without any evidence for the formation of dimers. The received mass spectra of the intramolecular end-to end-cyclized peptides cP8 and cP9 are shown in **Figure 62** and **Figure 63**. The summarized analytical data of cP8 and cP9 are illustrated in **Table 18**.

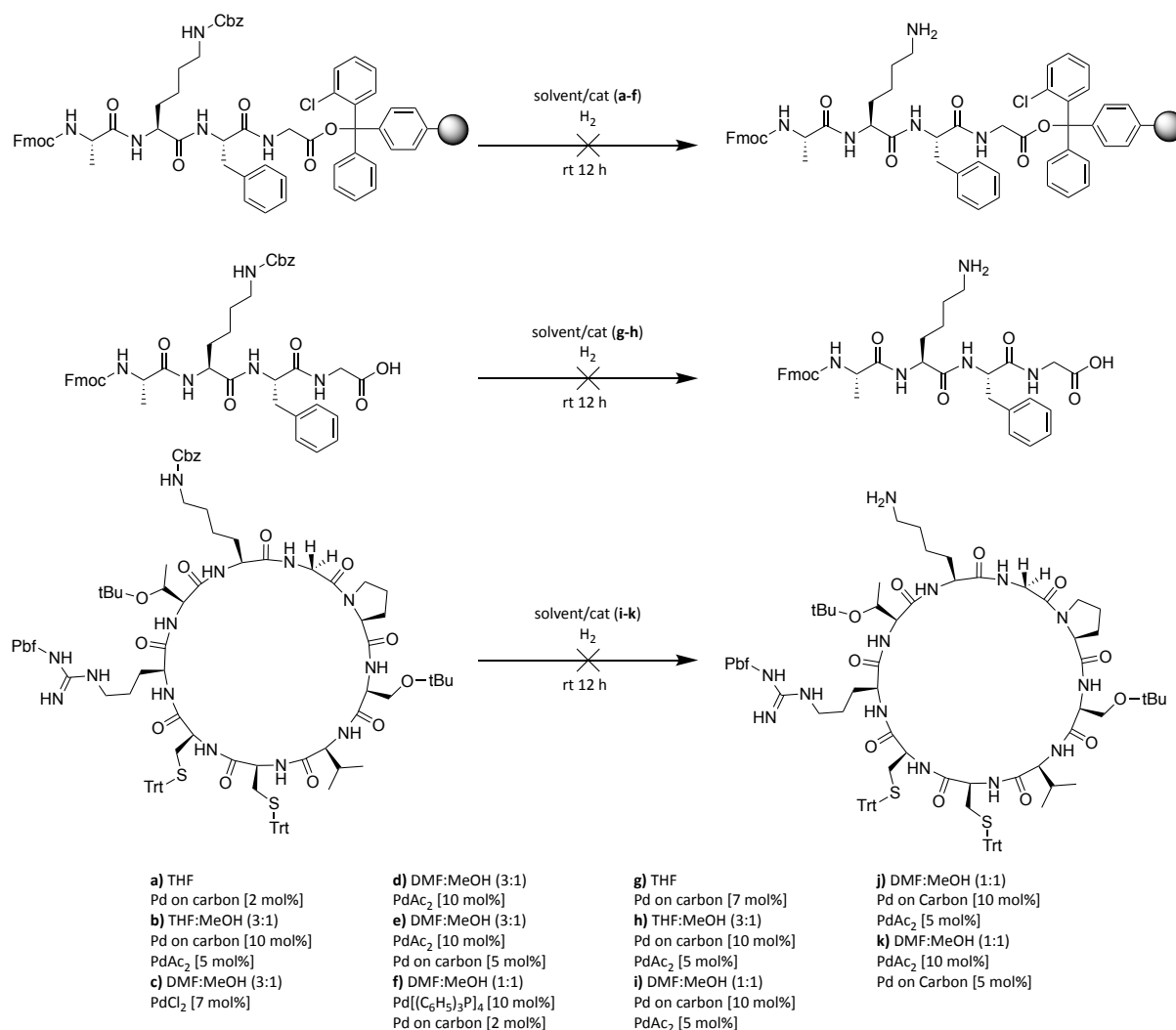
Table 18: Analytical data of cP8 and cP9: Sequence, modification, calculated and found mass (MALDI-TOF/MS).

Code	Peptide sequence N->C	Modification
cP8	IGPSVKCRT	N -> C cyclized
	Calcd. mass [M+K]⁺	Found mass [M+K]⁺
	1846.9	1847.2
Code	Peptide sequence N->C	Modification
cP9	KGPSVCCRT	N -> C cyclized
	Calcd. mass (with one tBu group fallen off) [M+K]⁺	Found mass (with one tBu group fallen off) [M+K]⁺
	1614.9	1615.1

After the isolation and characterization of the cyclic peptides, the orthogonal Alloc side chain protection group of the lysine was removed to make the amine accessible for follow-up coupling of the lipid anchor LA.

2.3.4.2.2 Orthogonal CBZ deprotection

Initially, a different synthetic approach had been attempted regarding the orthogonal deprotection of the side chain protecting group of the lysine. That attempt included the evaluation of an orthogonal CBZ (benzyloxycarbonyl) deprotection on resin. Therefore, a (H-Lys(Z)-OH) was installed during the synthesis of the peptide sequences P8 and P9. Beforehand, a short test sequence was synthesized on solid support containing a lysine (H-Lys(Z)-OH) to perform a test run of the CBZ deprotection with the peptide still on resin. Several different conditions were screened, but no conversion occurred. Next, an orthogonal CBZ deprotection conditions in solution were screened on the actual target sequences cP8 and cP9. Variations of the conditions included changes to the solvent system as well as the catalyst system used (**Scheme 1**). However, none of the attempts showed sufficient conversion.

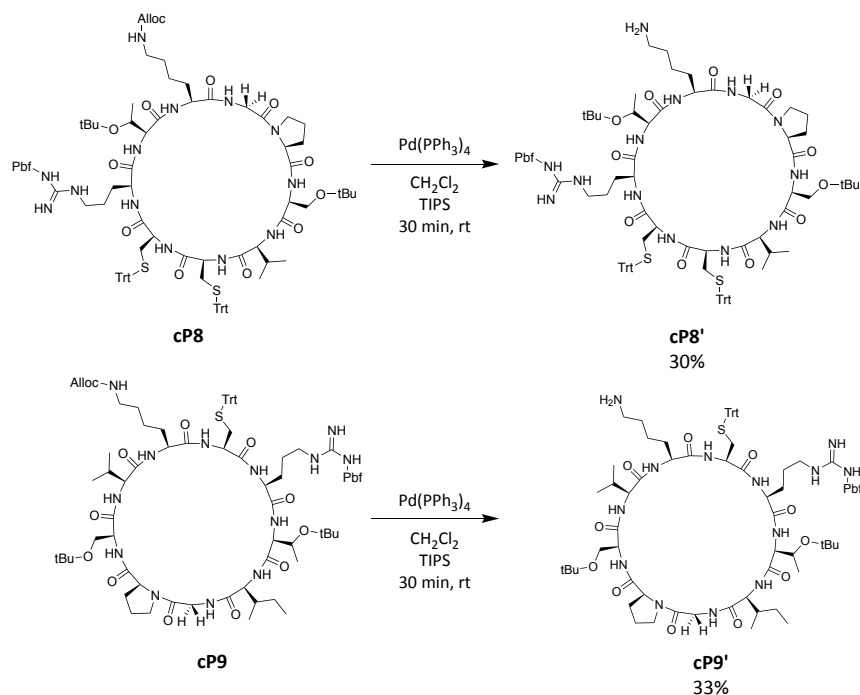


Scheme 1: Attempts to perform a CBZ deprotection of cP8 and cP9 under reductive conditions, utilizing different catalyst systems and solvent systems.

2.3.4.2.3 Orthogonal Alloc-deprotection

After the initial THF attempt of an orthogonal CBZ-deprotection did not show success, the lysine side chain protecting group was changed to Alloc. Therefore, Fmoc-Lys(Alloc)-OH were utilized during the synthesis of cP8 and cP9 and implemented in the sequence. To perform the orthogonal Alloc deprotection, tetrakis(triphenylphosphine)-palladium(0) was used as a catalyst, triisopropylsilane (TIPS) as a scavenger and dichloromethane as a solvent. Reaction time was 30 min at room temperature

Afterwards, the same conditions were applied to perform orthogonal Alloc-deprotection on cP8 and cP9 in solution (**Scheme 2**). Next, the cyclic peptides cP8' and cP9' were purified via reverse phase chromatography and after lyophilization cP8' yielded 30% and cP9' and 33%. Compared to similar reaction conditions but the utilization of an aqueous work-up reported in the literature, the obtained yields of cP8' and cP9' are three times lower. This is most likely due to compound loss during the reverse phase purification step due to sample sizes around the lower limit of the preparative column used. Furthermore, the received reaction products were analyzed by MALDI-TOF mass spectrometry (**Figure 64** and **Figure 65**). The crude peptides were directly used for the following synthetic step. The summarized analytical data are illustrated in **Table 19**.



Scheme 2: Alloc deprotection in solution to form cP8' and cP9'.

Table 19: Analytical data of cP8' and cP9': Sequence, modification, calculated and found mass (MALDI-TOF/MS)

Code	Peptide sequence N->C	Modification
	IGPSVKCRT	N -> C cyclized, Alloc deprotected
cP8'	Calcd. mass [M+H]⁺	Found mass [M+H]⁺
	1762.9	1762.8
Code	Peptide sequence N->C	Modification
	KGPSVCCRT	N -> C cyclized, Alloc deprotected
cP9'	Calcd. mass (with one tBu group fallen off) [M+K]⁺	Found mass (with one tBu group fallen off) [M+K]⁺
	1530.8	1531.1

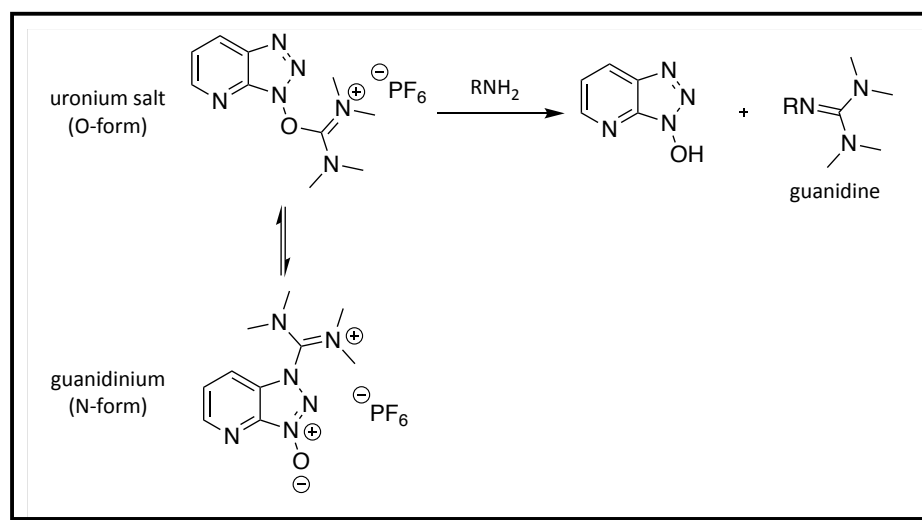
2.3.4.2.4 Installation of the lipid anchor

The installation of the lipid anchor LA was performed for both orthogonally deprotected peptides cP8' and cP9' in solution, utilizing HATU as a coupling reagent and DIPEA as a non nucleophilic base. The reactions were performed on a small scale to screen for the formation of the desired product. After 2 h of reaction time, both reaction mixtures were analyzed by MALDI-TOF mass spectrometry. Regarding the lipidation of cP9', the received spectra did not show the mass of the starting material, indicating that full conversion occurred. Furthermore, the desired reaction product mcP9 as well as the mass of the guanidylated starting material were identified in the reaction mixture (**Figure 66**). Similarly, the reaction mixture of cP8' showed full conversion of the starting material plus the guanidylation of the starting material, but no peak that corresponds to the mass of the desired reaction product mP8 occurred. The summarized analytical data of mcP9 are illustrated in **Table 20**.

Table 20: Analytical data of mcP9: Sequence, modification, calculated and found mass (MALDI-TOF/MS)

Code	Peptide sequence N->C	Modification
mcP9	IGPSVKCRT	N -> C cyclized, lysine side chain: modified with lipid anchor
	Calcd. mass [M+Na] ⁺	Found mass [M+Na] ⁺
	2150.3	2150.6

The guanidination is a known side reaction that can occur during the coupling process (**Scheme 3**). A way to diminish this side reaction would be the addition of 1-Hydroxybenzotriazol (HOBt) to the reaction. Overall, the identification of the desired product mcP9 in the reaction mixture showed that the selected synthetic strategy is successful. Furthermore, it needs to be tested if the undesired guanidylation of the starting material mP8 and mP9 could be suppressed by the utilization of 1-hydroxybenzotriazole hydrate (HOBt). A suppression could potentially enhance the yield of the lipidation.

**Scheme 3:** Equilibrium of uronium species (O-form) and guanidinium species (N-form) of HATU in solution and guanidylation as a side reaction during coupling reactions.

Synthesis of mcP10

All synthetic steps for making target sequence mcP10 accessible were carried out via solid phase peptide synthesis (SPPS) utilizing standard Fmoc-strategy on a Rink resin.¹⁷⁶ An overview of the synthetic strategy followed is shown in **Figure 28**.

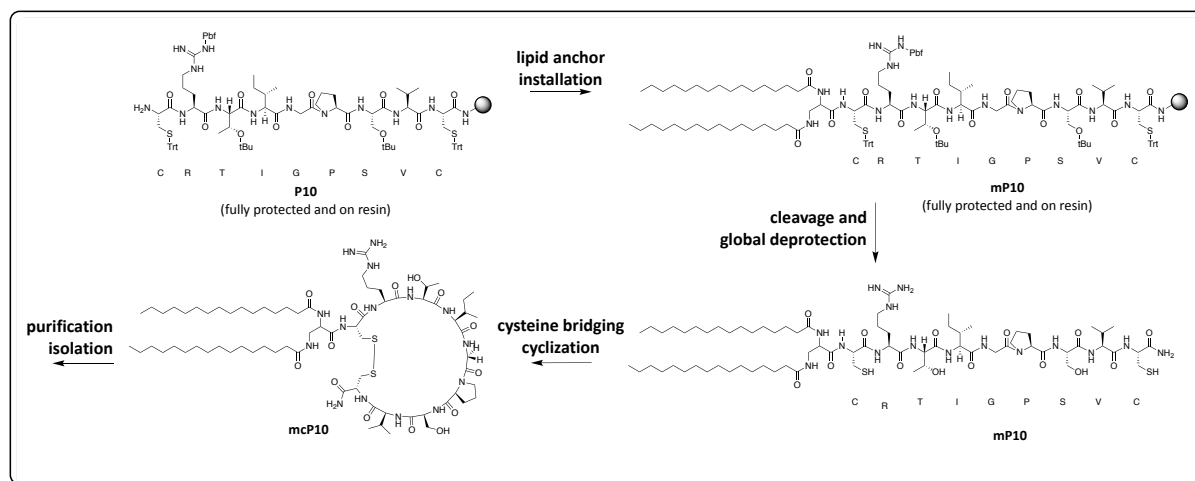
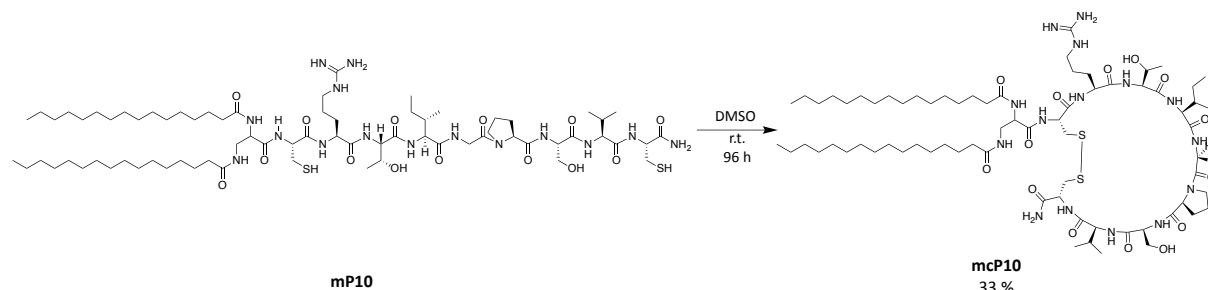


Figure 28: Overview of synthetic strategy used for making mcP10 accessible.

After the synthesis of P10 was completed with the peptide still on resin, a few beads were treated with 95% TFA to receive the globally unprotected peptide sequence to confirm the identity of the received product via reverse phase LC/MS (**Figure 67**). After the analysis had confirmed the identity of P10, the remaining peptide (still on solid support) was modified via stepwise installation of the lipid anchor (coupling of Dap followed by the coupling of palmitic acid residues to both N-terminals of the coupled Dap). The lipidation was also performed via standard SPPS conditions. Next, the modified linear sequence was cleaved from the resin using 95% TFA to receive the globally deprotected modified peptide mP10. The coupling product was verified via MALDI-TOF mass spectrometry (**Figure 68**) and used without further purification to undergo the cysteine bridging cyclization step in solution.

Therefore, mild oxidative conditions at room temperature were applied to mP10 to let side chain sulfhydryl groups of the two terminal cysteines form a disulfide bond (**Scheme 4**). After 96 h reaction time, a work-up of the reaction mixture utilizing normal phase chromatography was applied. The cyclization reaction yielded 33% and the reaction product mcP10 was verified via MALDI-TOF mass spectrometry (**Figure 69a** and **Figure 69b**). The peak corresponding to

the mass of the desired product was received in low intensity. The synthesis of mcP10 gave an overall yield of 9% based on the resin loading. This overall yield can be stated as reasonable based on the comparison to similar experiments reported in the literature.¹⁷⁶ The summarized analytical data of mP10 and mcP10 are illustrated in **Table 21**.



Scheme 4: Reaction equation of cysteine bridge formation step under mild oxidation conditions to make mcP10 accessible.

Table 21: Analytical data of mP10 and mcP10: Sequence, modification, calculated and found mass (MALDI-TOF/MS).

Code	Peptide sequence N->C	Modification
mP10	CRTIGPSVC	-
	Calcd. mass [M+H] ⁺	Found mass [M+H] ⁺
	1497.0	1497.3
Code	Peptide sequence N->C	Modification
mcP10	CRTIGPSVC	Cyclic: C -> C disulfide bond
	Calcd. mass [M+H] ⁺	Found mass [M+H] ⁺
	1495.0	1495.1

3 Conclusion and perspective

To conclude, a model system was rationally designed to investigate if oligonucleotide adaptors can reach cellular proximity and function as a recognition tool for fluorescent based cell sorting. The designed model system consists of two parts, System A and System B. The principle of the interaction studies is based on fluorescent readouts enabled by a FRET system installed on each system to monitor the interaction. The synthesis of System B was successfully carried out and is ready to be labeled with an appropriate fluorophore in order to perform interaction studies. Regarding System A, a way to realize protein-protein cross linking needs to be established prior to completing the system via appropriate fluorescent labeling. However, no further screening for protein-protein crosslinking conditions was carried out. This decision was based on economical reasons due to the use of the expensive and precious resource CD63. Consequently, the proteins used in the model system were changed to actin and gelsolin. The use of actin in one part of the system and gelsolin in another, brings along the advantage of a naturally occurring protein-protein interaction.

Furthermore, a model system to serve as an amplification-free method for detection of human cancer DNA was successfully designed and synthesized. An integral part of the system allows size exclusion of mutant DNA bound to an eight-arm-PEG-capture probe. Subsequent detection can be performed via formation of a fluorophore-peptide gel. After the peptide screening and the synthesis of the model system was finished, further investigations were performed and the establishment of a rapid and inexpensive method for human DNA detection with a promising method for future perspective for point-of-care applications was achieved.¹⁷⁷

Besides that, it was possible to isolate and characterize both linear target peptides mP6 and mP7 and the cyclic peptide mcP10. All three products were purified and are ready to be attached to LNPs to test their capability for enhancing the efficiency of BBB crossing. Modified peptides were received with sufficient overall yields (6-9 %).¹⁷⁵ After the initial attempt of orthogonal CBZ deprotection has not been successful, the orthogonal side chain protecting group was changed to Alloc. Ultimately, it was possible to show that the synthetic strategy

selected for the two end-to-end cyclic target peptides mcP8 and mcP9 is capable of making the cyclic target peptides accessible. The successful performance of orthogonal Alloc deprotection showed that the primary amine of lysine could be made selectively accessible to perform coupling of the lipid anchor. Finally, it was demonstrated that the synthetic strategy followed for the lipid anchor installation at the cyclic peptides is successful. Overall, it was possible to demonstrate that specific conjugation of rationally designed peptides, oligonucleotides and their conjugated products is a convenient and promising approach for developing potent diagnostic probes and therapeutics.

4 Experimental part

4.1 General

Reagents and solvents were obtained from Sigma-Aldrich, Merck, IDT and Lumiprobe LLC GlenResearch. Unmodified peptides (P1-P5) were purchased from Caslo Lab, Denmark. Azido-modified peptide reagents were provided by Prof. Knud Jensen, University of Copenhagen, Denmark. Cy3.5 azide was provided by Lumiprobe GmbH; AC was synthesized in house. AlexaFluor 547 was purchased from ThermoFisher Scientific. CuAAC and STP reagents were provided by Lumiprobe GmbH. 8× PEG azide was purchased from Creative PEG works, cat. no. PSB-881; MW 10 kDa.

TLC analysis was performed utilizing Merck Silica gel 60 F254 precoated plates and afterwards visualized by UV irradiation, development in 5% H₂SO₄ in methanol (v/v) or KMnO₄ solution charred with a heat gun. NMR spectrometry was performed on a Bruker AVANCE 400 MHz system 5mm CryoProbe Prodigy, utilizing DMSO-*d*₆ as solvent and internal reference. Manual normal phase chromatography was performed using Merck Silica gel (40-63 μm) with an appropriate solvent system. SDS-PAGE analysis was performed using 1× Tris-Glycine-SDS (25 mM Tris, 192 mM Glycine, 0.1% SDS (sodium-dodecyl-sulfate), pH 8.3) and GelRed as a staining solution for visualization. LC-MS analysis was performed using a Waters AQUITY UPLC equipped with an electron spray (ESI) as ionization source. HPLC analysis was performed on a Dionex UltiMate 3000 system equipped with a Thermo Scientific, Hypersil GOLD C18 column (5 μm, 175 Å, 150 x 4.6 mm) for reverse phase and with Thermo Scientific, DNAPac Pa-100 column (250 x 4 mm) for ion exchange analysis. Signal detection was performed by an UltiMate 3000 VWD, measuring the absorbance of UV-light at 214 nm and 260 nm. For each HPLC set-up (reverse phase and ion exchange) a separate solvent system was used to perform gradient elution. MALDI-TOF mass spectrometry analysis was performed using a Bruker AutoFlex 3000 instrument from Bruker using a matrix of 2-(4-hydroxyphenylazo)benzoic acid or 3-Hydroxypicolinic acid with di-ammoniumhydrogen citrate in MQ-water.

4.1.1 General procedure of oligonucleotide Synthesis (GP1)

4.1.1.1 Automated synthesis and Hand coupling procedure

Oligonucleotides with a 3'-alkyne modification were synthesized on an automated DNA synthesizer PerSpective Bio-systems Expedite 8909 using a standard protocol in 1.0 μ M scale. Modification was achieved by the use of a 3'-alkyne-modifier CPG. If LNA monomers were incorporated, a hand-coupling procedure was carried out. Hand-coupling was performed, by dissolving LNA phosphoramidite in DNA grade acetonitrile and coupling for 18 min with the use of 1H-tetrazole as an activator at room temperature.

4.1.1.2 Cleavage, washing and solvent removal

To cleave the synthesized sequence from the solid support, the column was dried and put into a PCR-vial together with filters and incubated with 1 mL methylamine (33% in ethanol) at 65°C for 2 hours. Next, the mixture was allowed to cool to rt and placed 30 min in a fridge. Then the mixture was filtered off and the filtrate was collected in a 2 mL Eppendorf Tube. The solid support and filters were washed with 1 mL of 50:50 (v:v) 96% ethanol and MQ-water, the wash was combined with the initial filtrate and the solvent was removed *in vacuo*.

4.1.1.3 DMT deprotection

DMT deprotection was achieved by adding 100 μ L 80% acetic acid at room temperature. After 30 min 200 μ L MQ water, 15 μ L 5 M NaClO₄ and 1.5 mL cold acetone were added to the mixture to precipitate the deprotected DNA/LNA oligonucleotide sequence. Then the mixture was kept for 48 h at -78 °C. The suspension was centrifuged for 2 min and the supernatant solution was removed via decantation. Then 1.5 mL cold acetone were added to the pellet and the resulting suspension was kept for additional 24 h at -78 °C. Again, the suspension was centrifuged and the supernatant solution was removed via decantation. Afterwards the remaining solvent in the pellet was removed *in vacuo* and HPLC and MALDI-TOF mass spectrometry was applied.

4.1.2 General procedure of peptide synthesis

4.1.2.1 General procedure of SPPS on 2-chlorotrityl resin (GP2)

4.1.2.1.1 Coupling of the first amino acid

The couplings of the first amino acid were performed in standard SPE filtration columns. Esterification of the 2-chlorotrityl linker with Fmoc amino acids was carried out with preactivation (5 min) of Fmoc amino acids (4 equiv.) using N,N-diisopropylethylamine (DIPEA) (6 equiv.) in DCM. The pre-activated reagents were added to the resin swollen in DCM and the coupling reaction time was 2 h. Manual stirring was applied approximately every 15 min. The coupling of the first amino acid was carried out twice to ensure coupling to the linker. Three times washing of the resin with each solvent in the given order DMF, DCM and DMF, was applied after every reaction step.

4.1.2.1.2 Elongations of the peptide sequence

Prolongation of peptide sequence was performed in standard SPE filtration columns. All peptide couplings on 2-chlorotrityl resin were carried out by preactivation (5 min) of Fmoc amino acid (4 equiv.) with 1-[bis(dimethylamino)methylene]-1H-1,2,3-triazolo[4,5-b]pyridinium 3-oxid hexafluorophosphate (HATU) (4 equiv.) and N,N-diisopropylethylamine (DIPEA) (6 equiv.) in DMF. The preactivated reagents were added to the resin swollen in DMF and coupling reaction time was 2 h. Manual stirring was applied approximately every 15 min. Fmoc cleavage to prepare the resin for the next coupling step was achieved by using 20% piperidine in DMF (1 x 2 min and 1 x 18 min). Three times washing of the resin with each solvent in the given order DMF, DCM and DMF, was applied after every reaction step.

4.1.2.1.3 Cleavage of the peptide from the resin

Cleavage of the synthesized amino acid sequence from the 2-chlorotrityl linker was performed using either hexafluoroisopropanol (HFIP) (20% in DCM, 3 x 20 min), to maintain sidechain

protection groups, or TFA cleavage mixture (TFA:phenol:H₂O:TIPS = 88:5:5:2, 3 x 60 min), to archive global deprotection. After the cleavage mixture was applied, extraction of remaining product in the resin with DCM (2 x 10 min) was performed. Finally, all DCM extracts received were combined with all TFA cleavage mixtures received and the resulting mixture was reduced under nitrogen flow. The solid product received was redissolved in DCM and reduced under nitrogen flow. Then the cycle of redissolving and reducing was applied for additional two times, followed by lyophilization to receive the crude peptide products.

4.1.2.1.4 Global deprotection in solution

Global deprotection in solution was performed using TFA cleavage mixture (TFA:phenol:H₂O:TIPS = 88:5:5:2). TFA cleavage reaction mixture was applied for 90 min to the protected peptide and after that period the reaction mixture was reduced under nitrogen flow. The solid product received was redissolved in DCM and reduced under nitrogen flow. This cycle of redissolving and reducing was applied for additional two times, followed by lyophilization to receive crude peptide product.

4.1.2.2 General procedure of SPPS on Rink resin (GP3)

4.1.2.2.1 Coupling of the first amino acid

Reactions were performed in standard SPE filtration columns. Prior first amino acid coupling, Fmoc group removal from the Rink linker was achieved by applying 20% piperidine in DMF (2 x 30 min). Preactivation of the Fmoc amino acid (4 equiv.) before first coupling was carried out with 1-[bis(dimethylamino)methylene]-1H-1,2,3-triazolo[4,5-b]pyridinium 3-oxid hexafluoro-phosphate (HATU) (4 equiv.) and N,N-diisopropylethylamine (DIPEA) (6 equiv.) in DMF. Then the reactivated mixture was added to the resin swollen in DMF and the coupling reaction time was 2 h. Manual stirring was applied approximately every 15 min. The coupling of the first amino acid was carried out twice to ensure coupling to the linker. Three times washing of the resin with each solvent in the given order DMF, DCM and DMF, was applied after every reaction step.

4.1.2.2.2 Elongations of the peptide sequence

All elongation steps were performed in standard SPE filtration columns. Preactivation of the Fmoc amino acid (4 equiv.) was achieved with 1-[bis(dimethylamino)methylene]-1H-1,2,3-triazolo[4,5-b]pyridinium 3-oxid hexafluorophosphate (HATU) (4 equiv.) and N,N-diisopropylethylamine (DIPEA) (6 equiv.) in DMF. The activated reagent mix was added to the resin swollen in DMF and the coupling reaction time was 2 h. Manual stirring was applied approximately every 15 min. Fmoc cleavage to prepare the resin for the next coupling step was achieved by using 20% piperidine in DMF (1 x 2 min and 1 x 18 min). Three times washing of the resin with each solvent in the given order DMF, DCM and DMF, was applied after every reaction step.

4.1.2.2.3 Cleavage of the peptide from the resin

Cleavage of the peptide sequence from the Rink resin was achieved by using TFA cleavage mixture (TFA:phenol:H₂O:TIPS = 88:5:5:2, 3 x 60 min) to obtain deprotected peptides. After the cleavage mixture was applied, extraction of the remaining resin with DCM (2 x 10 min) was performed. Finally, all DCM extracts received were combined with all TFA cleavage mixtures received and the resulting mixture was reduced under nitrogen flow. The solid product received was redissolved in DCM and reduced under nitrogen flow. Then the cycle of redissolving and reducing was applied for additional two times, followed by lyophilization to receive the crude peptide products.

4.2 Cell sorting

4.2.1 Oligonucleotide synthesis

4.2.1.1 ON1 and ON2

The oligonucleotide precursor ON1 (5'-5hexynyl/AAGACCTTCT/3AmMO-3') and ON2 (5'-hexynyl/iSP18/TCCACGTCTTC/3AmMO-3') were purchased at Integrated DNA Technologies (IDT) and were used without further purification for the following reaction steps.

4.2.1.2 Synthesis of oligonucleotide ON3

The DNA oligonucleotide ON3 with a 3'-alkyne modification was synthesized on an automated DNA synthesizer PerSpective Bio-systems Expedite 8909 following a standard protocol on 1.0 μ M scale. Synthesis was performed in the DMT-ON mode and modification was achieved by the use of a 3'-alkyne-modifier CPG. For cleaving ON3 from the solid support, an ammonia solution (28-30%) at 55 °C was applied overnight. After cleavage from the solid support DMT-deprotection was performed according to the general procedure (GP1). To characterize ON3, IE-HPLC and MALDI-TOF mass spectrometry were used. No further purification was conducted, the product was used directly in the following synthetic step.

MALDI-TOF-MS: Calculated [M+H]⁺: 11159

Found [M+2H]²⁺: 5579

IE-HPLC: RT [min]: 19.12

Purity [%]: 89

Appearance: Colorless solid

4.2.1.3 SC1

The alkyne amino modified oligonucleotide ON2 (20 μ L, 20 nm) were mixed together with bicarbonate buffer (5 μ L, 1 M), maleimide-PEG2-succinimidyl ester (8.5 μ L, 200 nmol) and MQ-water (16.5 μ L) in a 1.5 mL Eppendorf Tube. The reaction mixture with a total volume of 50 μ L was kept for 12 h in darkness at room temperature. Then the reaction mixture was filtered using Illustra NAP-5 columns and the solvent was evaporated *in vacuo*. The product SC1 was identified via MALDI- TOF mass spectrometry.

MALDI-TOF-MS: Calculated [M+H]⁺: 3683

Found [M+H]⁺: 3683

Appearance: Colorless solid

4.2.1.4 SC2

In a 1.5 mL Eppendorf Tube BSA (3 μ L, 1 nmol), 10 \times PBS (7 μ L), DTT (3.85 μ L, 100 nmol), DMSO (15 μ L) and MQ-water (1.15 μ L) were mixed together and degassed by bubbling argon through the reaction mixture. To this reaction mixture the maleimide STP labeled oligonucleotide SC1 (20 μ L, 20 nmol, in MQ-water) and additional degassing step utilizing argon. Then the reaction mixture with a total volume of 50 μ L was kept for 12 h in darkness at room temperature and occasionally gentle shaking was applied. Next, the reaction mixture was filtered using Illustra NAP-5 columns and the solvent was evaporated *in vacuo*. The product SC2 was analyzed by SDS-PAGE.

4.2.2 Bioconjugations

The calculation of the oligonucleotide concentration used for labeling, coupling and “click” reactions was based on the measured absorbance at 260 nm.

4.2.2.1 SC4

In a 1 mL Eppendorf Tube BSA (91 μL , 30 nmol), 10x bicarbonate buffer (50 μL , 1 M), DMSO (38 μL), MQ-water (299 μL) and STP-azide (sodium 4-(5-aminopentanoyl)-2,3,5,6-tetrafluorobenzenesulfonate) (12 μL , 178 nmol) were mixed together and occasionally gentle shaking was applied. The reaction mixture with a total volume of 490 μL was kept for 12 h in darkness at room temperature. Then the reaction mixture was filtered using Illustra NAP-5 columns and the collected filtrate was evaporated *in vacuo*. The received product SC4 was used for the next reaction step without any further purification and characterization.

4.2.2.2 SC5

SC4 (263 μL , 7.6 nmol), 4 \times PBS buffer (100 μL), AGH (amminoguanidinumhydrochloride) (6 μL , 10 mg/mL) oligo ON3 (11 μL , 18 nmol), oligo ON2 (19 μL , 18 nmol) and MQ-water (35.25 μL) was mixed together in a 2 mL Eppendorf Tube. The reaction mixture was degassed with argon. Then CuTHPTA (11.25 μL , 10 nM) and ascorbic acid (4.5 μL , 50 nM) were added to the mixture, followed by an additional degassing step utilizing argon. Next, the reaction mixture with a total volume of 450 μL was kept for 12 h in darkness at room temperature. Then the reaction mixture was filtered using Illustra NAP-5 columns and the collected filtrate was evaporated *in vacuo*. The product SC5 was analyzed by SDS-PAGE.

4.3 Mutation detection

4.3.1 Oligonucleotide precursors

4.3.1.1 ON4

The DNA oligonucleotide ON4 with a 3'-alkyne modification was synthesized on an automated DNA synthesizer PerSpective Bio-systems Expedite 8909 using a standard protocol in 1.0 μM scale. Synthesis was performed in the DMT-OFF mode and modification was achieved by the use of a 3'-alkyne-modifier CPG. For incorporation of LNA monomers, a hand-coupling procedure was carried out. Hand-coupling was performed, by dissolving LNA phosphoramidite in DNA grade acetonitrile and coupling for 18 min with the use of 1H-tetrazole as an activator. For cleaving ON4 from the solid support, an ammonia solution (28-30%) at 55 °C was applied overnight. To characterize of the received product ON4, IE-HPLC and MALDI-TOF mass spectrometry were used. The received reaction product was used for the following synthetic step without purification.

MALDI-TOF-MS: Calculated $[M+H]^+$: 5012

Found: 5011

IE-HPLC: RT [min]: 16.86

Purity [%]: 89

Appearance: Colorless solid

4.3.1.2 ON5'

The oligonucleotide precursor ON5 was purchased from Integrated DNA Technologies (IDT) and was used without any further purifications for the following synthetic step.

STP-alkyne labeling – ON5'

To make the 5'-AmMC12 modified ON5 oligonucleotide ready for CuAAC “click” reaction, STP-alkyne labeling was applied. To perform this labeling procedure the protocol “NHS ester labeling of amino biomolecules” from Lumiprobe was followed.¹⁶³ The ON5 oligonucleotide (70 μ L, 7 nmol), sodium bicarbonate solution (10 μ L, 1 M), MQ-water (15 μ L) and STP alkyne (5 μ L, 100 mg/mL) were mixed together in a 2 mL Eppendorf Tube. Afterwards the resulting reaction solution was vortexed and spun down before being kept for 12 h in darkness at rt with occasionally gentle shaking. Then the reaction mixture was filtered using Illustra NAP-5 columns. The resulting solution after gel filtration was evaporated *in vacuo*. The received reaction product ON5' was analyzed by IE-HPLC and MALDI-TOF mass spectrometry.

MALDI-TOF-MS:	Calculated [M+H] ⁺ : 7787
	Found: 7806 [deviation to calculated mass explained in 2.3.3.2.3]
IE-HPLC:	RT [min]: 5.34
	Purity [%]: 99
Appearance:	Colorless solid

4.3.2 Bioconjugations

The calculation of the oligonucleotide concentration used for the “click” reaction was based on the measured absorbance at 260 nm.

4.3.2.1 PEG

The alkyne labeled precursor ON5' (34.3 μL , 5.25 nmol, dissolved in MQ-water) was mixed with triethylammonium acetate buffer (TEAA) (7 μL , 1 M), formamide (20.55 μL), 8 \times PEG azide (4.2 μL , 0.21 nmol, dissolved in MQ-water) Cu (II) THBTA (5 μL , 10 mM in MQ-water:DMSO = 1:1) and ascorbic acid solution (2 μL , 50 mM in MQ-water), resulting in a final volume of 72 μL . The reaction was performed in a 5 mL round bottom flask using magnetic stirring. After mixing the starting materials together, the reaction mixture was degassed with argon and kept at room temperature overnight while stirring was applied. Then 428 μL MQ-water were added to the mixture and it was run through an Illustra NAP-5 column. The solvent from the received solution was evaporated *in vacuo* and the obtained product was analyzed using RP-HPLC and by denaturing PAGE.

MALDI-TOF-MS: Calculated $[\text{M}+\text{H}]^+$: 56837

Found: nd

IE-HPLC: RT [min]: 0.99

Purity [%]: 92

Appearance: Colorless solid

4.3.2.2 POC

The reaction was performed in a 1.5 mL Eppendorf Tube. For CuAAC “click” reaction, oligonucleotide ON4 (20 μ L, 20 nmol, dissolved in MQ-water) was mixed with triethylammonium acetate buffer (TEAA) (2 μ L, 1 M), aminoguanidine hydrochloride (0.4 μ L, 50 mM), azido-modified peptide reagent P1 (19.4 μ L, 150 nmol), Cu (II) THPTA (5 μ L, 10 mM in MQ-water:DMSO = 1:1), ascorbic acid solution (2 μ L, 50 mM in MQ-water) and MQ-water (16.2 μ L) resulting in a final volume of 65 μ L. After mixing the starting materials together the reaction mixture was degassed with argon, the tube was covered with tin foil and afterwards the reaction mixture was kept at 70 °C for 45 min. Next, the reaction mixture was allowed to reach room temperature and kept overnight at room temperature. The work-up was done using Illustra NAP-5 column, followed by the evaporation of the solvent *in vacuo*. The received reaction product and characterized using RP-HPLC and MALDI/TOF.

MALDI-TOF-MS: Calculated [M+H]⁺: 6310

Found [M+Na]⁺: 6332

IE-HPLC: RT [min]: 3.82

Purity [%]: 95

Appearance: Colorless solid

4.3.2.3 Control probe CP

The reaction was performed in a 1.5 mL Eppendorf Tube. For the CuAAC “click” reaction, the oligonucleotide ON4 (20 μ L, 20 nmol, dissolved in MQ-water) was mixed with triethylammonium acetate buffer (TEAA) (2 μ L, 1 M), Cy3.5 azide (5 μ L, 10 mM stock in DMSO), Cu (II) TBTA complex (5 μ L, 10 mM in MQ-water:DMSO = 1:1), ascorbic acid solution (2 μ L, 50 mM in MQ-water) and MQ-water (16.2 μ L). After mixing the starting materials together the reaction mixture was degassed with argon, the tube was covered with tin foil and afterwards the reaction mixture was kept at 70 °C for 20 min. Afterwards the reaction mixture was allowed to reach room temperature and was kept overnight at room temperature. The work-up was conducted using NAP-5 column, followed by the evaporation of the solvent in vacuo. The received reaction product was characterized using MALDI-TOF and RP-HPLC.

MALDI-TOF-MS: Calculated [M+H]⁺: 5655

Found [M+K]⁺: 5694

IE-HPLC: RT [min]: 7.61

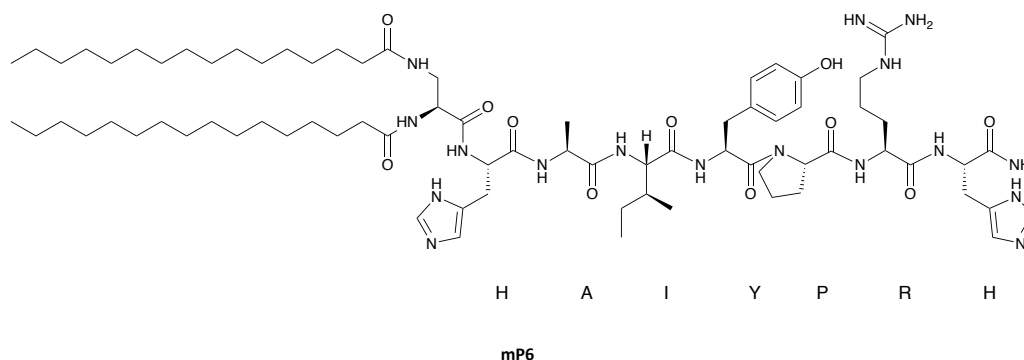
Purity [%]: 83

Appearance: Colorless solid

4.4 Peptide synthesis

4.4.1 Synthesis of linear peptides

4.4.1.1 mP6



Modified peptide mP6 with the sequence (2x palmitic acid)-Dap-His-Ala-Ile-Tyr-Pro-Arg-His-NH₂ was synthesized according to general procedure (GP3) on Rink-resin (133 mg, 0.75 mmol/g) using:

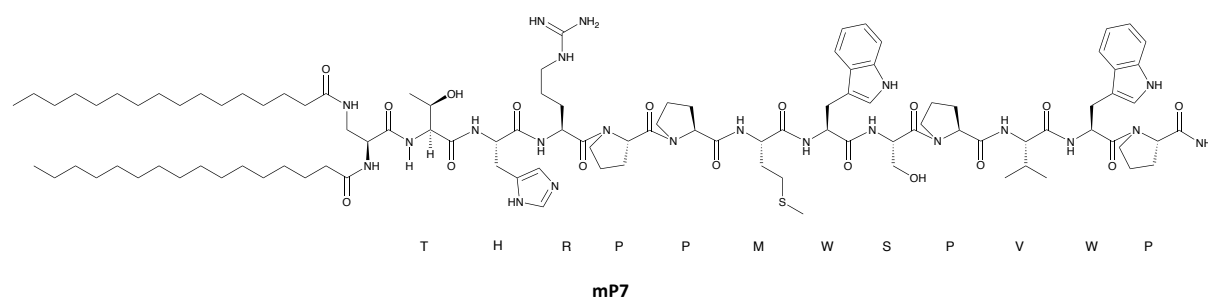
1	Fmoc-His(Trt)	248 mg	0.4 mmol	4 equiv.
2	Fmoc-Agr(Pbf)	260 mg	0.4 mmol	4 equiv.
3	Fmoc-Pro	135 mg	0.4 mmol	4 equiv.
4	Fmoc-Tyr(tBu)	184 mg	0.4 mmol	4 equiv.
5	Fmoc-Ile	141 mg	0.4 mmol	4 equiv.
6	Fmoc-Ala	125 mg	0.4 mmol	4 equiv.
7	Fmoc-His(Trt)	248 mg	0.4 mmol	4 equiv.
8	Fmoc-Dap(Fmoc)-OH	219 mg	0.4 mmol	4 equiv.
9	palmitic acid	205 mg	0.8 mmol	8 equiv.

Cleavage of mP6 was carried out using TFA cleavage mixture. The compound received was purified by manual normal phase column utilizing gradient elution (2-50% MeOH in DCM) and was the desired peptide mP6 (9 mg, 6 μmol, 6%) was isolated.

MALDI-TOF-MS: Calculated [M+H]⁺: 1455.9
 Found [M+H]⁺: 1455.5

Appearance: Colorless solid

4.4.1.2 mP7



Modified peptide mP7 with the sequence H-Thr-His-Arg-Pro-Pro-Met-Trp-Ser-Pro-Val-Trp-Pro-NH₂ was synthesized according to general procedure (GP3) on Rink-resin (133 mg, 0.75 mmol/g) using:

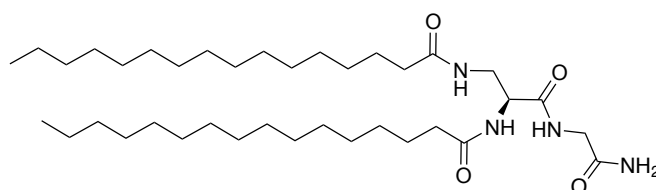
1	Fmoc-Pro	135 mg	0.4 mmol	4 equiv.
2	Fmoc-Trp(Boc)	211 mg	0.4 mmol	4 equiv.
3	Fmoc-Val	136 mg	0.4 mmol	4 equiv.
4	Fmoc-Pro	135 mg	0.4 mmol	4 equiv.
5	Fmoc-Ser(tBu)	153 mg	0.4 mmol	4 equiv.
6	Fmoc-Trp(Boc)	211 mg	0.4 mmol	4 equiv.
7	Fmoc-Met	149 mg	0.4 mmol	4 equiv.
8	Fmoc-Pro	135 mg	0.4 mmol	4 equiv.
9	Fmoc-Pro	135 mg	0.4 mmol	4 equiv.
10	Fmoc-Agr(Pbf)	260 mg	0.4 mmol	4 equiv.
11	Fmoc-His(Trt)	248 mg	0.4 mmol	4 equiv.
12	Fmoc-Thr(tBU)	159 mg	0.4 mmol	4 equiv.
13	Fmoc-Dap(Fmoc)-OH	219 mg	0.4 mmol	4 equiv.
14	palmitic acid	205 mg	0.8 mmol	8 equiv.

Cleavage of mP7 was carried out using TFA cleavage mixture. The compound received was dissolved in a mixture of 85% ACN in MQ-water with 0.1% FA and purified via reverse phase chromatography and the desired peptide mP7 (14 mg, 7 μmol, 7%) was isolated.

MALDI-TOF-MS: Calculated [M+H]⁺: 2053.2
Found [M+H]⁺: 2053.7

Appearance: Colorless solid

4.4.1.3 Lipid anchor LA



LA

The lipid anchor LA with the sequence (2x palmitic acid)-DAP-Gly-OH was synthesized according to general procedure (GP2) on 2-chlorotrytyl resin (300 mg, 1.0 mmol/g) using:

1	Fmoc-Gly	357 mg	1.2 mmol	4 equiv.
2	Fmoc-Dap(Fmoc)-OH	657 mg	1.2 mmol	4 equiv.
3	palmitic acid	615 mg	2.4 mmol	8 equiv.

Cleavage of the lipid anchor LA from the resin was carried out via standard cleavage procedure using TFA cleavage mixture to receive the crude reaction product LA (62 mg, 97 μ mol, 32% (crude)) as a brownish solid.

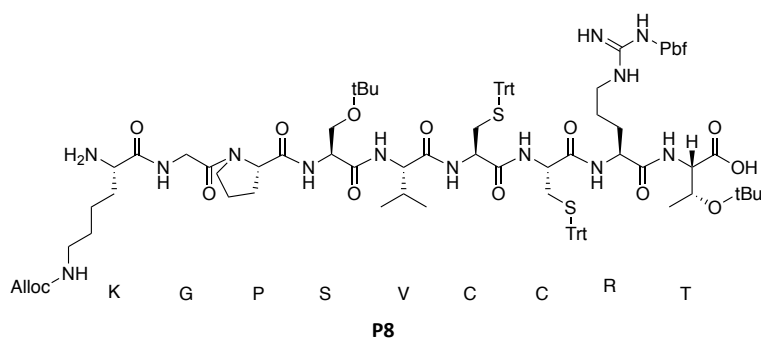
MALDI-TOF-MS: Calculated $[M+Na]^+$: 660.6

Found $[M+Na]^+$: 660.7

Appearance: Brownish solid

4.4.2 Synthesis of cyclic peptides

4.4.2.1 P8



The synthesis of peptide P8 with the sequence H-Lys-Gly-Pro-Ser-Val-Cys-Cys-Arg-Thr-OH was carried out according to general procedure (GP2) on 2-chlorotrytyl resin (300 mg, 1.0 mmol/g) using:

1	Fmoc-Thr(tBu)	477 mg	1.2 mmol	4 equiv.
2	Fmoc-Agr(Pbf)	780 mg	1.2 mmol	4 equiv.
3	Fmoc-Cys(Trt)	702 mg	1.2 mmol	4 equiv.
4	Fmoc-Cys(Trt)	702 mg	1.2 mmol	4 equiv.
5	Fmoc-Val	408 mg	1.2 mmol	4 equiv.
6	Fmoc-Ser(tBu)	459 mg	1.2 mmol	4 equiv.
7	Fmoc-Pro	405 mg	1.2 mmol	4 equiv.
8	Fmoc-Gly	357 mg	1.2 mmol	4 equiv.
9	Fmoc-Lys(Alloc)	543 mg	1.2 mmol	4 equiv.

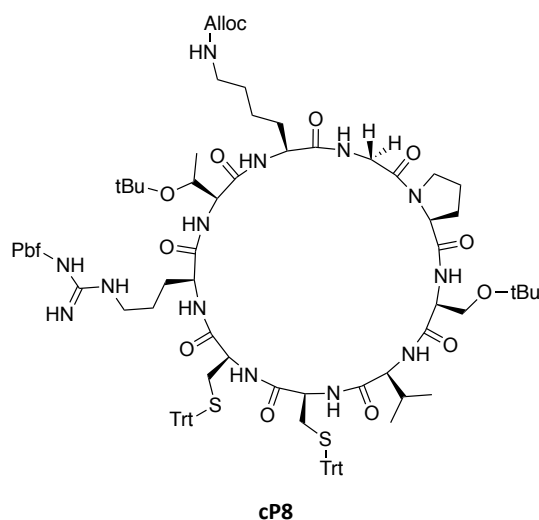
The N-terminal Fmoc group was removed followed by cleavage of the sequence from the 2-chlorotrytyl linker using hexafluoroisopropanol (HFIP) (20% in DCM, 3 x 20 min). The received crude solid was dissolved in 75% ACN in MQ-water with 0.1% FA and purification via reverse phase chromatography was applied. The received reaction product was lyophilized and the desired product P8 was received as a colorless solid (93 mg, 49 μ mol, 24%). For analytical purpose a small number of beads were treated with TFA cleavage mixture to receive the globally deprotected (except Lys(Alloc)) sequence and the identity of the received sequence was analyzed via MALDI-TOF mass spectrometry.

MALDI-TOF-MS: Calculated $[M+H]^+$: 1034.5

Found $[M+H]^+$: 1034.6

Appearance: Colorless solid

4.4.2.2 cP8



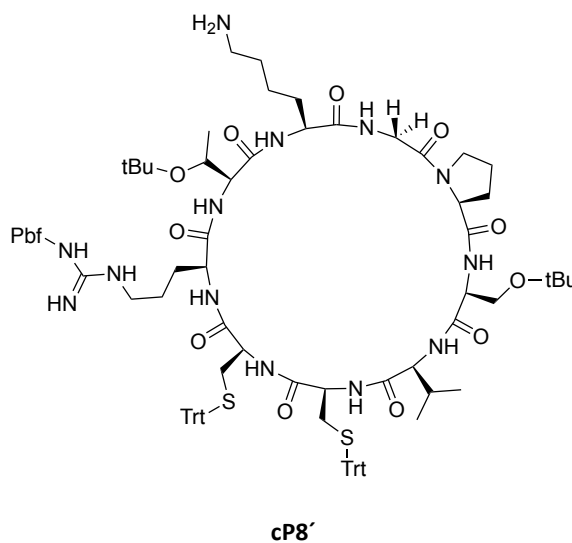
P8 (93 mg, 49 μmol) was dissolved in DMF (3 mL) and added dropwise via a syringe to a mixture of 1-[bis(dimethylamino)methylene]-1H-1,2,3-triazolo[4,5-b]pyridinium 3-oxid hexafluorophosphate (HATU) (149 mg, 392 μmol , 8 equiv.) and diisopropylethylamine (DIPEA) (76 mg, 588 μmol , 12 equiv.) in DMF (5 mL). The reaction was carried out at rt and magnetic stirring was applied. After 40 min the addition of the dissolved P8 was completed and the reaction mixture was stirred for additional 90 min at rt. Then the solvent was evaporated *in vacuo*, the received crude solid was dissolved in a mixture of 80% ACN in MQ-water with 0.1% FA (2 mL) and purified via reverse phase preparative chromatography. The received reaction product was lyophilized and cP8 was received as a colorless solid (38 mg 21 μmol , 42%).

MALDI-TOF-MS: Calculated $[M+K]^+$: 1846.9

Found $[M+K]^+$: 1847.2

Appearance: Colorless solid

4.4.2.3 cP8'



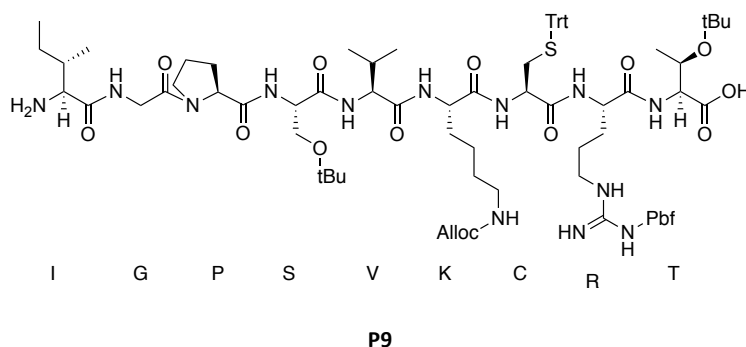
To a mixture of cP8 (38 mg 21 μ mol) in DCM (2 mL) was added tetrakis(triphenylphosphine)palladium(0) (5 mg, 4 μ mol 0.2 equiv.) dissolved in DCM (1 mL) and triisopropylsilane (TIPS) (67 mg, 420 μ mol, 20 equiv.). The resulting reaction mixture was stirred at room temperature for 30 min. Then the solvent was removed *in vacuo* and the crude reaction product was received and dissolved in a mixture of 80% ACN in MQ-water with 0.1% FA and purified via reverse phase preparative chromatography. The received reaction product was lyophilized and cP8' was received as a colorless solid (11 mg, 6 μ mol, 30%).

MALDI-TOF-MS: Calculated [M+H]⁺: 1762.9

Found [M+H]⁺: 1762.8

Appearance: Colorless solid

4.4.2.4 P9



The synthesis of peptide P9 with the sequence H-Ile-Gly-Pro-Ser-Val-Lys-Cys-Arg-Thr-OH was carried out according to general procedure (GP2) on 2-chlorotrytyl resin (300 mg, 1.0 mmol/g) using:

1	Fmoc-Thr(tBu)	477 mg	1.2 mmol	4 equiv.
2	Fmoc-Agr(Pbf)	780 mg	1.2 mmol	4 equiv.
3	Fmoc-Cys(Trt)	702 mg	1.2 mmol	4 equiv.
4	Fmoc-Lys(Alloc)	543 mg	1.2 mmol	4 equiv.
5	Fmoc-Val	408 mg	1.2 mmol	4 equiv.
6	Fmoc-Ser(tBu)	459 mg	1.2 mmol	4 equiv.
7	Fmoc-Pro	405 mg	1.2 mmol	4 equiv.
8	Fmoc-Gly	357 mg	1.2 mmol	4 equiv.
9	Fmoc-Ile	423 mg	1.2 mmol	4 equiv.

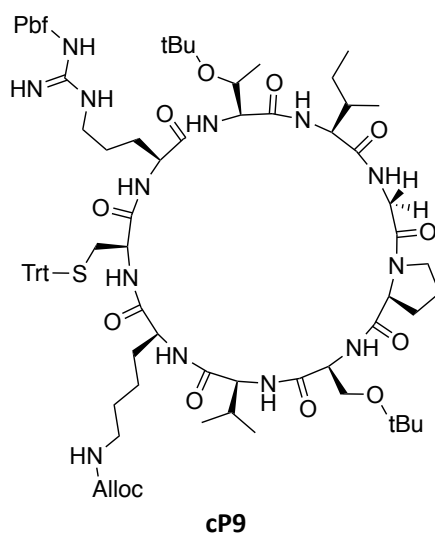
The N-terminal Fmoc protecting group was removed and the sequence was cleavage from the 2-chlorotrytyl linker using hexafluoroisopropanol (HFIP) (20% in DCM, 3 x 20 min). The received crude solid was dissolved in 75% ACN in MQ-water with 0.1% FA and purification via reverse phase chromatography. The received reaction product was lyophilized and the desired product P9 was received as a colorless solid (104 mg, 63 μ mol, 21%). For analytical purpose a small number of beads were treated with TFA cleavage mixture to receive the globally deprotected (except Lys(Alloc)) sequence and the identity of the received sequence was analyzed via MALDI-TOF mass spectrometry.

MALDI-TOF-MS: Calculated $[M+H]^+$: 1044.6

Found $[M+H]^+$: 1044.7

Appearance: Colorless solid

4.4.2.5 cP9



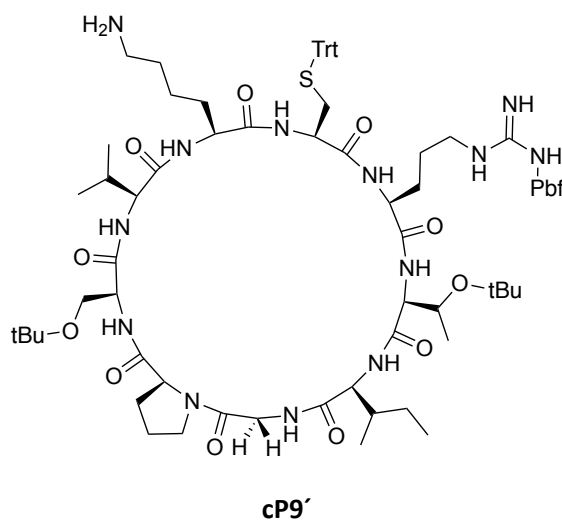
P9 (77 mg, 74 μmol) was dissolved in DMF (3 mL) and added dropwise via syringe to a mixture of 1-[bis(dimethylamino)methylene]-1H-1,2,3-triazolo[4,5-b]pyridinium 3-oxide hexafluorophosphate (HATU) (225 mg, 592 μmol , 8 equiv.) and diisopropylethylamine (DIPEA) (115 mg, 1.2 μmol , 12 equiv.) in DMF (5 mL). The reaction was carried out at rt and magnetic stirring was applied. After 40 min the addition of the dissolved P9 was completed and the reaction mixture was stirred for additional 90 min at rt. Then the solvent was evaporated *in vacuo*, the received crude solid was dissolved in a mixture of 80% ACN in MQ-water with 0.1% FA (2 mL) and purified via reverse phase preparative chromatography. The received reaction product was lyophilized and cP9 was received as a colorless solid (49 mg, 30 μmol , 41%).

MALDI-TOF-MS: Calculated (with one tBu group fallen off) $[\text{M}+\text{K}]^+$: 1614.9

Found (with one tBu group fallen off) $[\text{M}+\text{K}]^+$: 1615.1

Appearance: Colorless solid

4.4.2.6 cP9'



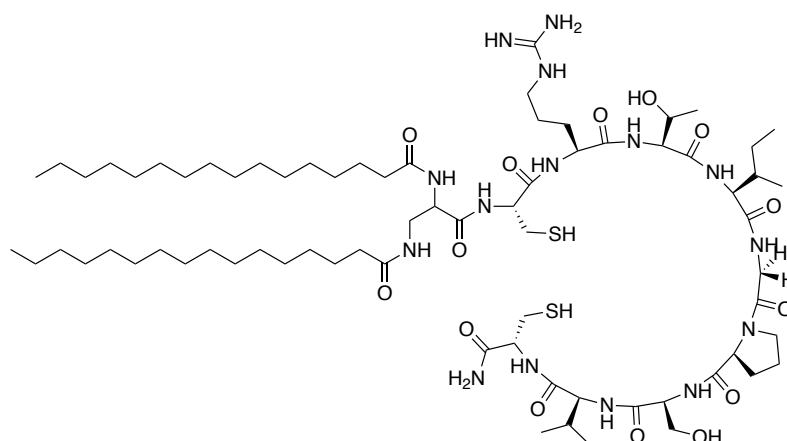
To a mixture of cP9 (49 mg, 30 μ mol) in DCM (2 mL) was added tetrakis(triphenylphosphine)-palladium(0) (7 mg, 6 μ mol, 0.2 equiv.) dissolved in DCM (1 mL) and triisopropylsilane (TIPS) (95 mg, 600 μ mol, 20 equiv.). The resulting reaction mixture was stirred at rt for 30 min. Then the solvent was removed *in vacuo* and the crude reaction product was received and dissolved in a mixture of 80% ACN in MQ-water with 0.1% FA and purified via reverse phase preparative chromatography. The received reaction product was lyophilized and cP9' was received as a colorless solid (15 mg, 9 μ mol, 33%).

MALDI-TOF-MS: Calculated (one tBu group fallen off) $[M+K]^+$: 1530.8

Found (one tBu group fallen off) $[M+K]^+$: 1531.1

Appearance: Colorless solid

4.4.2.7 mP10



mP10

The synthesis of peptide P10 with the sequence H-Cys-Arg-Thr-Ile-Gly-Pro-Ser-Val-Cys-OH was carried out according to general procedure (GP3) on Rink resin (133 mg, 0.75 mmol/g) using:

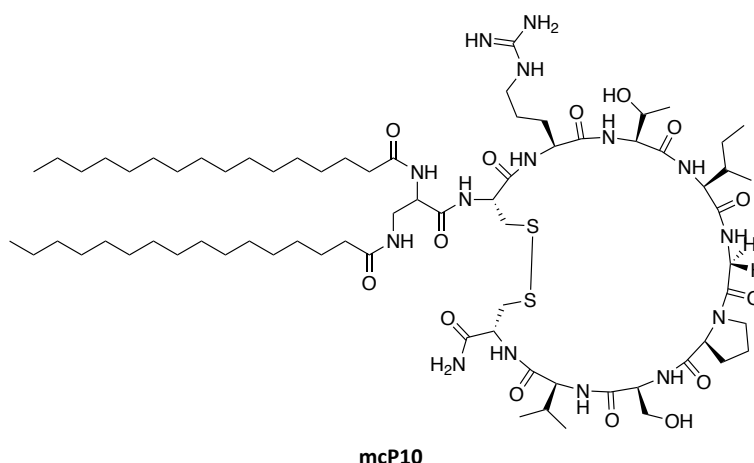
1	Fmoc-Cys(Trt)	234 mg	0.4 mmol	4 equiv.
2	Fmoc-Val	136 mg	0.4 mmol	4 equiv.
3	Fmoc-Ser(tBu)	153 mg	0.4 mmol	4 equiv.
4	Fmoc-Pro	135 mg	0.4 mmol	4 equiv.
5	Fmoc-Gly	119 mg	0.4 mmol	4 equiv.
6	Fmoc-Ile	141 mg	0.4 mmol	4 equiv.
7	Fmoc-Thr(tBu)	159 mg	0.4 mmol	4 equiv.
8	Fmoc-Agr(Pbf)	260 mg	0.4 mmol	4 equiv.
9	Fmoc-Cys(Trt)	234 mg	0.4 mmol	4 equiv.
10	Fmoc-Dap(Fmoc)-OH	110 mg	0.4 mmol	4 equiv.
11	palmitic acid	205 mg	0.8 mmol	8 equiv.

The final Fmoc group was removed followed by cleavage from the 2-chlorotrityl linker using hexafluoroisopropanol (HFIP) (20% in DCM, 3 x 20 min). The crude modified peptide mP10 was received as a colorless solid (39 mg, 26.1 μ mol, 27% (crude)).

MALDI-TOF-MS: Calculated $[M+H]^+$: 1497.0
Found $[M+H]^+$: 1497.3

Appearance: Colorless solid

4.4.2.8 mcP10



Crude modified peptide mP10 (6 mg, 4.0 μmol) was mixed together with DMSO (1 mL) in a 5 mL glass vial and the resulting reaction mixture was stirred for 96 h at room temperature. Then the solvent was reduced under nitrogen flow, received crude reaction product was purified via manual normal phase chromatography and then lyophilized to receive the desired product mcP10 as a colorless solid (1.9 mg, 1,4 μmol , 33%).

MALDI-TOF-MS: Calculated $[\text{M}+\text{H}]^+$: 1495.0

Found $[\text{M}+\text{H}]^+$: 1495.1

Appearance: Colorless solid

5 Appendix

5.1 Analytical data

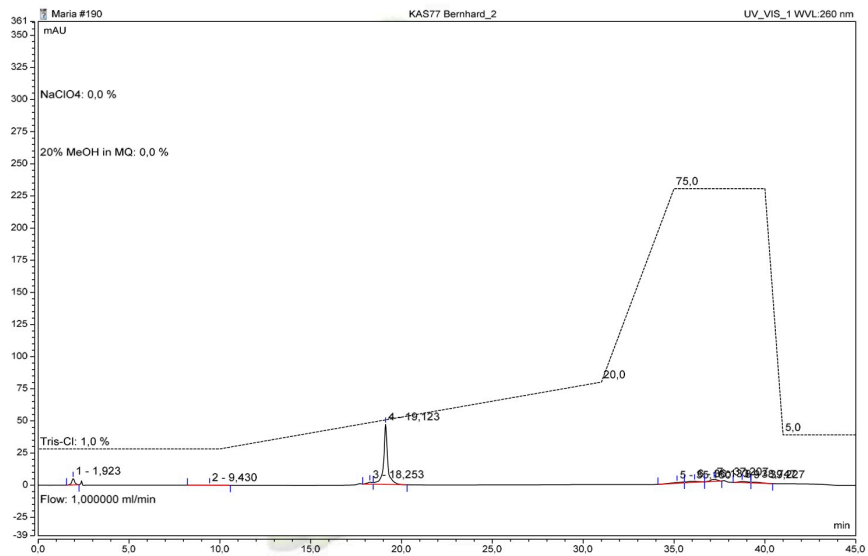


Figure 29: IE-HPLC chromatogram from ON3.

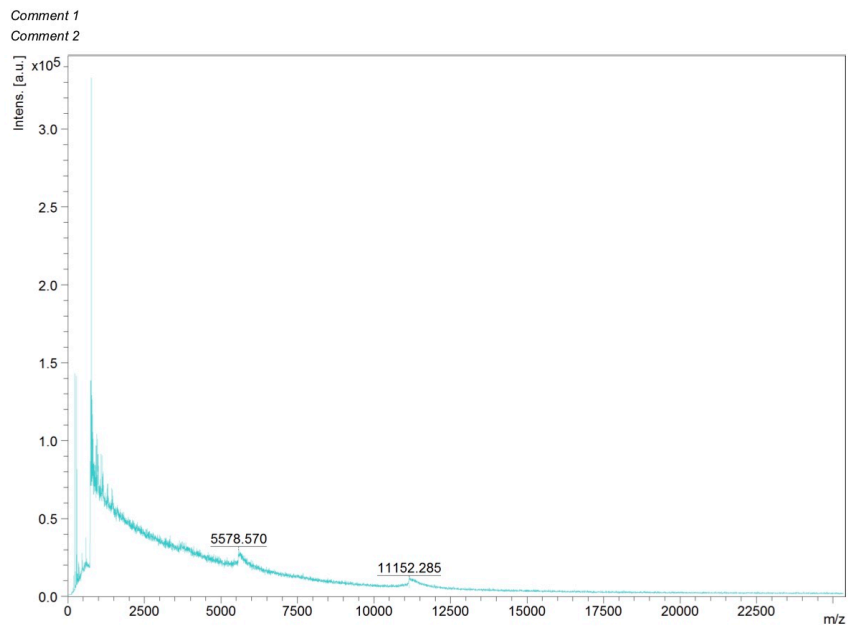


Figure 30: MALDI-TOF from ON3.

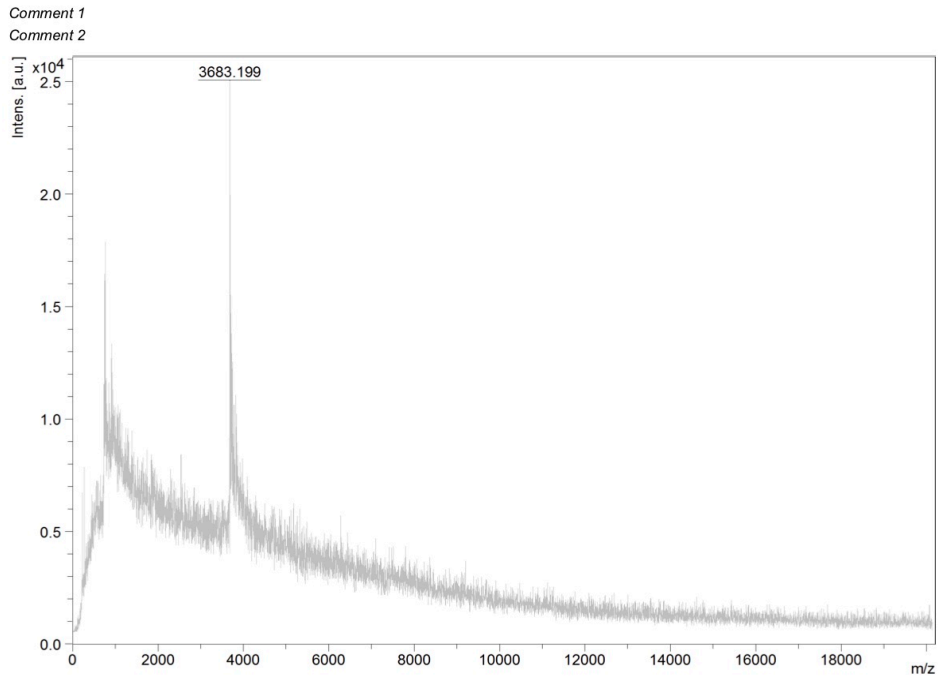


Figure 31: MALDI-TOF spectra of SC1.

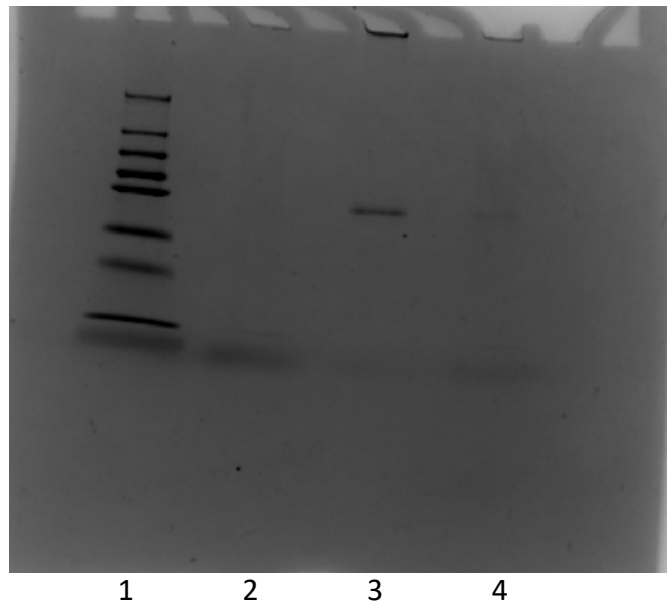


Figure 32: SDS-PAGE of ladder (lane 1), CD63 (lane 2), SC2 (lane 3) and SC3e (lane 4); stained with GelRed.

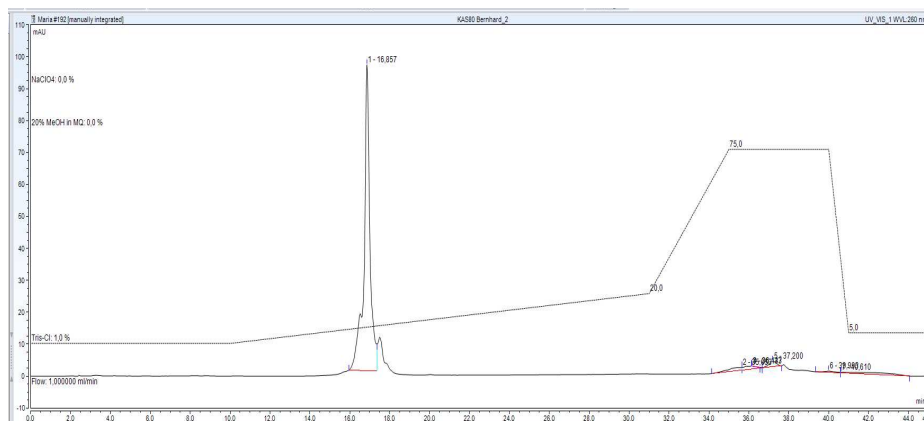


Figure 33: IE-HPLC chromatogram from ON4.

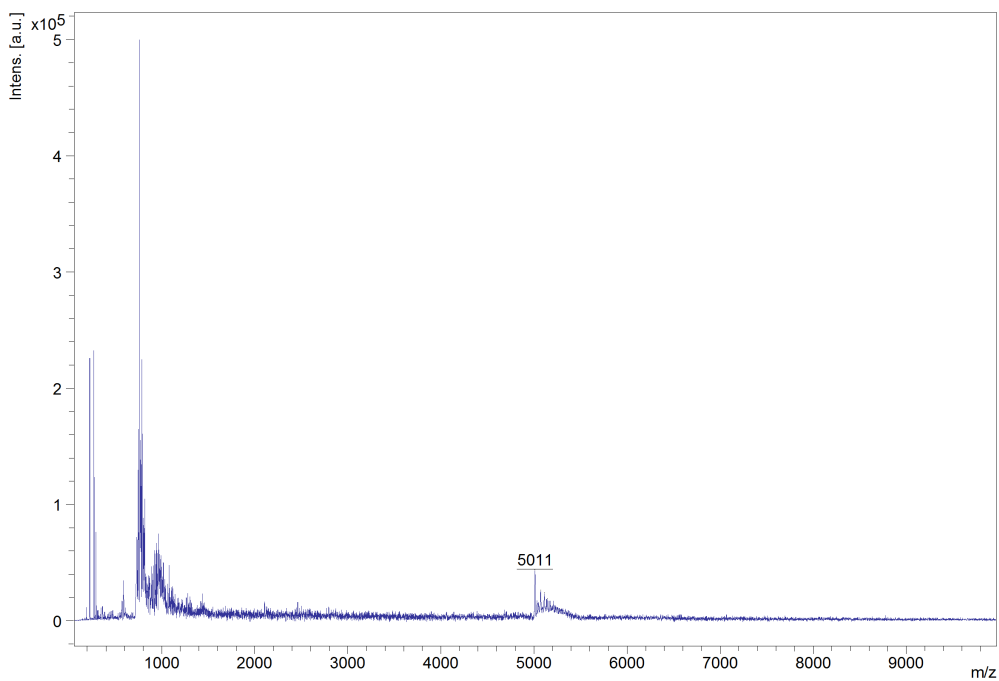


Figure 34: MALDI-TOF from ON4.

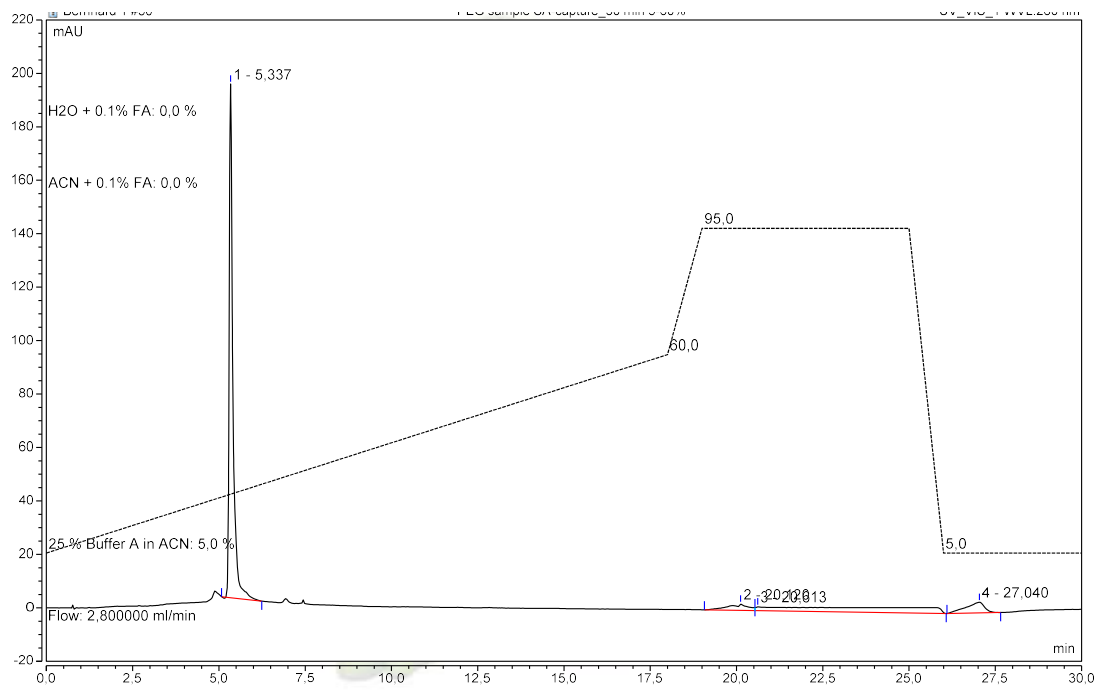


Figure 35: RP-HPLC chromatogram of ON5'.

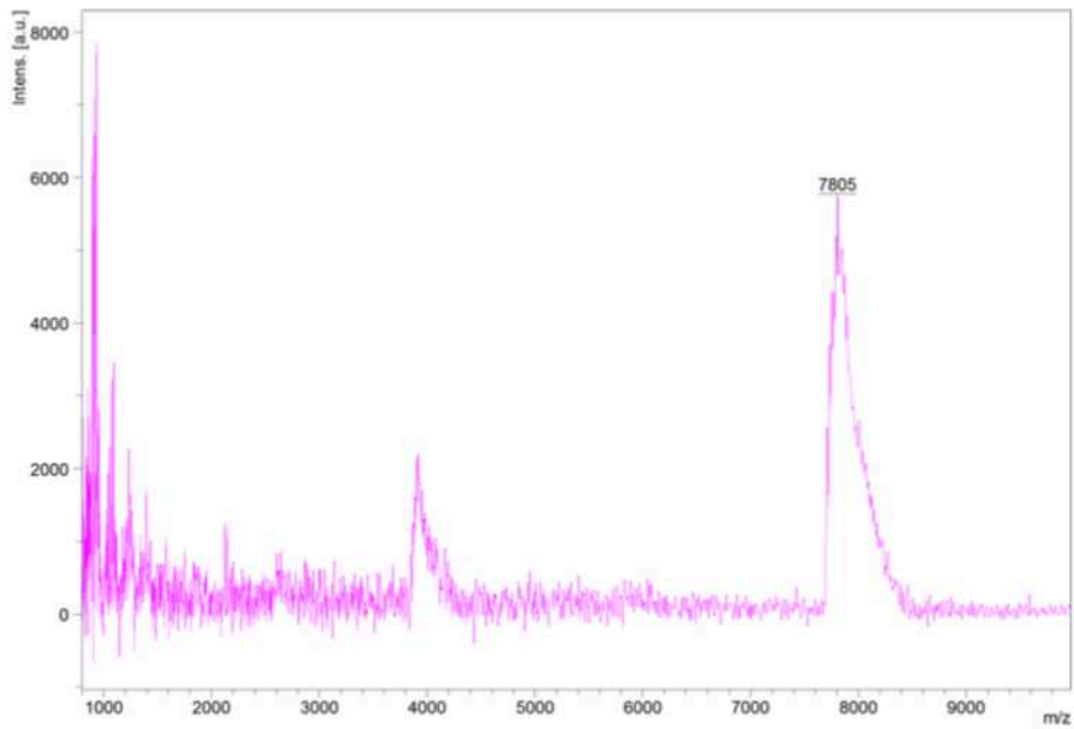


Figure 36: MALDI-TOF mass spectra of ON5'.

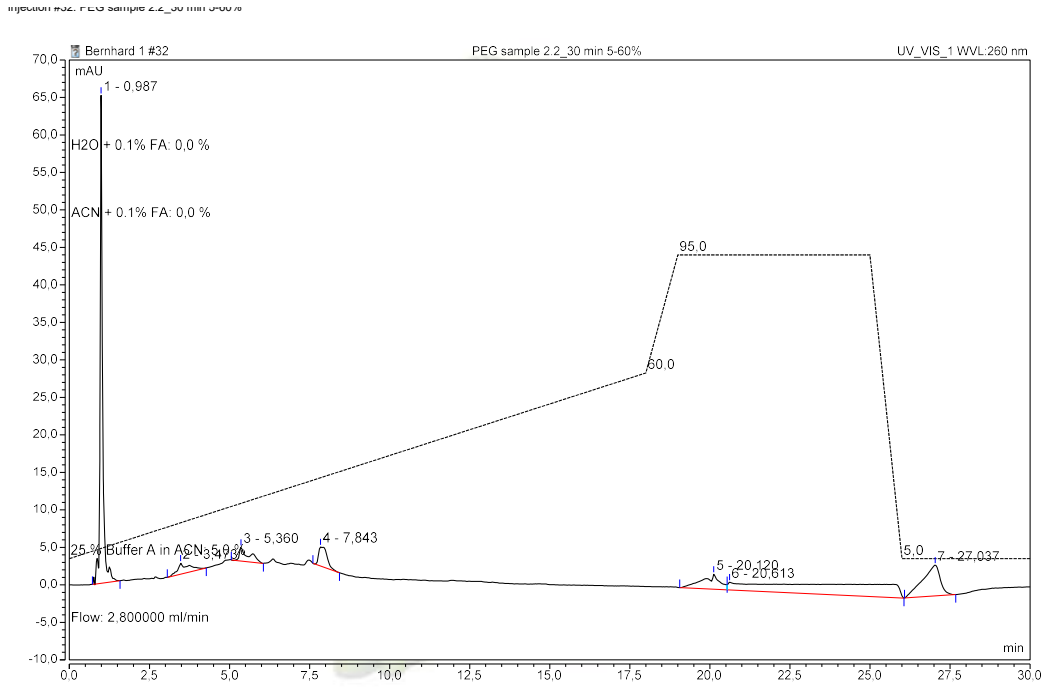


Figure 37: RP-HPLC chromatogram of PEG (260 nm).

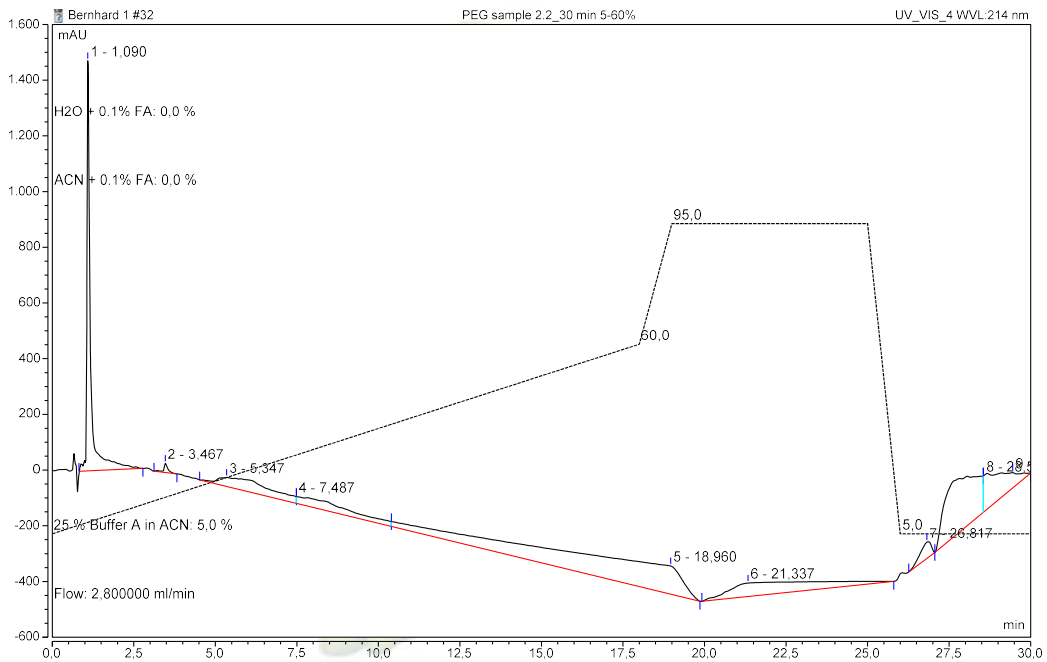


Figure 38: RP-HPLC chromatogram of PEG (214 nm).

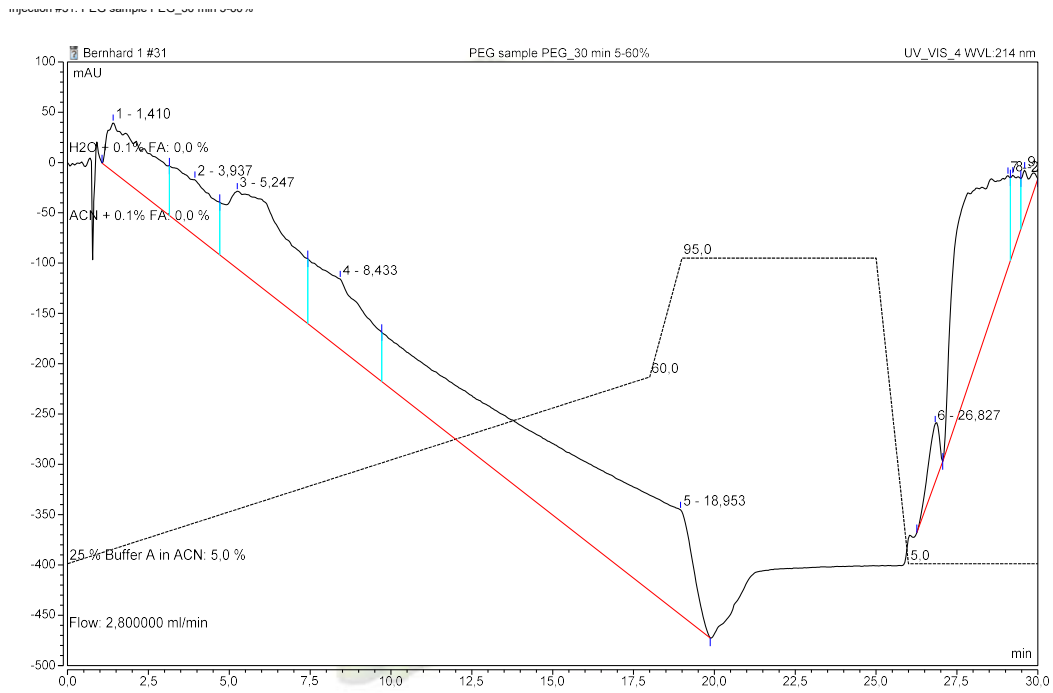


Figure 39: RP-HPLC chromatogram of 8× PEG-azide (214 nm).

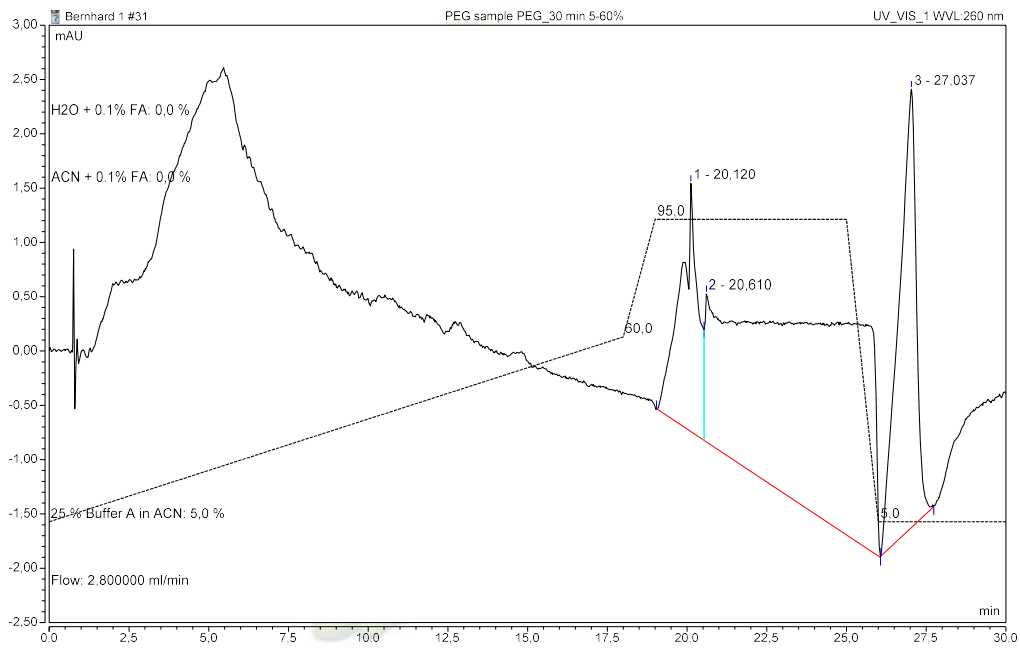
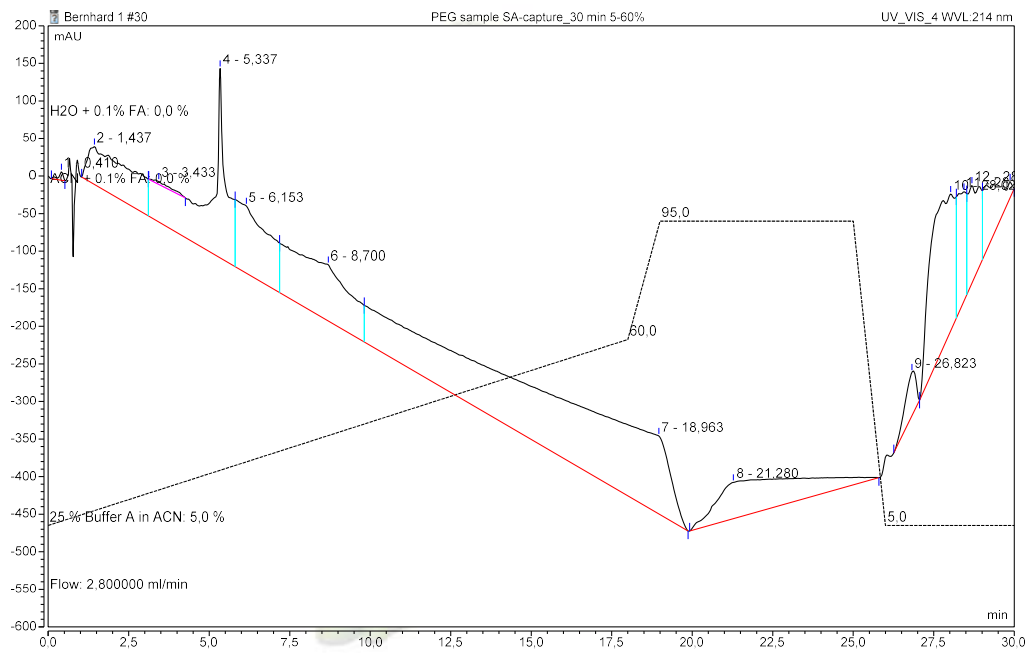


Figure 40: RP-HPLC chromatogram of 8× PEG-azide (260 nm).

Sequence: Bernhard 1
Injection #30: PEG sample SA-capture_30 min 5-60%

Chromatogram



Chromleon 7,
Version 7.2.7.10369, Thermo Fisher Scientific

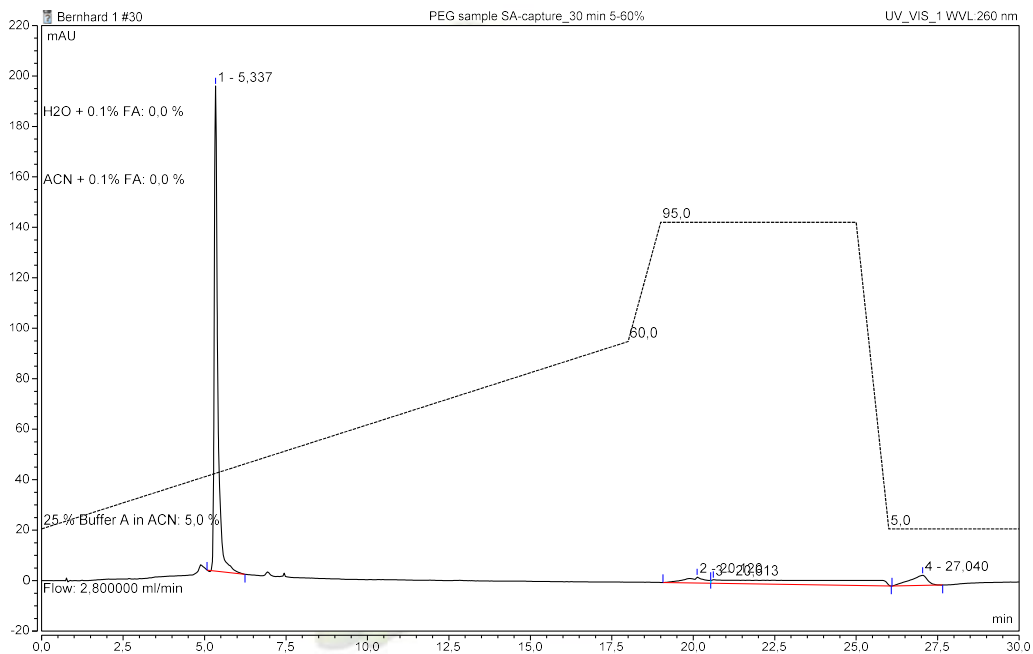
Page 1 of 1

Printed by KEMI-KAS-HPLC
27-02-19 13:51

Figure 41: RP-HPLC chromatogram of ON5' (PEG) (214 nm).

Sequence: Bernhard 1
Injection #30: PEG sample SA-capture_30 min 5-60%

Chromatogram



Chromleon 7,
Version 7.2.7.10369, Thermo Fisher Scientific

Page 1 of 1

Printed by KEMI-KAS-HPLC
27-02-19 13:50

Figure 42: RP-HPLC chromatogram of ON5' (PEG) (260 nm).

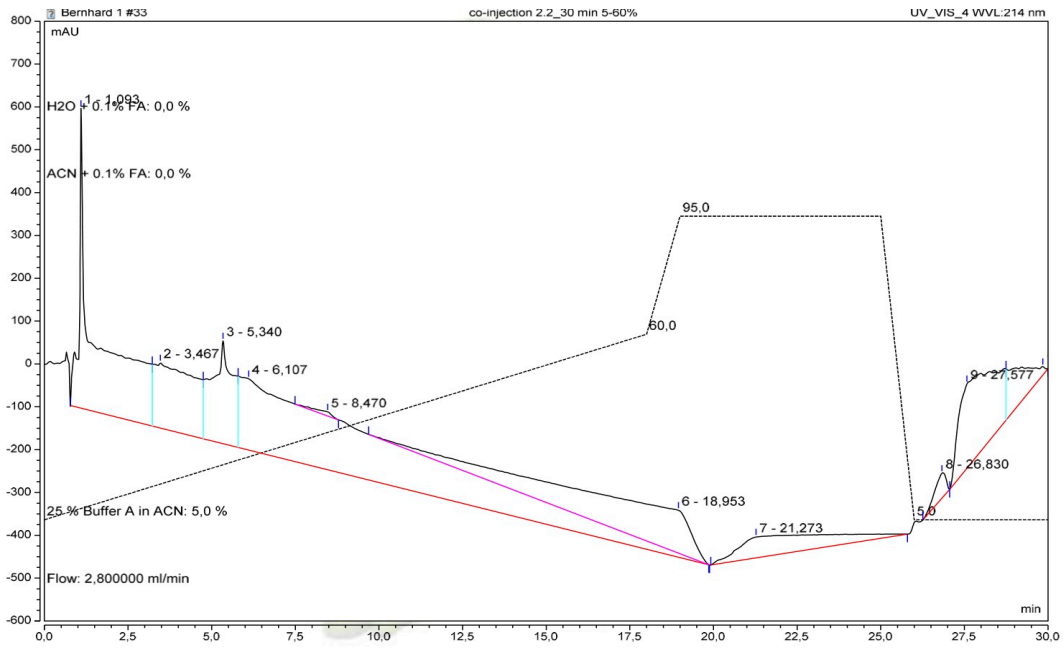


Figure 43: RP-HPLC chromatogram of co-injection (PEG) (214 nm).

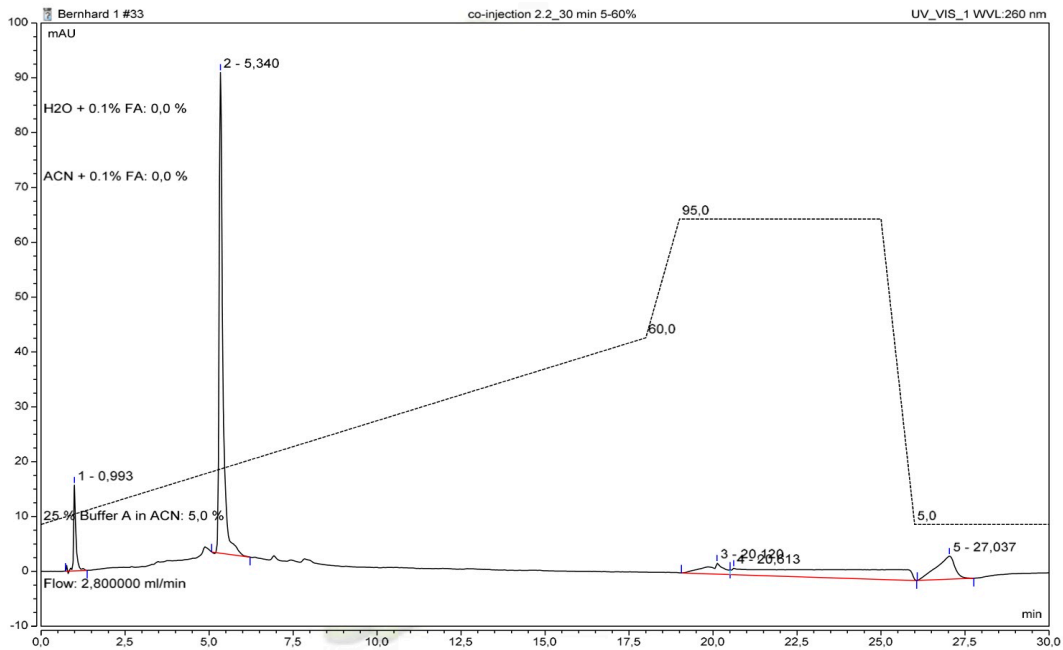


Figure 44: RP-HPLC chromatogram of co-injection (PEG) (260 nm).

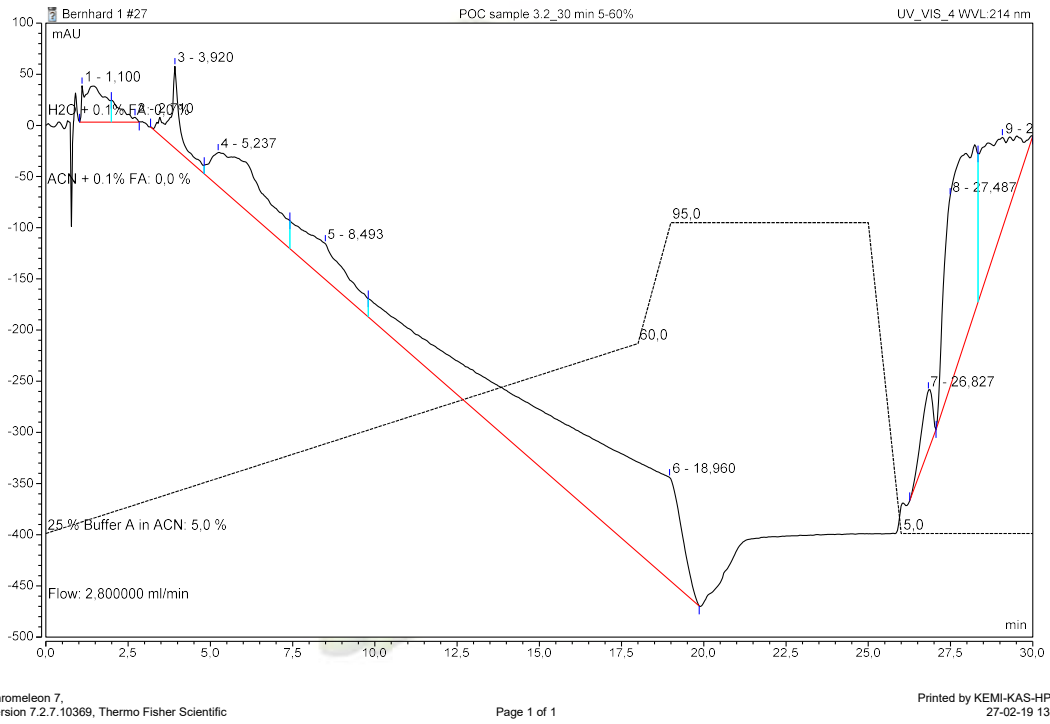


Figure 45: RP-HPLC chromatogram of POC (214 nm).

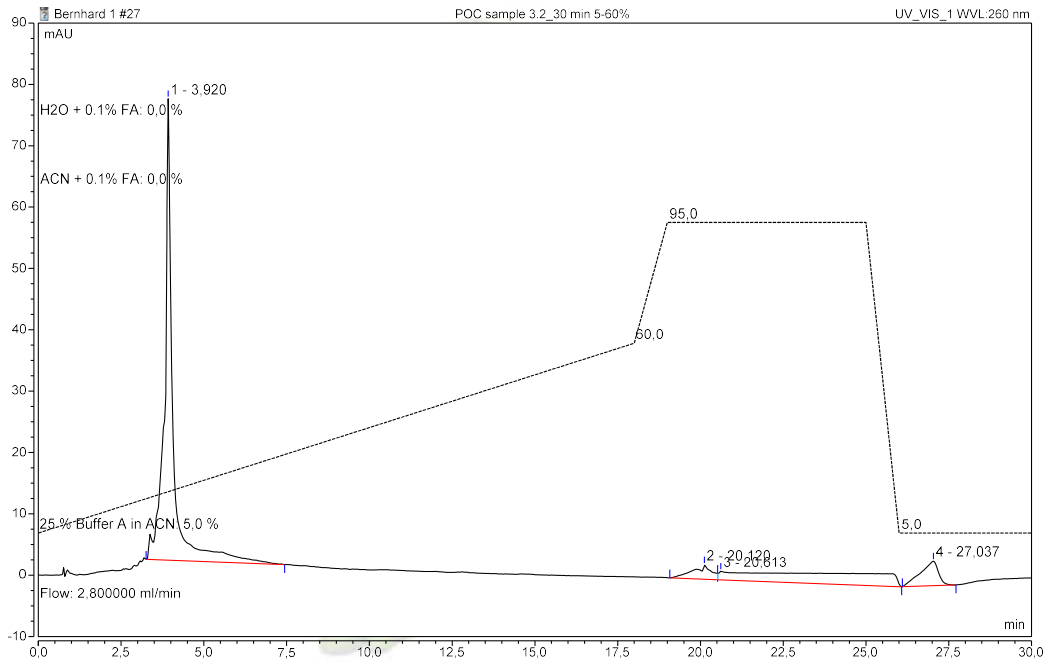
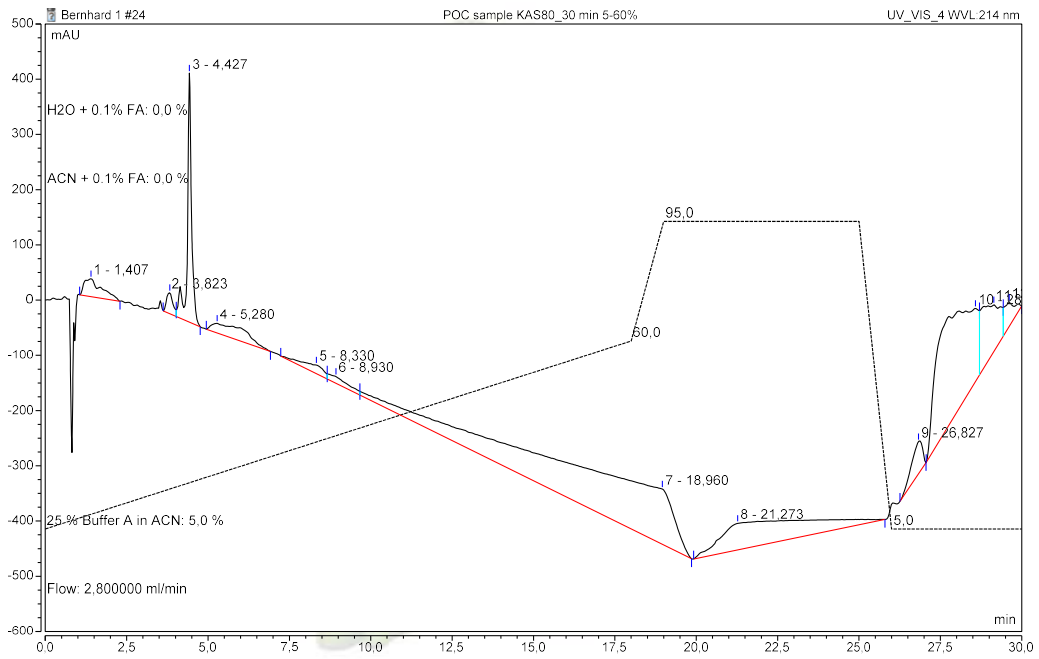


Figure 46: RP-HPLC chromatogram of POC (260 nm).

Sequence: Bernhard 1
Injection #24: POC sample KAS80_30 min 5-60%

Chromatogram



Chromleon 7,
Version 7.2.7.10369, Thermo Fisher Scientific

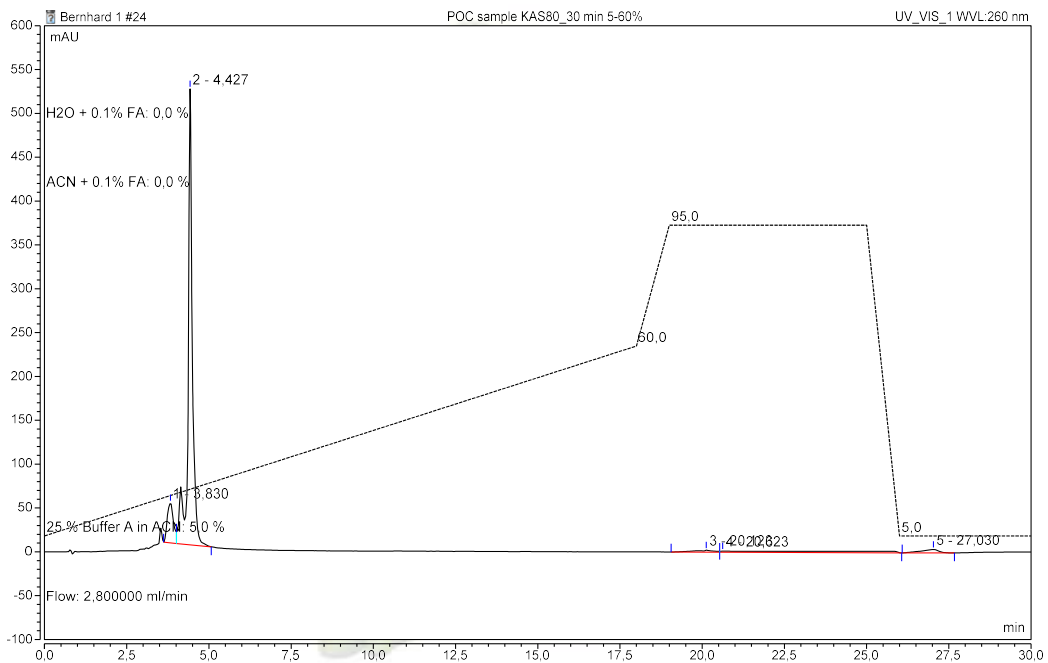
Page 1 of 1

Printed by KEMI-KAS-HPLC
27-02-19 13:43

Figure 47: RP-HPLC chromatogram of ON4 (214 nm).

Sequence: Bernhard 1
Injection #24: POC sample KAS80_30 min 5-60%

Chromatogram



Chromleon 7,
Version 7.2.7.10369, Thermo Fisher Scientific

Page 1 of 1

Printed by KEMI-KAS-HPLC
27-02-19 13:44

Figure 48: RP-HPLC chromatogram of ON4 (260 nm).

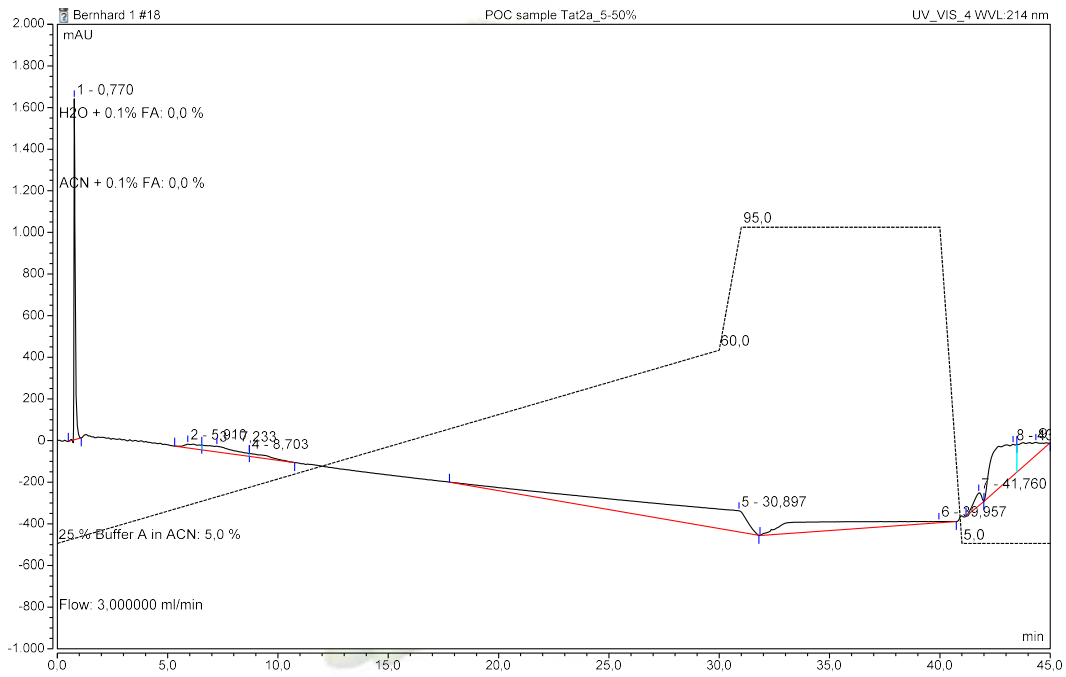


Figure 49: RP-HPLC chromatogram of P1 (214 nm).

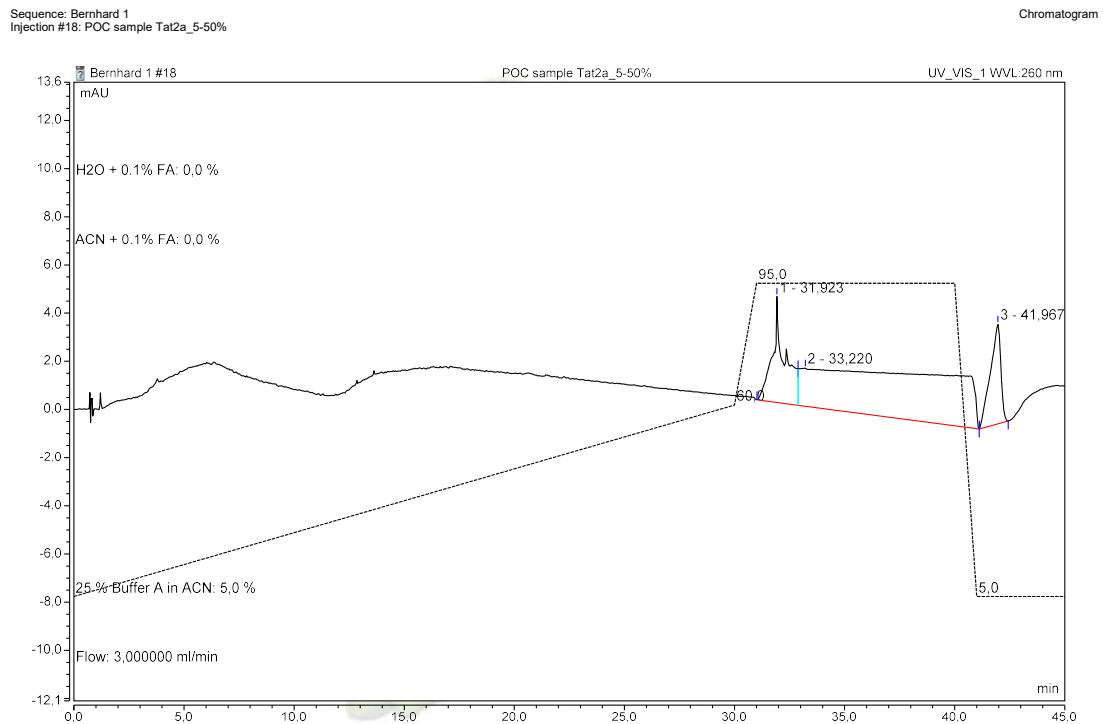


Figure 50: RP-HPLC chromatogram of P1 (260 nm).

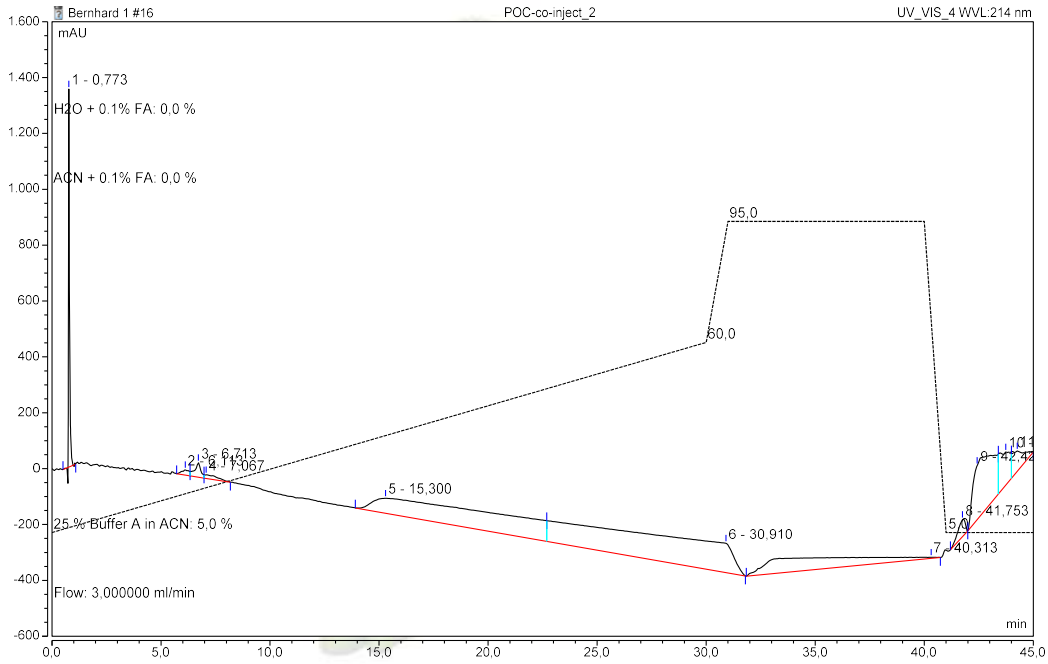


Figure 51: RP-HPLC chromatogram of POC co-injection (214 nm).

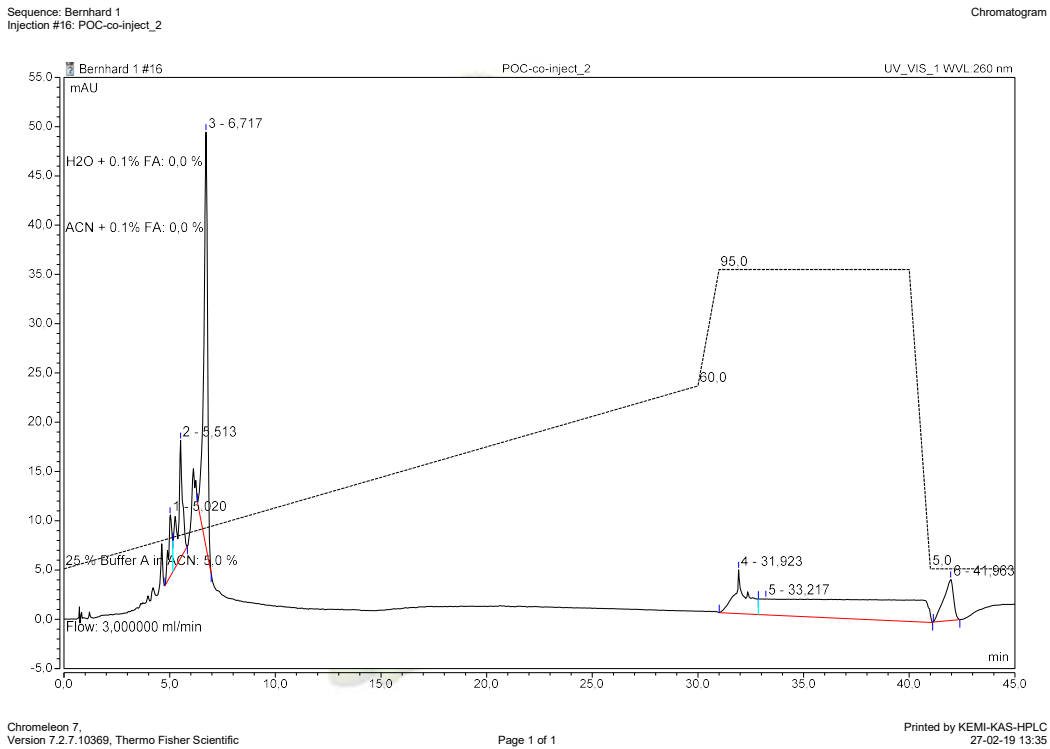


Figure 52: RP-HPLC chromatogram of POC co-injection (260 nm).

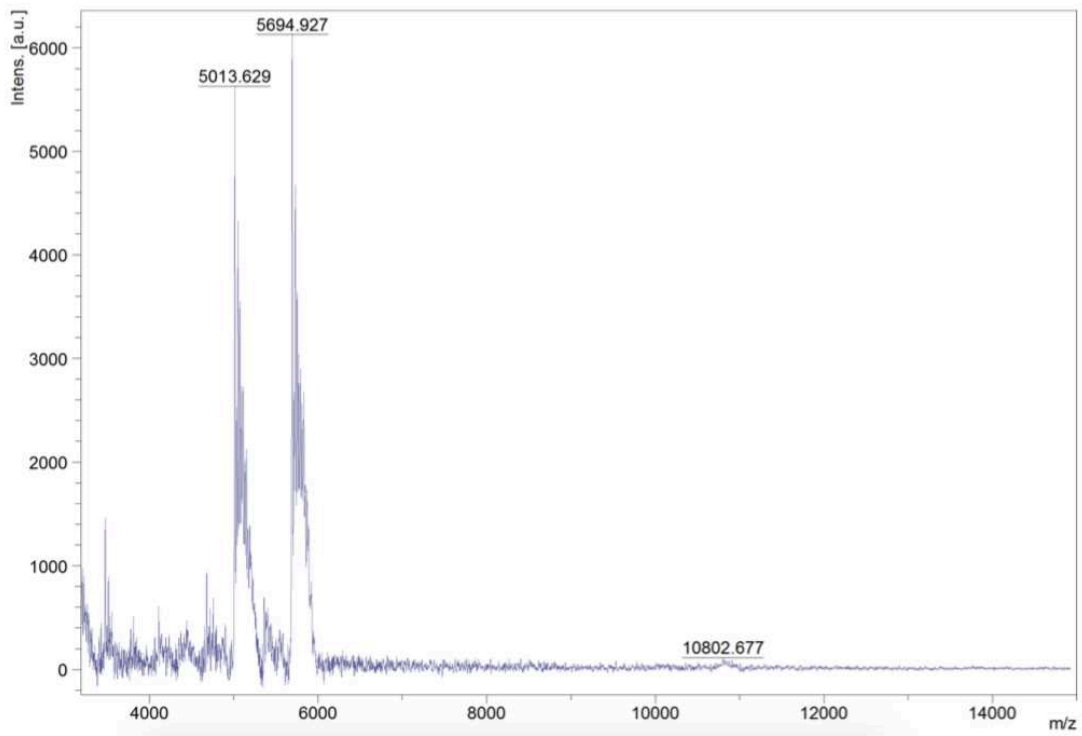


Figure 53: MALDI-TOF mass spectra CP.

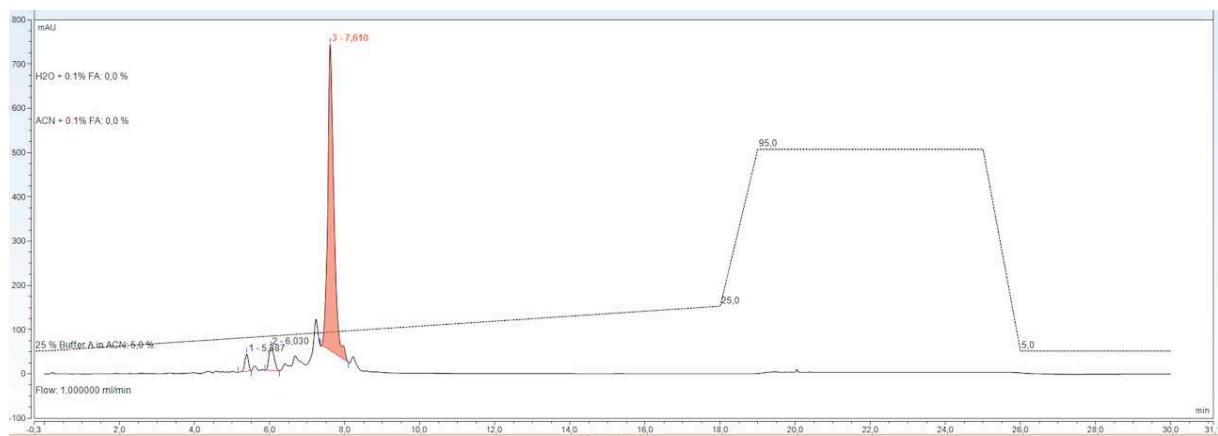


Figure 54: RP-HPLC chromatogram of CP (260 nm).

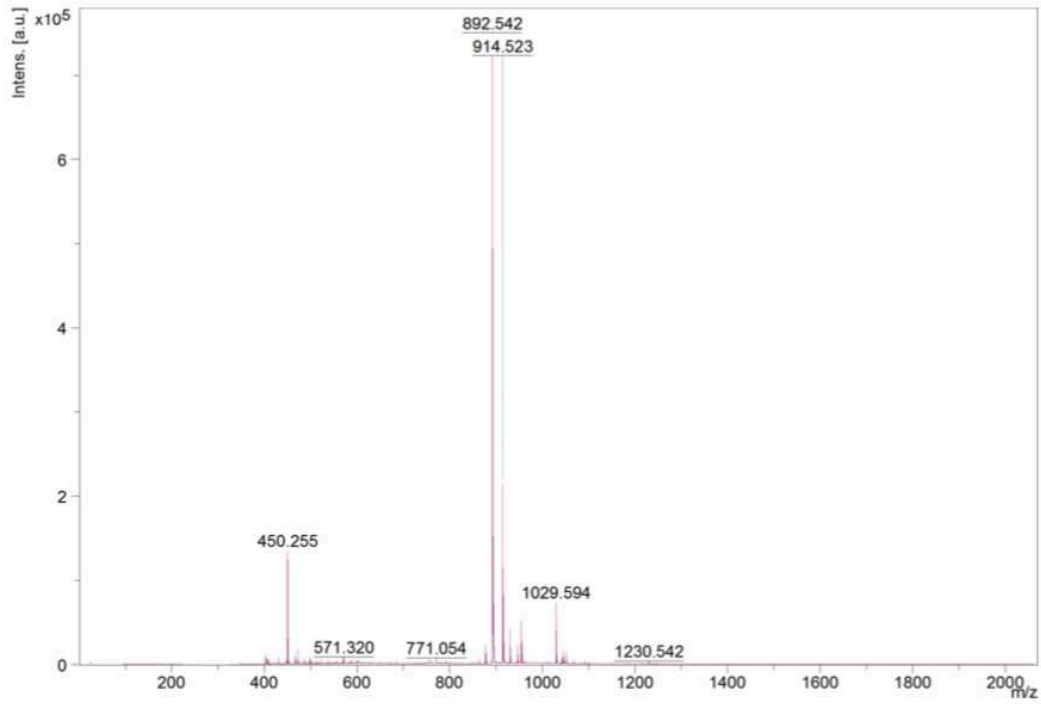


Figure 55: MALDI-TOF mass spectra P6.

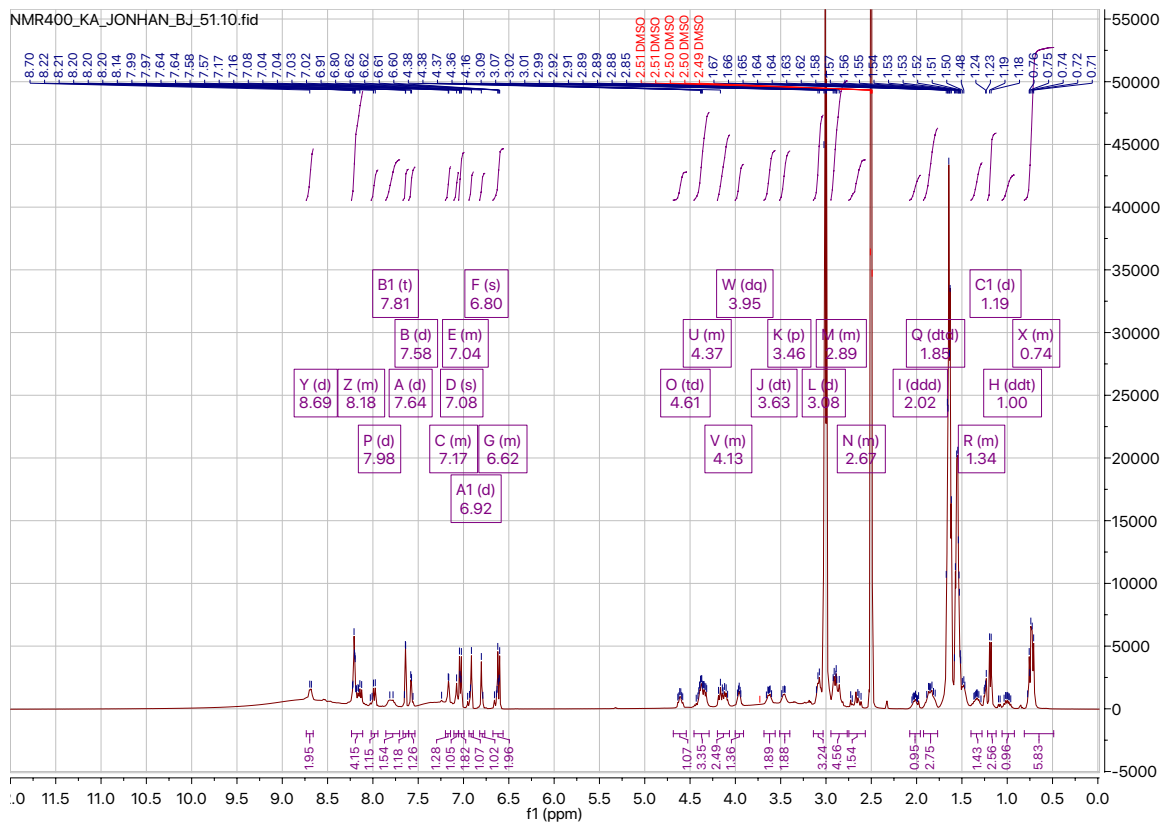


Figure 56a: ¹H-NMR spectrum of P6 (400 MHz, DMSO-*d*₆).

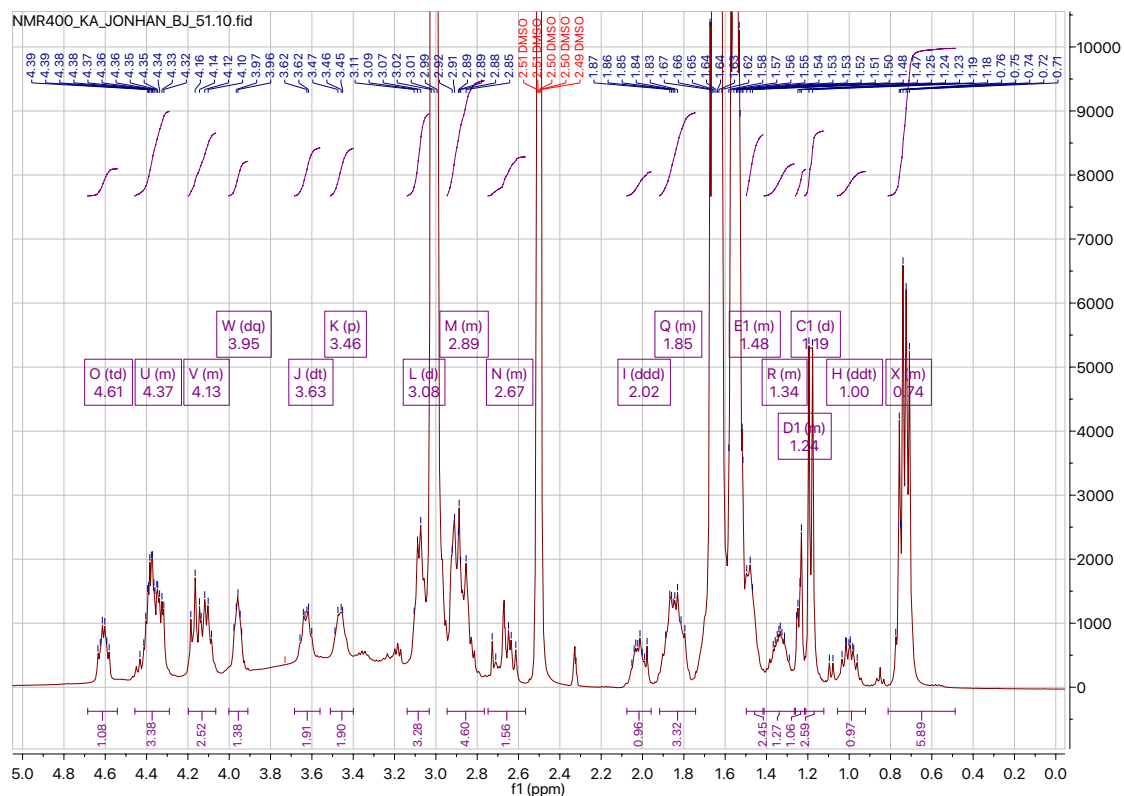


Figure 56b: ¹H-NMR spectrum of P6 (400 MHz, DMSO-*d*₆, 0-5 ppm).

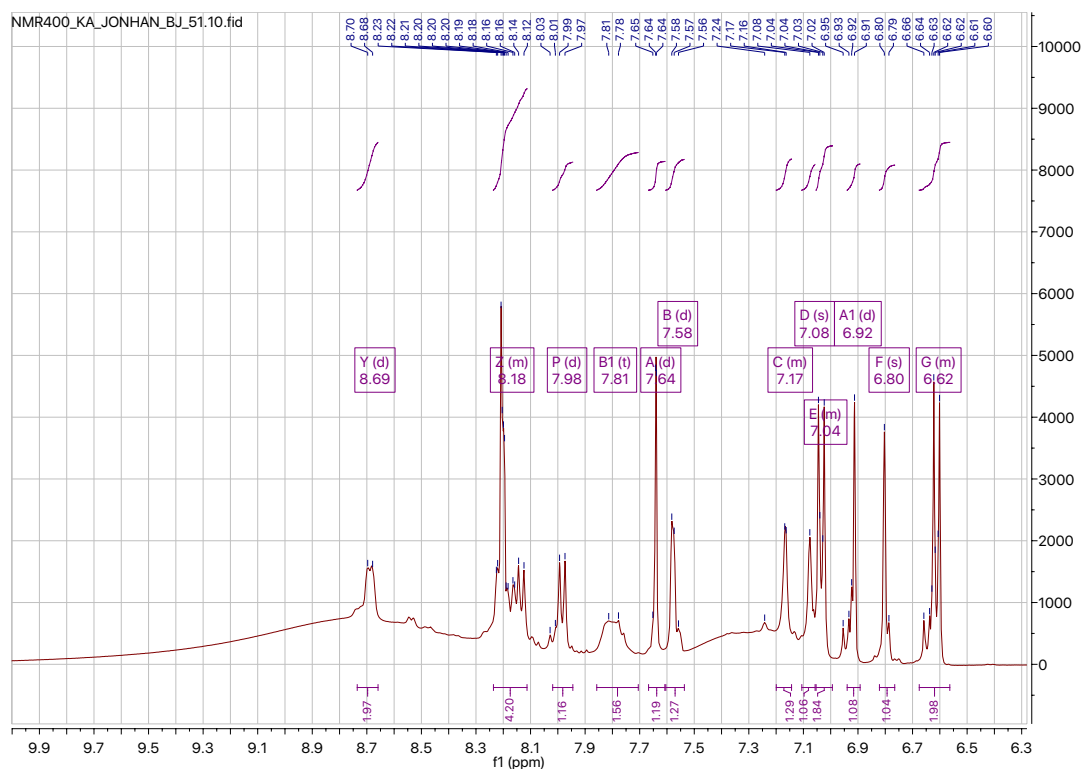


Figure 56c: ¹H-NMR spectrum of P6 (400 MHz, DMSO-*d*₆, 6.3-10 ppm).

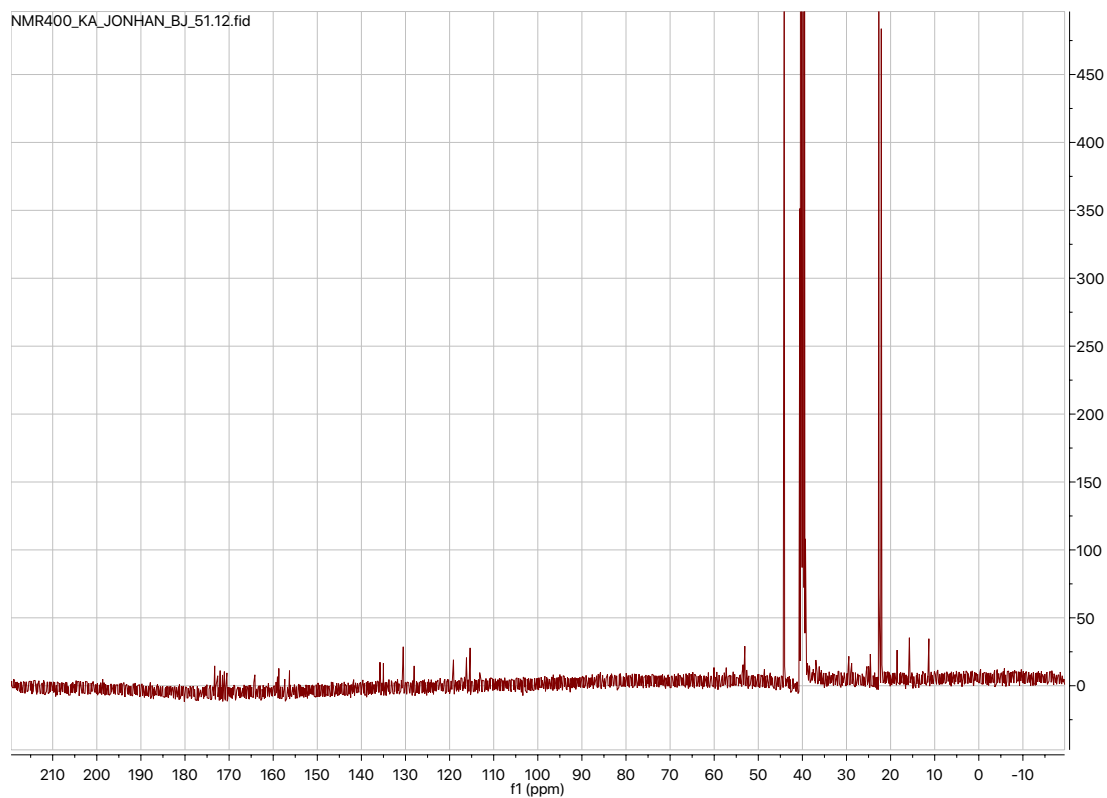


Figure 56d: ^{13}C -NMR spectrum of P6 (101MHz, $\text{DMSO-}6d_6$).

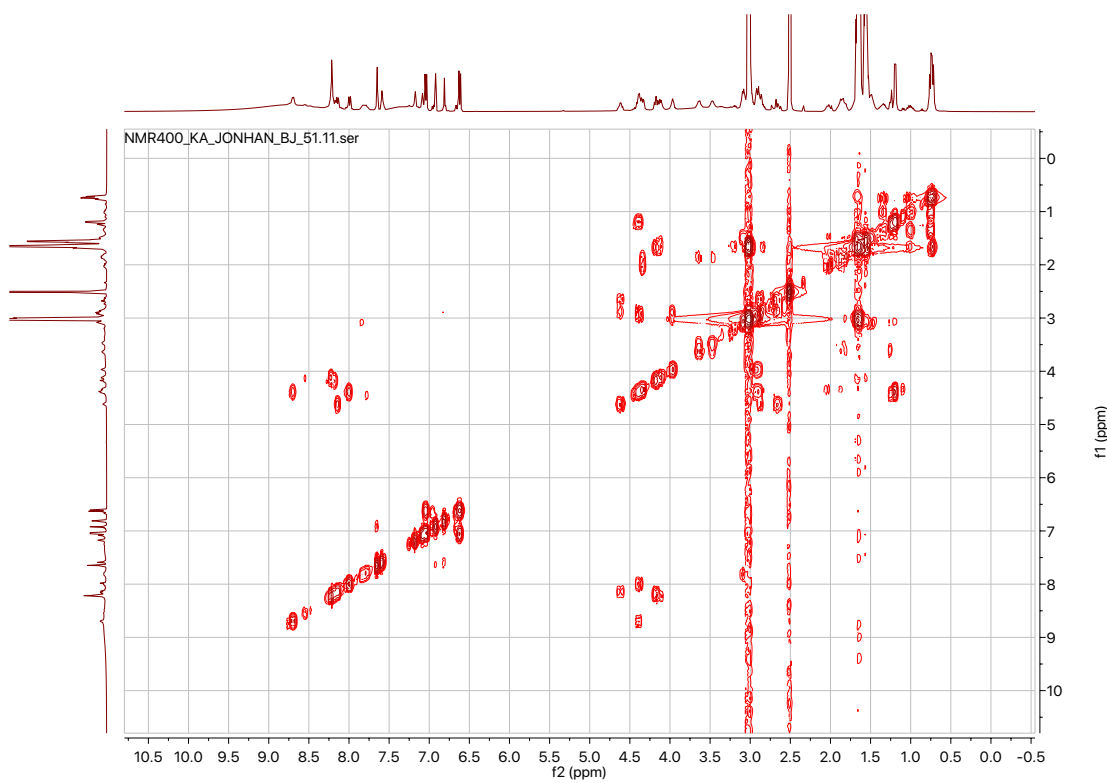


Figure 56e: COSY spectrum of P6 ($\text{DMSO-}6d_6$).

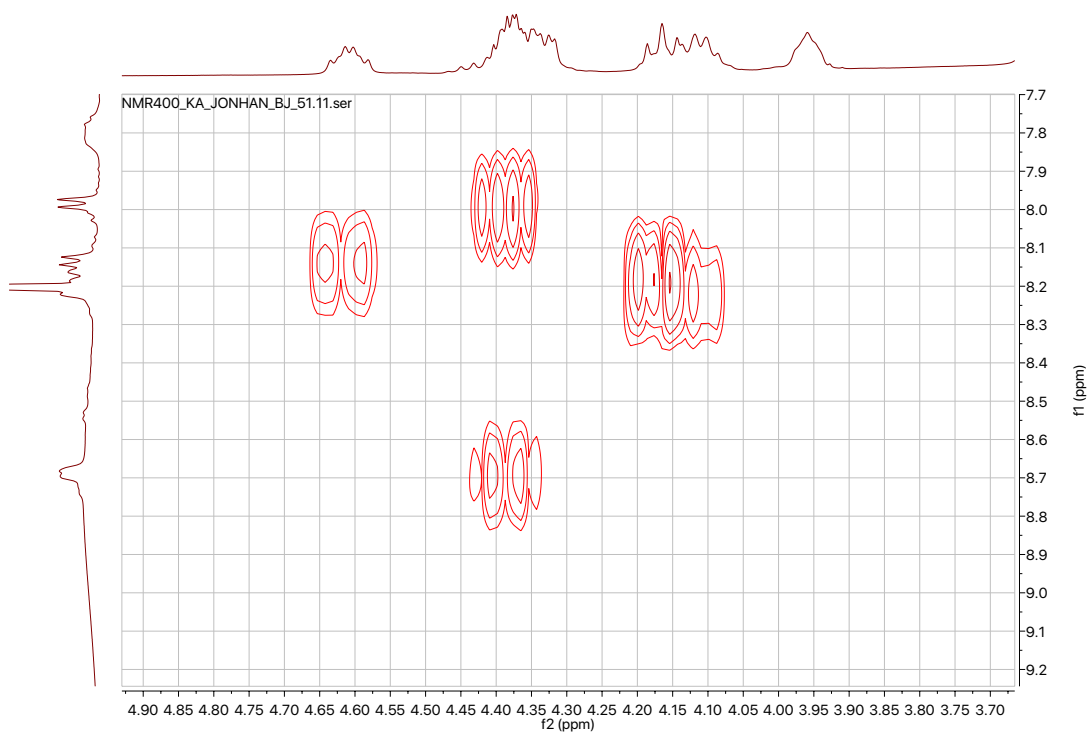


Figure 56f: Close up of COSY spectrum of P6 (DMSO- d_6).

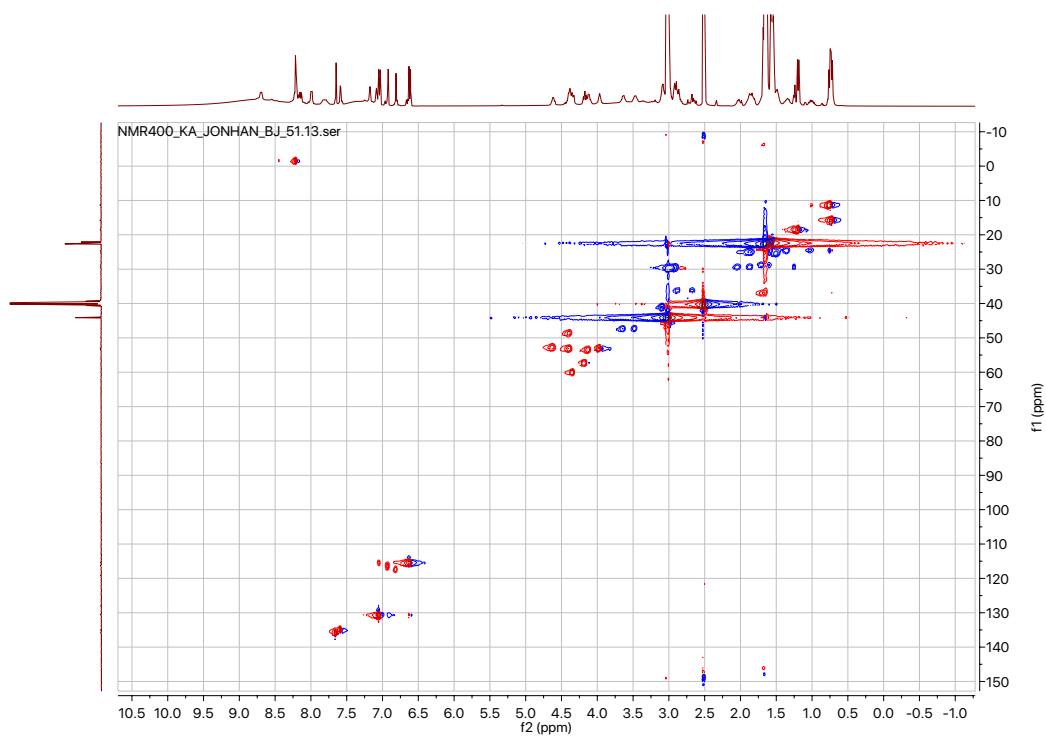


Figure 56g: HSQC spectrum of P6 (DMSO- d_6).

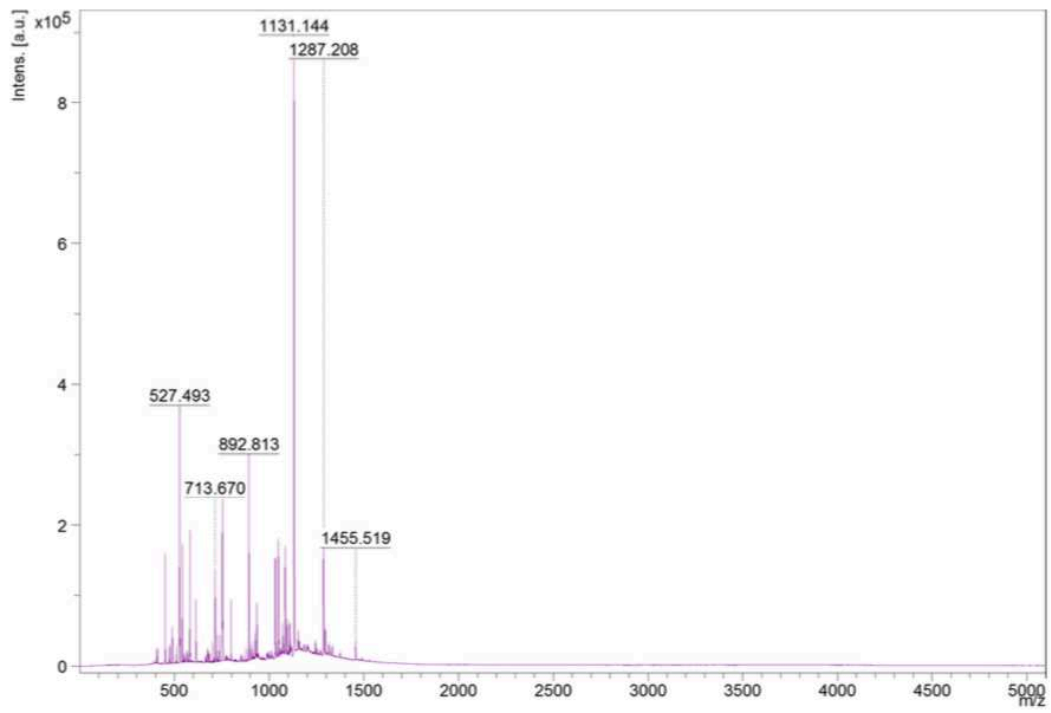


Figure 57: MALDI-TOF mass spectra mP6.

Comment 1
Comment 2

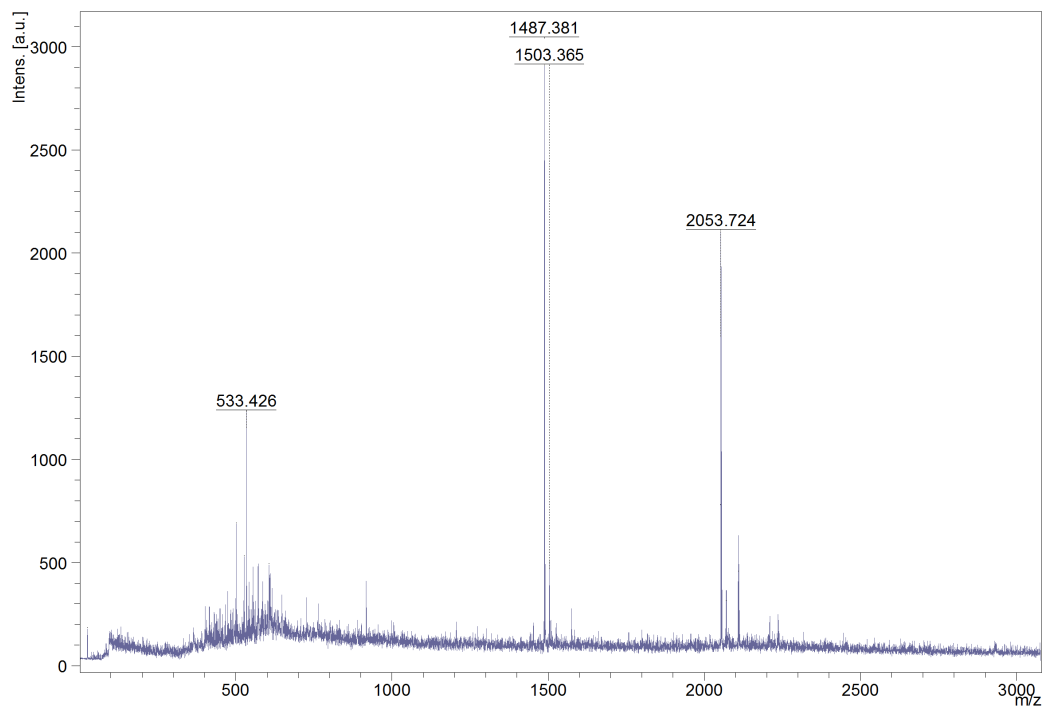


Figure 58: MALDI-TOF mass spectra mP7.

Comment 1
Comment 2

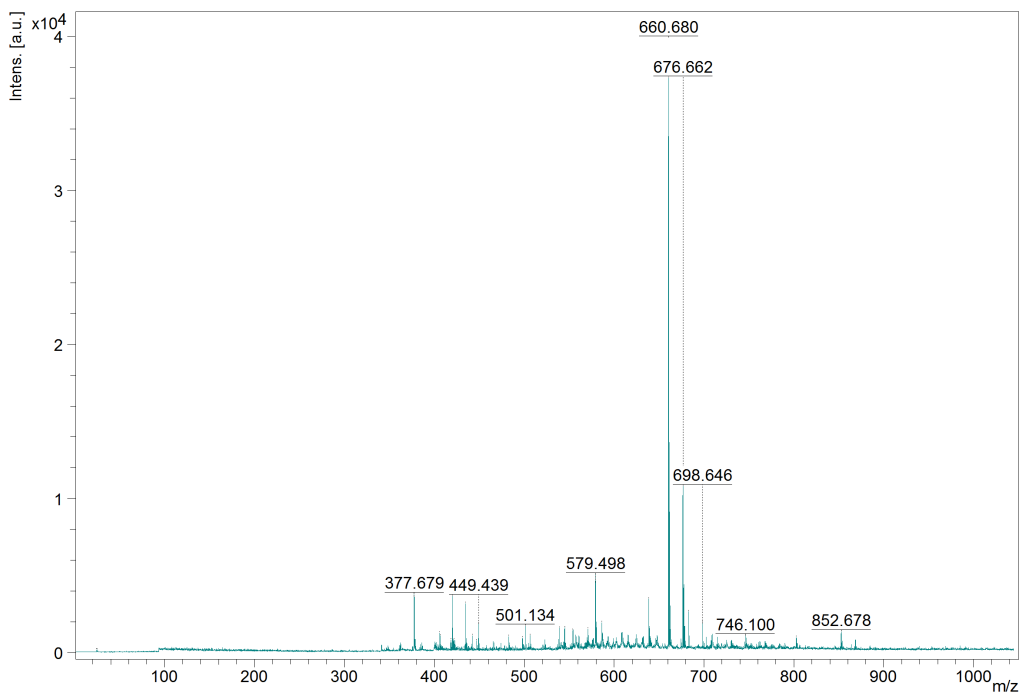


Figure 59: MALDI-TOF mass spectra of the lipid anchor LA.

Comment 1
Comment 2

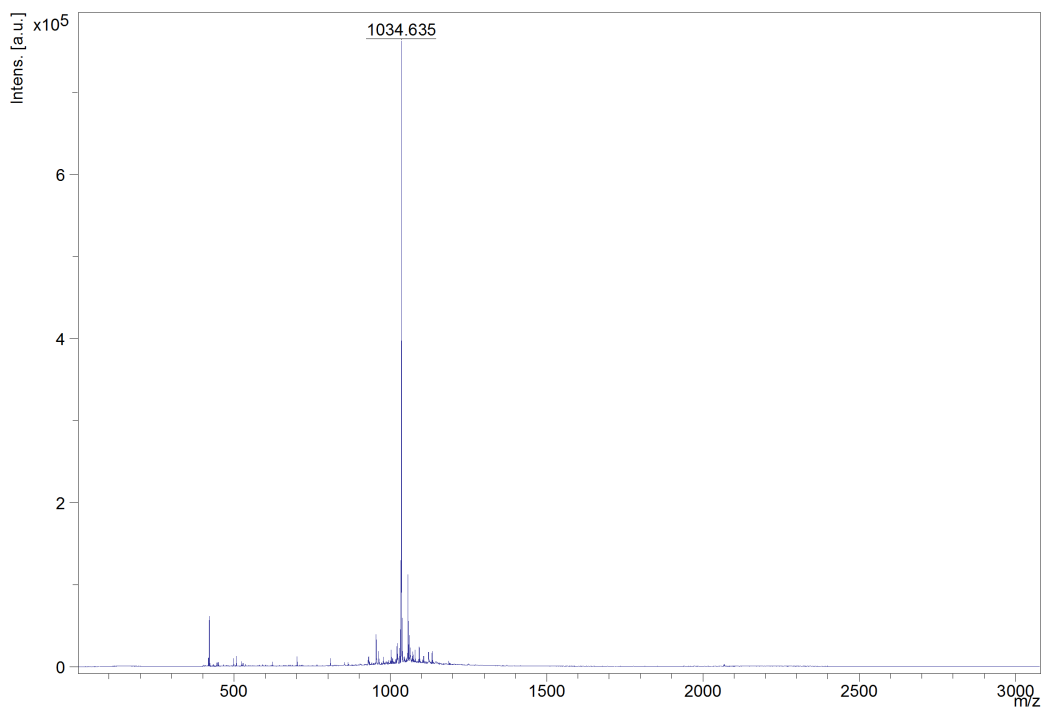


Figure 60: MALDI-TOF mass spectra of P8.

Comment 1
Comment 2

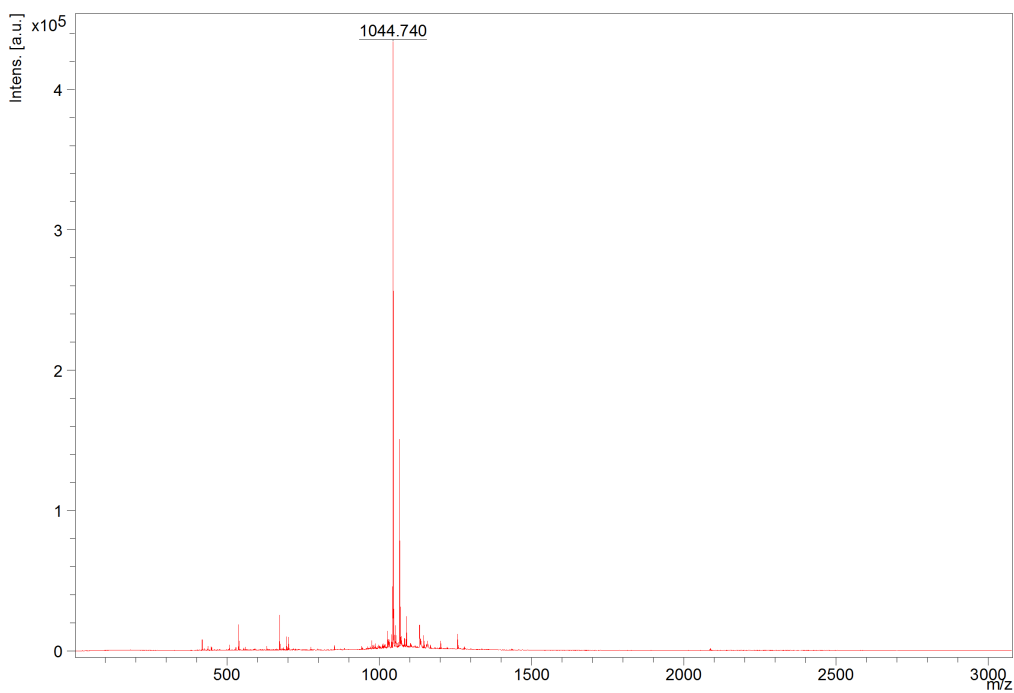


Figure 61: MALDI-TOF mass spectra of P9.

Comment 1
Comment 2

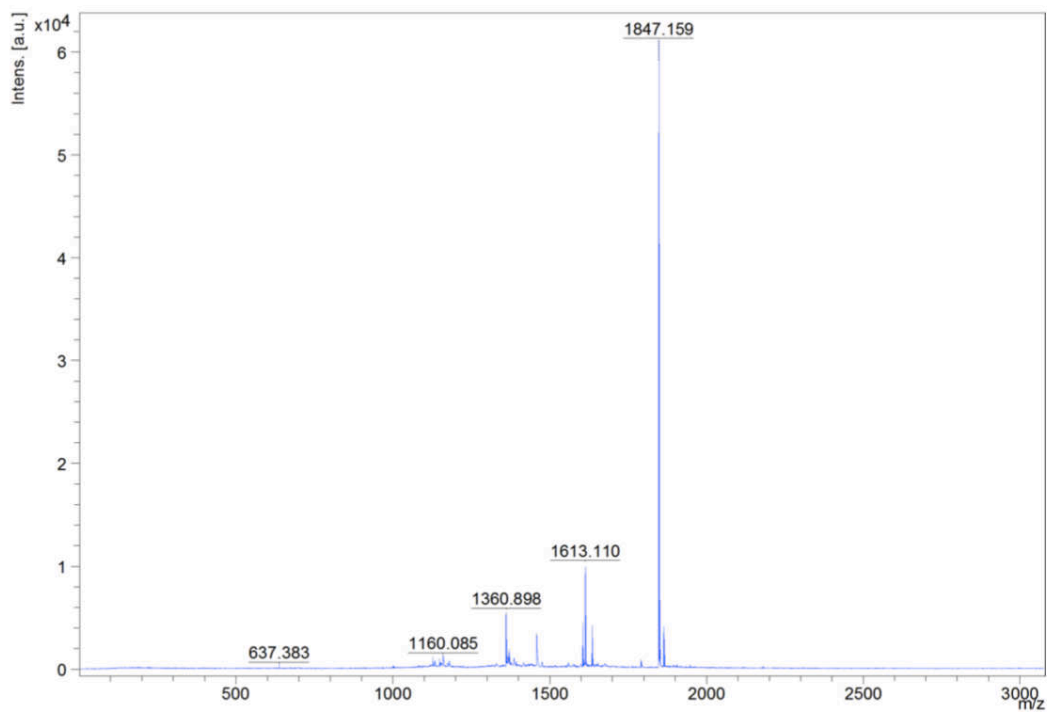


Figure 62: MALDI-TOF mass spectra of cP8.

Comment 1
Comment 2

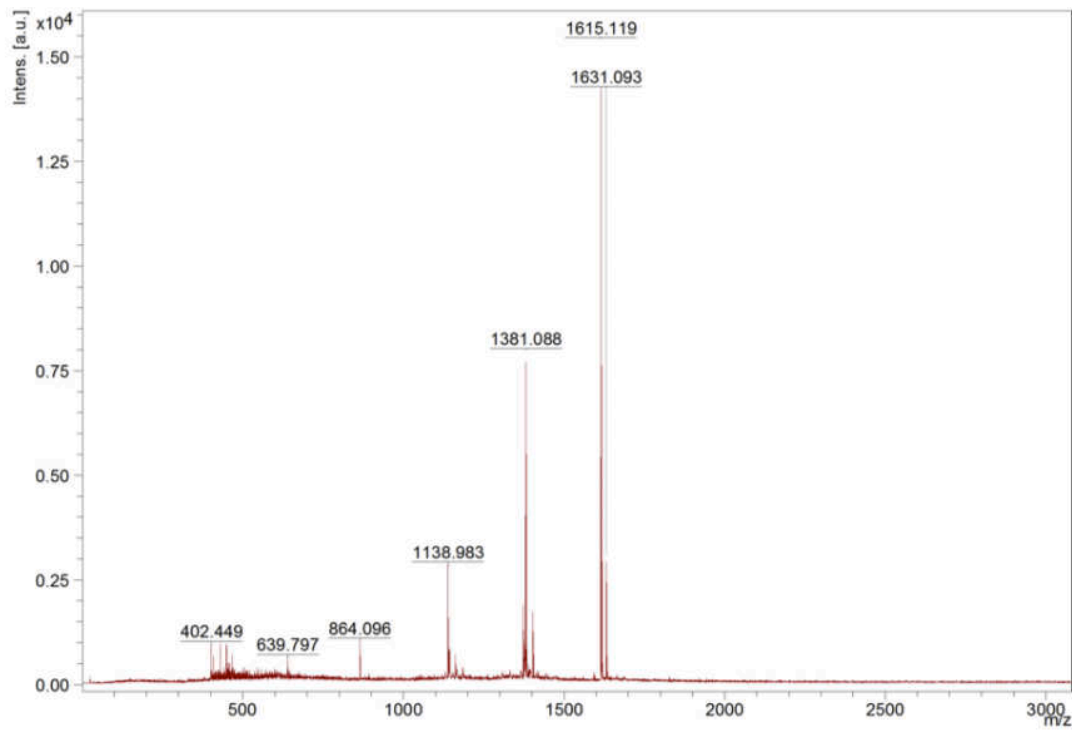


Figure 63: MALDI-TOF mass spectra of cP9.

Comment 1
Comment 2

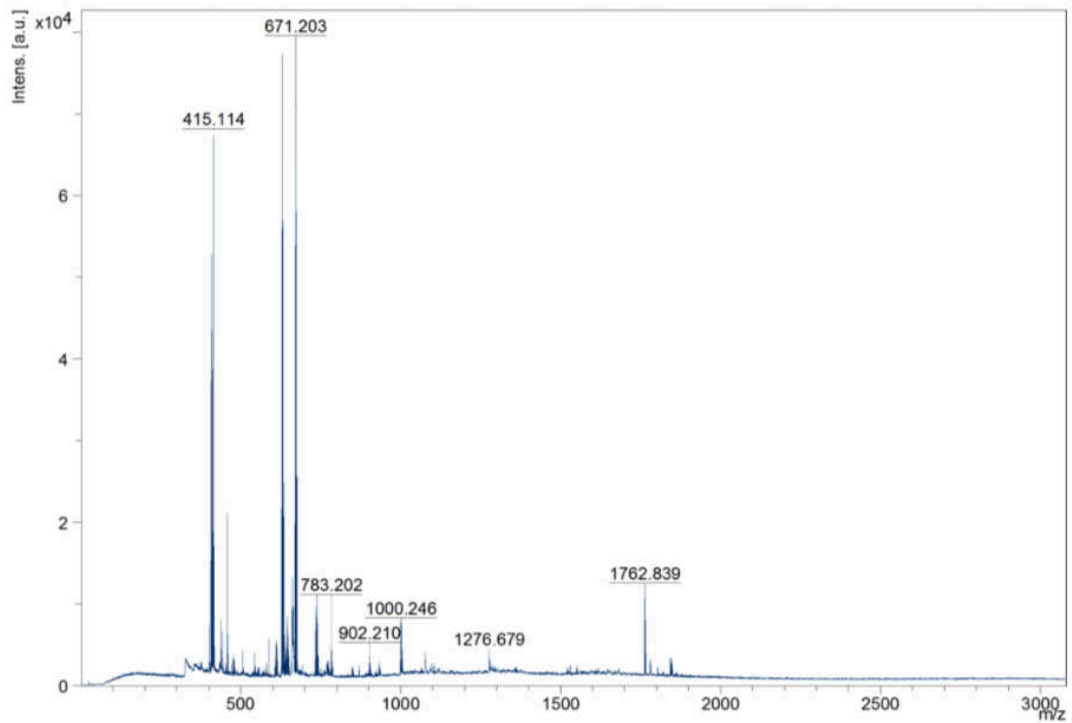


Figure 64: MALDI-TOF mass spectra of cP8'.

Comment 1
Comment 2

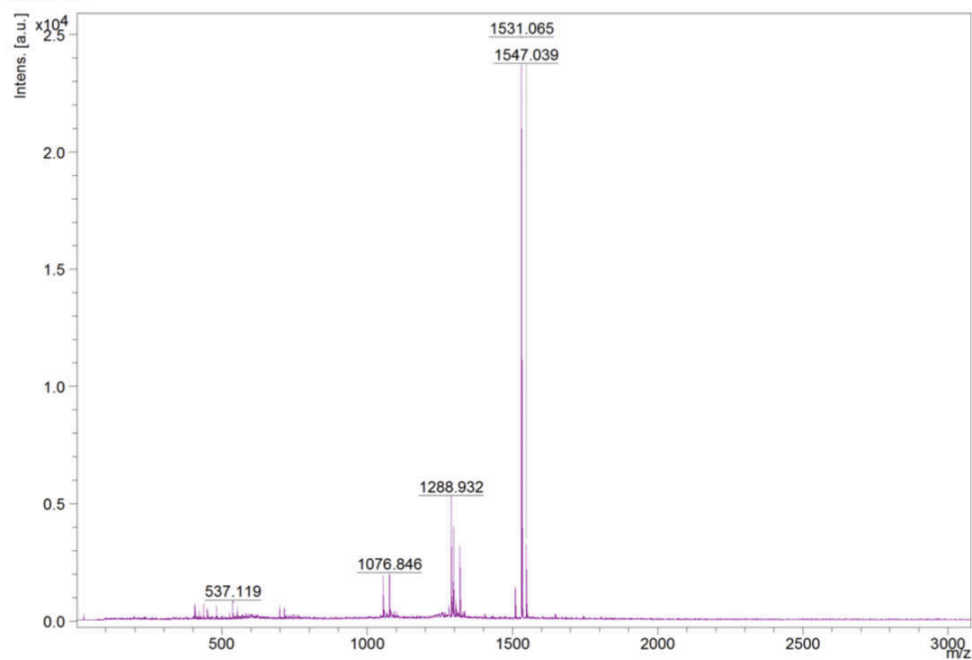


Figure 65: MALDI-TOF mass spectra of cP9'.

Comment 1
Comment 2

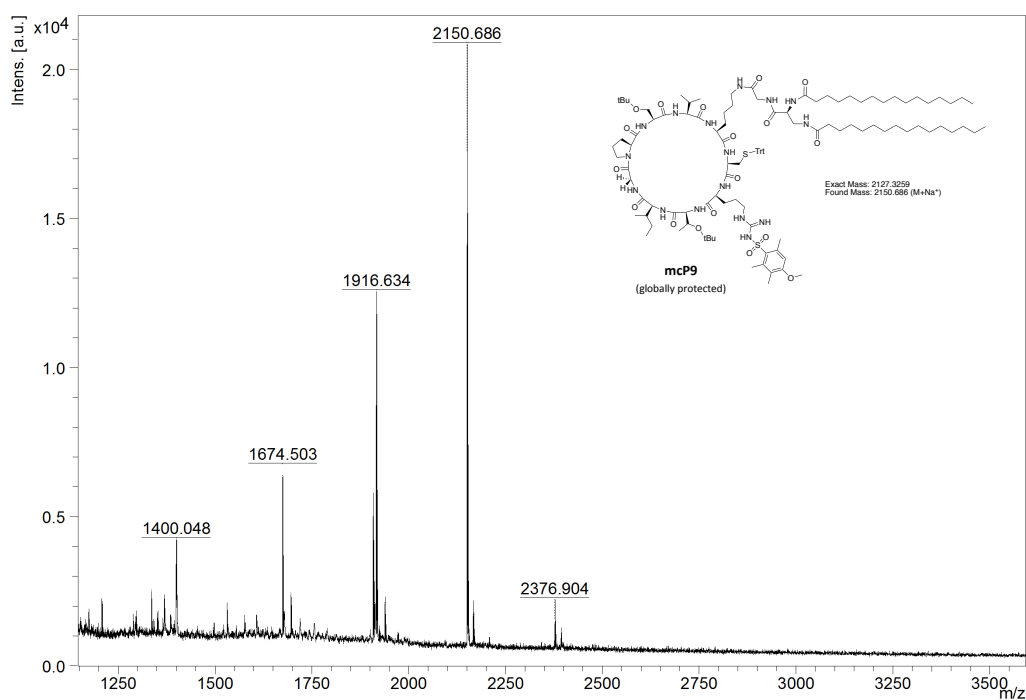


Figure 66: MALDI-TOF mass spectra mcP9.

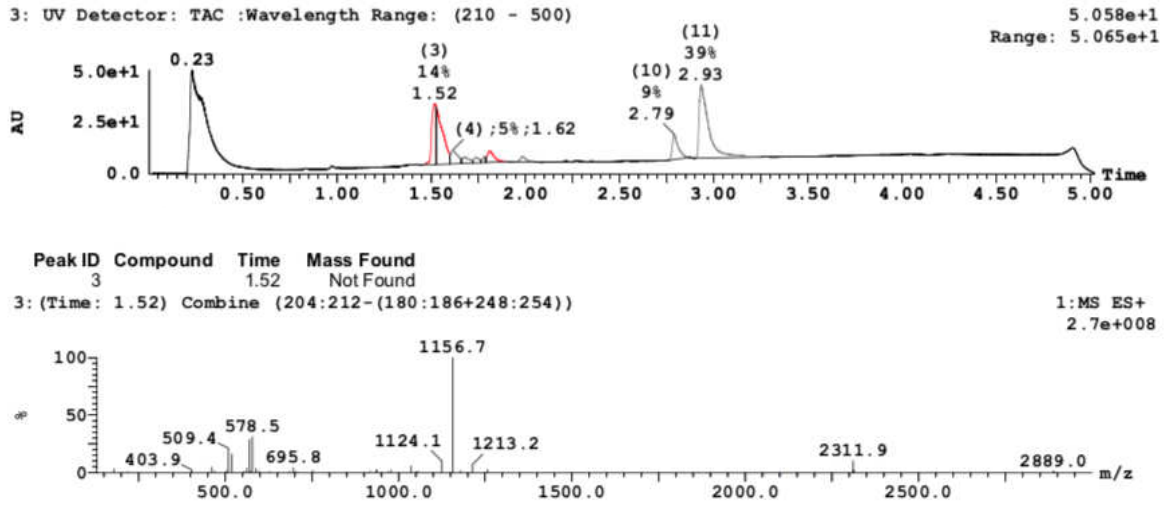


Figure 67: Received UV and mass spectra of LC-MS run of P10.

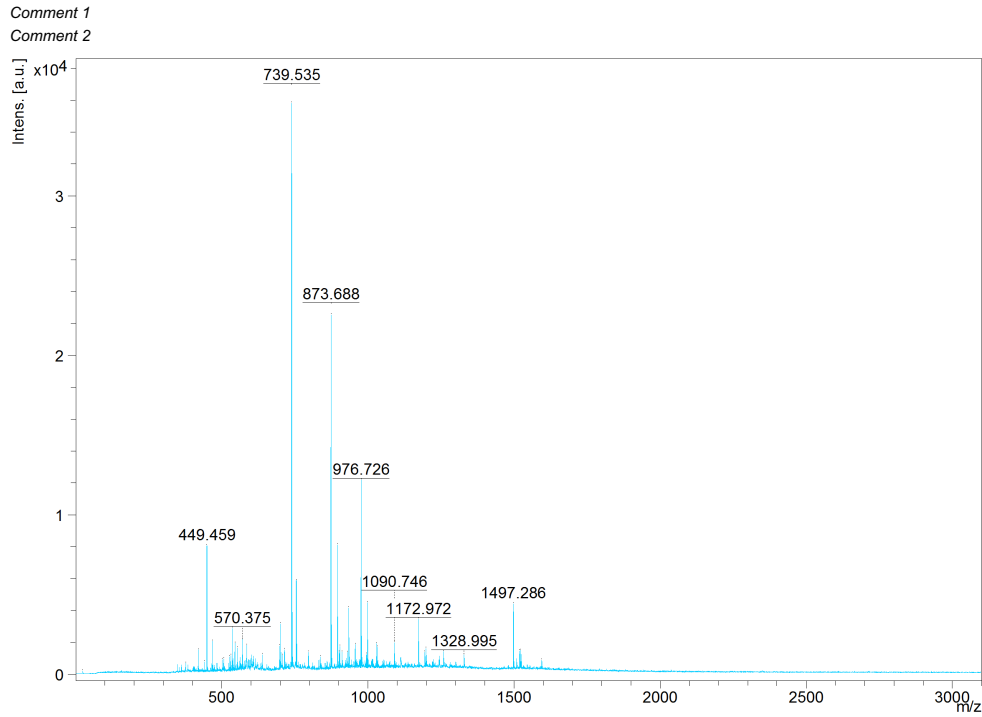


Figure 68: MALDI-TOF mass spectra of mP10.

Comment 1
Comment 2

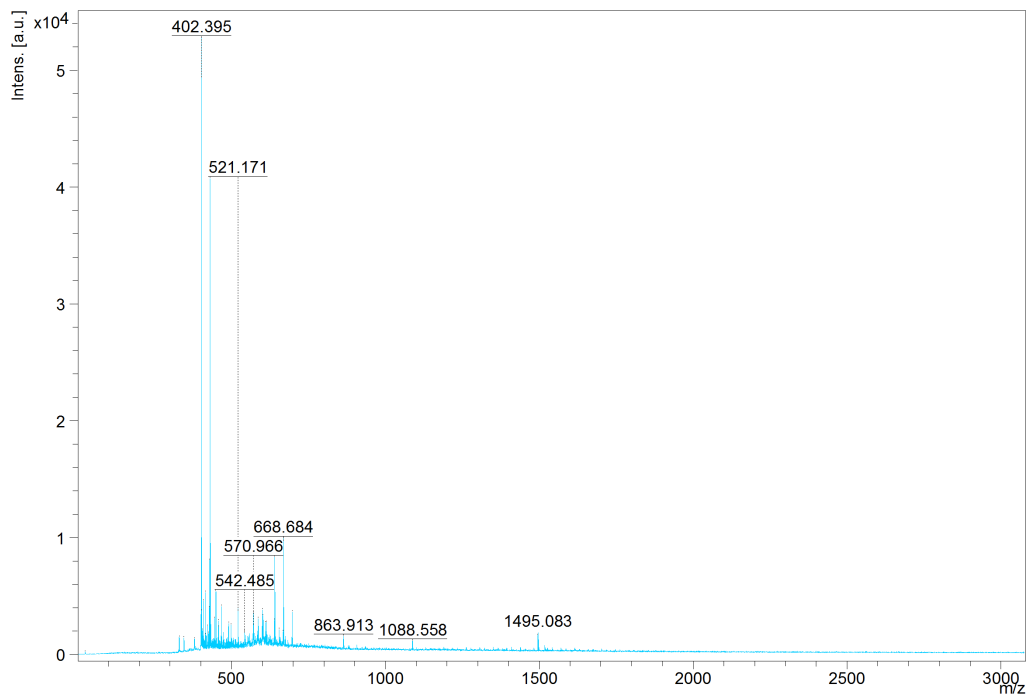


Figure 69a: Close up of MALDI-TOF mass spectra of mcP10.

Comment 1
Comment 2

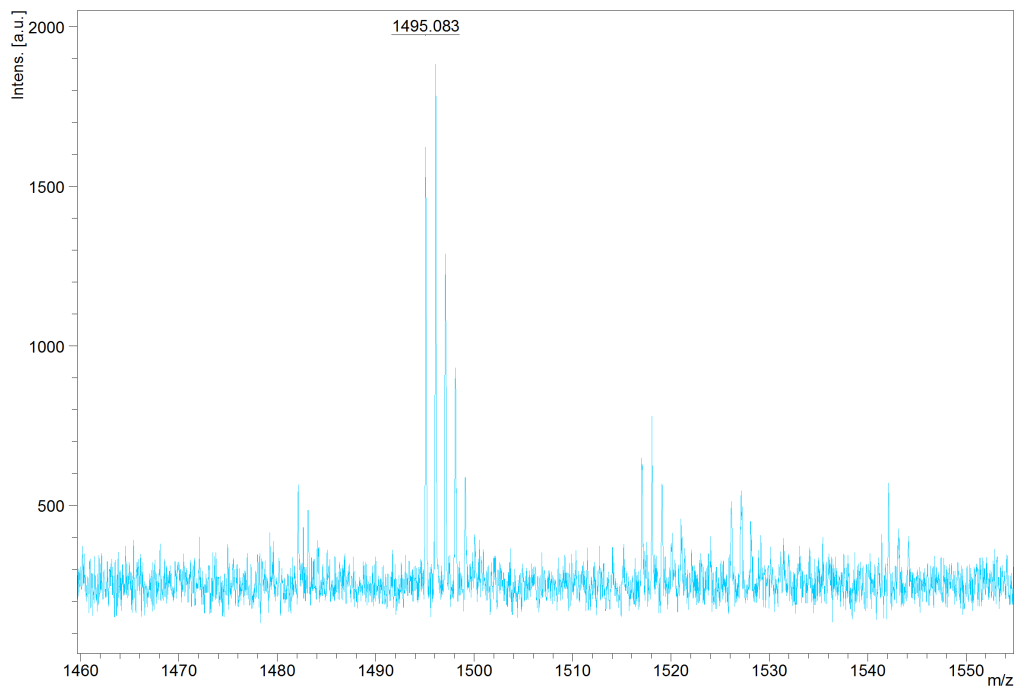


Figure 69b: Close up of MALDI-TOF mass spectra of mcP10.

5.2 Curriculum Vitae

Bernhard Jandl, BSc

Mollardgasse 29/12, 1060 Vienna

+ 43 664 54 15 924

jandl_berni@gmx.at

date/place of birth: 04.04.1993/Klagenfurt

citizenship: Austria



Education

Apr. 2016 – present

**Master's program: Technical Chemistry
University of Technology Vienna (TU Wien)**

Specialization: Applied Synthetic Chemistry

Master thesis at **Technical University of Denmark (DTU)**

Novel nucleoside analogues for diagnosis and treatment of infectious diseases

Research area: *Bioorganic Chemistry and Chemical Biology*

(Supervision: Univ. Prof. Marko Mihovilovic (TU Wien), Assoc. Prof. Kira Astakhova (DTU))

Thesis defense presumably Feb. 2020

Oct. 2011 – Apr. 2016

**Bachelor's program: Technical Chemistry
University of Technology Vienna (TU Wien)**

Triazoloquinazoliniones as ligands for the alpha+/beta- interface

Research area: *Medicinal Chemistry and Organic Synthesis*

Supervision: Assoc. Prof. Michael Schnürch (TU Wien)

Sept. 2003 – Jun. 2011

Bg/Brg St. Veit a. d. Glan

specializing in languages (6 years Italian; 4 years Latin)

Sept. 1999 – Jun. 2003

Primary school Brückl

Work Experience

Sept. 2018 – Feb. 2019

Visiting Researcher - Technical University of Denmark (DTU)

Research group of Assoc. Prof. Kira Astakhova

Apr. – May 2018

Semperit AG Wimpassing - Research and Development

Project Researcher - Method evaluation and optimization (*TGA and DSC*)

Sept. 2017	Technical University of Vienna (TU Wien) Lab course assistant - Institute of Applied Synthetic Chemistry
Jul. – Aug. 2017	Semperit AG Wimpassing - Research and Development Laboratory scientist - method development (<i>TGA and DSC</i>)
Jul. – Aug. 2016	Semperit AG Wimpassing - Research and Development Laboratory scientist - Chemical quality control (<i>AAS, DSC, TGA, titrimetric and gravimetric methods</i>)
Feb. 2016	Semperit AG Wimpassing - Research and Development Laboratory scientist - Chemical quality control (<i>AAS, DSC, TGA, titrimetric and gravimetric methods</i>)
Jul. – Sept. 2014	Semperit AG Wimpassing - Research and Development Laboratory scientist - method evaluation and optimization (<i>DSC and TGA</i>)
Jul. – Sept. 2013	Semperit AG Wimpassing - Research and Development Laboratory scientist - Chemical quality control (<i>AAS, DSC, TGA, titrimetric and gravimetric</i>)

Additional Skills

Language Skills

German	native
English	fluent in speech and writing
Italian	basic communication skills
Latin	basic translation skills

IT-Skills

MS-Office (Word, Excel, PPT)	advanced
Chem-Draw	advanced
MestReNova	advanced
Chromeleon	basics
Proteus	basics
Biotyper	basics
Mendeley	advanced

Interests

Music (Guitar, and Drums)
Theater/Art/Photography
Sports (cycling, climbing, athletics...)

5.3 Publications resulting from this thesis

1. **Jandl, B.;** Sedghiniya, S.; Carstens, A.; Astakhova, K. Peptide–Fluorophore Hydrogel as a Signal Boosting Approach in Rapid Detection of Cancer DNA. *ACS Omega* **2019**, 4 (9), 13889–13895. <https://doi.org/10.1021/acsomega.9b01586>.

5.4 References

- (1) Liang, L.; Astruc, D. The Copper(I)-Catalyzed Alkyne-Azide Cycloaddition (CuAAC) "Click" Reaction and Its Applications. An Overview. *Coord. Chem. Rev.* **2011**, *255* (23–24), 2933–2945. <https://doi.org/10.1016/j.ccr.2011.06.028>.
- (2) Kolb, H. C.; Finn, M. G.; Sharpless, K. B. Click Chemistry: Diverse Chemical Function from a Few Good Reactions. *Angew. Chem. Int. Ed. Engl.* **2001**, *40* (11), 2004–2021.
- (3) Benizri, S.; Gissot, A.; Martin, A.; Violet, B.; Grinstaff, M. W.; Barthelemy, P. B. Bioconjugated Oligonucleotides: Recent Developments and Therapeutic Applications. **2019**. <https://doi.org/10.1021/acs.bioconjchem.8b00761>.
- (4) Wu, X.; Shaikh, A. B.; Yu, Y.; Li, Y.; Ni, S.; Lu, A.; Zhang, G. Potential Diagnostic and Therapeutic Applications of Oligonucleotide Aptamers in Breast Cancer. *Int. J. Mol. Sci.* **2017**, *18* (9). <https://doi.org/10.3390/ijms18091851>.
- (5) Wang, D.; Bodovitz, S. Single Cell Analysis: The New Frontier in "Omics." *Trends in Biotechnology.* 2010. <https://doi.org/10.1016/j.tibtech.2010.03.002>.
- (6) Hodzic, E. Single-Cell Analysis: Advances and Future Perspectives. *Bosn. J. basic Med. Sci.* **2016**, *16* (4), 313–314. <https://doi.org/10.17305/bjbms.2016.1371>.
- (7) Zhao, X.; Wu, S.; Fang, N.; Sun, X.; Fan, J. Evaluation of Single-Cell Classifiers for Single-Cell RNA Sequencing Data Sets. *Brief. Bioinform.* **2019**. <https://doi.org/10.1093/bib/bbz096>.
- (8) Pickens, C. J.; Johnson, S. N.; Pressnall, M. M.; Leon, M. A.; Berkland, C. J. Practical Considerations, Challenges, and Limitations of Bioconjugation via Azide-Alkyne Cycloaddition. *Bioconjug. Chem.* **2018**, *29* (3), 686–701. <https://doi.org/10.1021/acs.bioconjchem.7b00633>.
- (9) Letsinger, R. L.; Mahadevan, V.; Fessenden, R. W.; Ogawa, S.; Strauss, H. L.; Katz, T. J.; Fraenkel, G. K.; Silvers tone, H. J.; Wood, D. E.; McConnell, M.; et al. Chart I I a 0 °C-C-Cl4 (a) Communications to the Editor 3527. *J. Am. Chem. Soc.* **1964**, *86* (5), 1481.
- (10) Hughes, R. A.; Ellington, A. D. Synthetic DNA Synthesis and Assembly: Putting the Synthetic in Synthetic Biology. *Cold Spring Harb. Perspect. Biol.* **2017**, *9* (1). <https://doi.org/10.1101/cshperspect.a023812>.
- (11) Wang, L.; Jiang, S.; Chen, C.; He, W.; Wu, X.; Wang, F.; Tong, T.; Zou, X.; Li, Z.; Luo, J.; et al. Synthetic Genomics: From DNA Synthesis to Genome Design. *Angew. Chemie - Int. Ed.* **2018**, *57* (7), 1748–1756. <https://doi.org/10.1002/anie.201708741>.
- (12) Wang, L.; Jiang, S.; Chen, C.; He, W.; Wu, X.; Wang, F.; Tong, T.; Zou, X.; Li, Z.; Luo, J.; et al. Synthetic Genomics: From DNA Synthesis to Genome Design. *Angew. Chemie Int. Ed.* **2017**, *57* (7), 1748–1756. <https://doi.org/10.1002/anie.201708741>.
- (13) Agard, N. J.; Prescher, J. A.; Bertozzi, C. R. A Strain-Promoted [3 + 2] Azide-Alkyne Cycloaddition for Covalent Modification of Biomolecules in Living Systems. *J. Am. Chem. Soc.* **2004**, *126* (46), 15046–15047. <https://doi.org/10.1021/ja044996f>.
- (14) Hogrefe, Richard; Midthune, Brea; Lebedev, A. Current Challenges in Nucleic Acid Synthesis. *Isr. J. Chem.* **2013**, *24*.
- (15) Hillebrand, G. G.; McCluskey, A. H.; Abbott, K. A.; Revich, G. G.; Beattie, K. L. Misincorporation during DNA Synthesis, Analyzed by Gel Electrophoresis. *Nucleic Acids Res.* **1984**, *12* (7), 3155–3171. <https://doi.org/10.1093/nar/12.7.3155>.
- (16) Merrifield, R. B. Synthesis of a Tetrapeptide. *J. Am. Chem. Soc.* **1963**, *85*, 2149–2154.
- (17) Palomo, J. M. Solid-Phase Peptide Synthesis: An Overview Focused on the Preparation of Biologically Relevant Peptides. *RSC Adv.* **2014**, *4* (62), 32658–32672. <https://doi.org/10.1039/c4ra02458c>.
- (18) Presolski, S. I.; Hong, V. P.; Finn, M. G. Copper-Catalyzed Azide-Alkyne Click Chemistry for Bioconjugation. *Curr. Protoc. Chem. Biol.* **2011**, *3* (4), 153–162. <https://doi.org/10.1002/9780470559277.ch110148>.
- (19) Tang, W.; Becker, M. L. "click" Reactions: A Versatile Toolbox for the Synthesis of Peptide-Conjugates. *Chem. Soc. Rev.* **2014**, *43* (20), 7013–7039. <https://doi.org/10.1039/c4cs00139g>.
- (20) Pickens, C. J.; Johnson, S. N.; Pressnall, M. M.; Leon, M. A.; Berkland, C. J. Practical Considerations, Challenges, and Limitations of Bioconjugation via Azide-Alkyne Cycloaddition. *Bioconjug. Chem.* **2018**, *29* (3), 686–701. <https://doi.org/10.1021/acs.bioconjchem.7b00633>.
- (21) Bock, V. D.; Hiemstra, H.; Van Maarseveen, J. H. Cu I-Catalyzed Alkyne-Azide "Click" Cycloadditions from a Mechanistic and Synthetic Perspective. *European J. Org. Chem.* **2006**, *2006* (1), 51–68. <https://doi.org/10.1002/ejoc.200500483>.
- (22) Golas, P. L.; Tsarevsky, N. V.; Sumerlin, B. S.; Matyjaszewski, K. Catalyst Performance in "Click" Coupling Reactions of Polymers Prepared by ATRP: Ligand and Metal Effects. *Macromolecules* **2006**, *39* (19), 6451–6457. <https://doi.org/10.1021/ma061592u>.
- (23) Nair, D. P.; Podgórski, M.; Chatani, S.; Gong, T.; Xi, W.; Fenoli, C. R.; Bowman, C. N. The Thiol-Michael Addition Click Reaction: A Powerful and Widely Used Tool in Materials Chemistry. *Chem. Mater.* **2014**, *26* (1), 724–744. <https://doi.org/10.1021/cm402180t>.
- (24) Hong, V.; Presolski, S. I.; Ma, C.; Finn, M. G. Analysis and Optimization of Copper-Catalyzed Azide-Alkyne Cycloaddition for Bioconjugation. *Angew. Chemie - Int. Ed.* **2009**, *48* (52), 9879–9883. <https://doi.org/10.1002/anie.200905087>.
- (25) Besanceney-Webler, C.; Jiang, H.; Zheng, T.; Feng, L.; Soriano Del Amo, D.; Wang, W.; Klivansky, L. M.; Marlow, F. L.; Liu, Y.; Wu, P. Increasing the Efficacy of Bioorthogonal Click Reactions for Bioconjugation: A Comparative Study. *Angew. Chemie - Int. Ed.* **2011**, *50* (35), 8051–8056. <https://doi.org/10.1002/anie.201101817>.
- (26) Fontaine, S. D.; Reid, R.; Robinson, L.; Ashley, G. W.; Santi, D. V. Long-Term Stabilization of Maleimide-Thiol Conjugates. *Bioconjug. Chem.* **2015**, *26* (1), 145–152. <https://doi.org/10.1021/bc5005262>.
- (27) Northrop, B. H.; Frayne, S. H.; Choudhary, U. Thiol-Maleimide "Click" Chemistry: Evaluating the Influence of Solvent, Initiator, and Thiol on the Reaction Mechanism, Kinetics, and Selectivity. *Polym. Chem.* **2015**, *6* (18), 3415–3430. <https://doi.org/10.1039/C5PY00168D>.
- (28) Meinkoth, J.; Wahl, G. Hybridization of Nucleic Acids Immobilized on Solid Supports. *Anal. Biochem.* **1984**, *138* (2), 267–284.
- (29) Southern, E. M. Detection of Specific Sequences among DNA Fragments Separated by Gel Electrophoresis. *J. Mol. Biol.* **1975**, *98* (3), 503–517. [https://doi.org/10.1016/S0022-2836\(75\)80083-0](https://doi.org/10.1016/S0022-2836(75)80083-0).
- (30) WATSON, J. D.; CRICK, F. H. C. Molecular Structure of Nucleic Acids: A Structure for Deoxyribose Nucleic Acid. *Nature* **1953**, *171* (4356), 737–738. <https://doi.org/10.1038/171737a0>.
- (31) Kim, J. H.; Kalitsis, P.; Pertile, M. D.; Magliano, D.; Wong, L.; Choo, A.; Hudson, D. F. Nucleic Acids: Hybridisation. In *eLS*; John Wiley & Sons, Ltd: Chichester, UK, 2012. <https://doi.org/10.1002/9780470015902.a0003148.pub2>.
- (32) de Planell-Saguer, M.; Rodicio, M. C. Detection Methods for MicroRNAs in Clinic Practice. *Clin. Biochem.* **2013**, *46* (10–11), 869–878. <https://doi.org/10.1016/j.clinbiochem.2013.02.017>.
- (33) Jiang, L.; Qian, J.; Yang, X.; Yan, Y.; Liu, Q.; Wang, K.; Wang, K. Amplified Impedimetric Aptasensor Based on Gold Nanoparticles

- Covalently Bound Graphene Sheet for the Picomolar Detection of Ochratoxin A. *Anal. Chim. Acta* **2014**, *806*, 128–135. <https://doi.org/10.1016/j.aca.2013.11.003>.
- (34) Hindson, B. J.; Ness, K. D.; Masquelier, D. A.; Belgrader, P.; Heredia, N. J.; Makarewicz, A. J.; Bright, I. J.; Lucero, M. Y.; Hiddessen, A. L.; Legler, T. C.; et al. High-Throughput Droplet Digital PCR System for Absolute Quantitation of DNA Copy Number. *Anal. Chem.* **2011**, *83* (22), 8604–8610. <https://doi.org/10.1021/ac202028g>.
- (35) Zuiderwijk, M.; Tanke, H. J.; Sam Niedbala, R.; Corstjens, P. L. A. M. An Amplification-Free Hybridization-Based DNA Assay to Detect *Streptococcus Pneumoniae* Utilizing the up-Converting Phosphor Technology. *Clin. Biochem.* **2003**, *36* (5), 401–403. [https://doi.org/10.1016/S0009-9120\(03\)00057-2](https://doi.org/10.1016/S0009-9120(03)00057-2).
- (36) Jin, Z.; Geißler, D.; Qiu, X.; Wegner, K. D.; Hildebrandt, N. A Rapid, Amplification-Free, and Sensitive Diagnostic Assay for Single-Step Multiplexed Fluorescence Detection of MicroRNA. *Angew. Chemie Int. Ed.* **2015**, *54* (34), 10024–10029. <https://doi.org/10.1002/anie.201504887>.
- (37) Lesner, A. Reporter Fluorescent Molecules in Biological Systems: The Current Overview. *Biochem. Anal. Biochem.* **2012**, *01* (04), 1–3. <https://doi.org/10.4172/2161-1009.1000e111>.
- (38) Juskowiak, B. Nucleic Acid-Based Fluorescent Probes and Their Analytical Potential. *Anal. Bioanal. Chem.* **2011**, *399* (9), 3157–3176. <https://doi.org/10.1007/s00216-010-4304-5>.
- (39) Marras, S. A. E.; Kramer, F. R.; Tyagi, S. Efficiencies of Fluorescence Resonance Energy Transfer and Contact-Mediated Quenching in Oligonucleotide Probes. *Nucleic Acids Res.* **2002**, *30* (21), e122.
- (40) Herzenberg, L. A.; Sweet, R. G.; Herzenberg, L. A. Fluorescence-Activated Cell Sorting. *Sci. Am.* **1976**, *234* (3), 108–117.
- (41) Gross, A.; Schoendube, J.; Zimmermann, S.; Steeb, M.; Zengerle, R.; Koltay, P. Technologies for Single-Cell Isolation. *Int. J. Mol. Sci.* **2015**, *16* (8), 16897. <https://doi.org/10.3390/IJMS160816897>.
- (42) Emmert-Buck, M. R.; Bonner, R. F.; Smith, P. D.; Chuaqui, R. F.; Zhuang, Z.; Goldstein, S. R.; Weiss, R. A.; Liotta, L. A. Laser Capture Microdissection. *Science* **1996**, *274* (5289), 998–1001.
- (43) Hu, P.; Zhang, W.; Xin, H.; Deng, G. Single Cell Isolation and Analysis. *Front. Cell Dev. Biol.* **2016**, *4*. <https://doi.org/10.3389/FCELL.2016.00116>.
- (44) Hwang, B.; Lee, J. H.; Bang, D. Single-Cell RNA Sequencing Technologies and Bioinformatics Pipelines. *Exp. Mol. Med.* **2018**, *50* (8), 96. <https://doi.org/10.1038/s12276-018-0071-8>.
- (45) Bandura, D. R.; Baranov, V. I.; Ornatsky, O. I.; Antonov, A.; Kinach, R.; Lou, X.; Pavlov, S.; Vorobiev, S.; Dick, J. E.; Tanner, S. D. Mass Cytometry: Technique for Real Time Single Cell Multitarget Immunoassay Based on Inductively Coupled Plasma Time-of-Flight Mass Spectrometry. *Anal. Chem.* **2009**, *81* (16), 6813–6822. <https://doi.org/10.1021/ac901049w>.
- (46) Spitzer, M. H.; Nolan, G. P. Mass Cytometry: Single Cells, Many Features. *Cell* **2016**, *165* (4), 780–791. <https://doi.org/10.1016/j.cell.2016.04.019>.
- (47) Schatz, D. G.; Swanson, P. C. V(D)J Recombination: Mechanisms of Initiation. *Annu. Rev. Genet.* **2011**, *45* (1), 167–202. <https://doi.org/10.1146/annurev-genet-110410-132552>.
- (48) Heath, J. R.; Ribas, A.; Mischel, P. S. Single-Cell Analysis Tools for Drug Discovery and Development. *Nat. Rev. Drug Discov.* **2016**, *15* (3), 204–216. <https://doi.org/10.1038/nrd.2015.16>.
- (49) Kanter, I.; Kalisky, T. Single Cell Transcriptomics: Methods and Applications. *Front. Oncol.* **2015**, *5*, 53. <https://doi.org/10.3389/fonc.2015.00053>.
- (50) Bacher, R.; Kendziorski, C. Design and Computational Analysis of Single-Cell RNA-Sequencing Experiments. *Genome Biol.* **2016**, *17* (1), 63. <https://doi.org/10.1186/s13059-016-0927-y>.
- (51) Su, Y.; Shi, Q.; Wei, W. Single Cell Proteomics in Biomedicine: High-Dimensional Data Acquisition, Visualization, and Analysis. *Proteomics* **2017**, *17* (3–4), 1600267. <https://doi.org/10.1002/pmic.201600267>.
- (52) Gawad, C.; Koh, W.; Quake, S. R. Single-Cell Genome Sequencing: Current State of the Science. *Nat. Rev. Genet.* **2016**, *17* (3), 175–188. <https://doi.org/10.1038/nrg.2015.16>.
- (53) Mullis, K. B. The Unusual Origin of the Polymerase Chain Reaction. *Sci. Am.* **1990**, *262* (4), 56–61, 64–65.
- (54) Saiki, R. K.; Scharf, S.; Faloona, F.; Mullis, K. B.; Horn, G. T.; Erlich, H. A.; Arnheim, N. Enzymatic Amplification of Beta-Globin Genomic Sequences and Restriction Site Analysis for Diagnosis of Sickle Cell Anemia. *Science* **1985**, *230* (4732), 1350–1354.
- (55) Shendure, J.; Balasubramanian, S.; Church, G. M.; Gilbert, W.; Rogers, J.; Schloss, J. A.; Waterston, R. H. DNA Sequencing at 40: Past, Present and Future. *Nature* **2017**, *550* (7676), 345–353. <https://doi.org/10.1038/nature24286>.
- (56) Holley, R. W.; Apgar, J.; Everett, G. A.; Madison, J. T.; Marquisee, M.; Merrill, S. H.; Penswick, J. R.; Zamir, A. Structure of a Ribonucleic Acid. *Science*. American Association for the Advancement of Science pp 1462–1465. <https://doi.org/10.2307/1715055>.
- (57) Levene, M. J.; Korlach, J.; Turner, S. W.; Foquet, M.; Craighead, H. G.; Webb, W. W. Zero-Mode Waveguides for Single-Molecule Analysis at High Concentrations. *Science (80-.)*. **2003**, *299* (5607), 682–686. <https://doi.org/10.1126/science.1079700>.
- (58) Eid, J.; Fehr, A.; Gray, J.; Luong, K.; Lyle, J.; Otto, G.; Peluso, P.; Rank, D.; Baybayan, P.; Bettman, B.; et al. Real-Time DNA Sequencing from Single Polymerase Molecules. *Science (80-.)*. **2009**, *323* (5910), 133–138. <https://doi.org/10.1126/science.1162986>.
- (59) Telenius, H.; Carter, N. P.; Bebb, C. E.; Nordenskjöld, M.; Ponder, B. A.; Tunnacliffe, A. Degenerate Oligonucleotide-Primed PCR: General Amplification of Target DNA by a Single Degenerate Primer. *Genomics* **1992**, *13* (3), 718–725.
- (60) Zhang, D.; Brandwein, M.; Hsuih, T.; Li, H. B. Ramification Amplification: A Novel Isothermal DNA Amplification Method. *Mol. Diagnosis* **2001**, *6* (2), 141–150. <https://doi.org/10.1054/modi.2001.25323>.
- (61) Langmore, J. P. Rubicon Genomics, Inc. *Pharmacogenomics* **2002**, *3* (4), 557–560. <https://doi.org/10.1517/14622416.3.4.557>.
- (62) Zong, C.; Lu, S.; Chapman, A. R.; Xie, X. S. Genome-Wide Detection of Single-Nucleotide and Copy-Number Variations of a Single Human Cell. *Science (80-.)*. **2012**, *338* (6114), 1622–1626. <https://doi.org/10.1126/science.1229164>.
- (63) Theodor Förster. *Delocalized Excitation and Excitation Transfer - Theodor Förster - Google Books*.
- (64) Förster, T. Energiewanderung Und Fluoreszenz. *Naturwissenschaften* **1946**, *33* (6), 166–175. <https://doi.org/10.1007/BF00585226>.
- (65) Lerner, E.; Cordes, T.; Ingargiola, A.; Alhadid, Y.; Chung, S.; Michalet, X.; Weiss, S. Toward Dynamic Structural Biology: Two Decades of Single-Molecule Förster Resonance Energy Transfer. *Science (80-.)*. **2018**, *359* (6373), eaan1133. <https://doi.org/10.1126/science.aan1133>.
- (66) Didenko, V. V. DNA Probes Using Fluorescence Resonance Energy Transfer (FRET): Designs and Applications. *Biotechniques* **2001**, *31* (5), 1106–1121. <https://doi.org/10.2144/01315rv02>.
- (67) Zheng, J.; Yang, R.; Shi, M.; Wu, C.; Fang, X.; Li, Y.; Li, J.; Tan, W. Rationally Designed Molecular Beacons for Bioanalytical and Biomedical Applications. *Chem. Soc. Rev.* **2015**, *44* (10), 3036–3055. <https://doi.org/10.1039/C5CS00020C>.

- (68) Wang, K.; Tang, Z.; Yang, C. J.; Kim, Y.; Fang, X.; Li, W.; Wu, Y.; Medley, C. D.; Cao, Z.; Li, J.; et al. Molecular Engineering of DNA: Molecular Beacons. *Angew. Chem. Int. Ed. Engl.* **2009**, *48* (5), 856–870. <https://doi.org/10.1002/anie.200800370>.
- (69) Tyagi, S.; Kramer, F. R. Molecular Beacons: Probes That Fluoresce upon Hybridization. *Nat. Biotechnol.* **1996**, *14* (3), 303–308. <https://doi.org/10.1038/nbt0396-303>.
- (70) Stobiecka, M.; Chafupa, A. Biosensors Based on Molecular Beacons. *Chem. Pap.* **2015**, *69* (1). <https://doi.org/10.1515/chempap-2015-0026>.
- (71) Hepel, M.; Stobiecka, M.; Peachey, J.; Miller, J. Intervention of Glutathione in Pre-Mutagenic Catechol-Mediated DNA Damage in the Presence of Copper(II) Ions. *Mutat. Res.* **2012**, *735* (1–2), 1–11. <https://doi.org/10.1016/j.mrfmmm.2012.05.005>.
- (72) Caliendo, A. M.; Gilbert, D. N.; Ginocchio, C. C.; Hanson, K. E.; May, L.; Quinn, T. C.; Tenover, F. C.; Alland, D.; Blaschke, A. J.; Bonomo, R. A.; et al. Better Tests, Better Care: Improved Diagnostics for Infectious Diseases. *Clin. Infect. Dis.* **2013**, *57* (suppl 3), S139–S170. <https://doi.org/10.1093/cid/cit578>.
- (73) Venter, J. C.; Adams, M. D.; Myers, E. W.; Li, P. W.; Mural, R. J.; Sutton, G. G.; Smith, H. O.; Yandell, M.; Evans, C. A.; Holt, R. A.; et al. The Sequence of the Human Genome. *Science* **2001**, *291* (5507), 1304–1351. <https://doi.org/10.1126/science.1058040>.
- (74) Cancer Genome Atlas Network. Comprehensive Genomic Characterization of Head and Neck Squamous Cell Carcinomas. *Nature* **2015**, *517* (7536), 576–582. <https://doi.org/10.1038/nature14129>.
- (75) McLendon, R.; Friedman, A.; Bigner, D.; Van Meir, E. G.; Brat, D. J.; M. Mastrogiannis, G.; Olson, J. J.; Mikkelsen, T.; Lehman, N.; Aldape, K.; et al. Comprehensive Genomic Characterization Defines Human Glioblastoma Genes and Core Pathways. *Nature* **2008**, *455* (7216), 1061–1068. <https://doi.org/10.1038/nature07385>.
- (76) Roy, S. Molecular Pathology Informatics. *Surg. Pathol. Clin.* **2015**, *8* (2), 187–194. <https://doi.org/10.1016/J.PATH.2015.02.013>.
- (77) Nagahashi, M.; Wakai, T.; Shimada, Y.; Ichikawa, H.; Kameyama, H.; Kobayashi, T.; Sakata, J.; Yagi, R.; Sato, N.; Kitagawa, Y.; et al. Genomic Landscape of Colorectal Cancer in Japan: Clinical Implications of Comprehensive Genomic Sequencing for Precision Medicine. *Genome Med.* **2016**, *8* (1), 136. <https://doi.org/10.1186/s13073-016-0387-8>.
- (78) Daniel A. Goldstein, M. W. L. S. M. C. R. F. M. M. Costs and Effectiveness of Genomic Testing in the Management of Colorectal Cancer. **2015**.
- (79) Méhes, G. Liquid Biopsy for Predictive Mutational Profiling of Solid Cancer: The Pathologist’s Perspective. *J. Biotechnol.* **2019**, *297*, 66–70. <https://doi.org/10.1016/j.jbiotec.2019.04.002>.
- (80) Cangiarella, J.; Simsir, A. Advantages and Disadvantages of FNA and Core Biopsies: Diagnostic Accuracy and Precision for Aspiration Biopsy in the Diagnosis of Lesions of the Breast. In *Breast Cytohistology*; Cangiarella, J., Simsir, A., Tabbara, S. O., Eds.; Cambridge University Press: Cambridge, 2013; pp 19–26. <https://doi.org/10.1017/CBO9780511979941.002>.
- (81) Zheng, P.; Liang, C.; Ren, L.; Zhu, D.; Feng, Q.; Chang, W.; He, G.; Ye, L.; Chen, J.; Lin, Q.; et al. Additional Biomarkers beyond RAS That Impact the Efficacy of Cetuximab plus Chemotherapy in MCRC: A Retrospective Biomarker Analysis. *J. Oncol.* **2018**, *2018*, 1–14. <https://doi.org/10.1155/2018/5072987>.
- (82) Politaki, E.; Agelaki, S.; Apostolaki, S.; Hatzidakis, D.; Strati, A.; Koinis, F.; Perraki, M.; Saloustrou, G.; Stoupis, G.; Kallergi, G.; et al. A Comparison of Three Methods for the Detection of Circulating Tumor Cells in Patients with Early and Metastatic Breast Cancer. *Cell. Physiol. Biochem.* **2017**, *44* (2), 594–606. <https://doi.org/10.1159/000485115>.
- (83) Schindlbeck, C.; Andergassen, U.; Jueckstock, J.; Rack, B.; Janni, W.; Jeschke, U. Disseminated and Circulating Tumor Cells in Bone Marrow and Blood of Breast Cancer Patients: Properties, Enrichment, and Potential Targets. *J. Cancer Res. Clin. Oncol.* **2016**, *142* (9), 1883–1895. <https://doi.org/10.1007/s00432-016-2118-3>.
- (84) Manier, S.; Park, J.; Capelletti, M.; Bustoros, M.; Freeman, S. S.; Ha, G.; Rhoades, J.; Liu, C. J.; Huynh, D.; Reed, S. C.; et al. Whole-Exome Sequencing of Cell-Free DNA and Circulating Tumor Cells in Multiple Myeloma. <https://doi.org/10.1038/s41467-018-04001-5>.
- (85) Ellison, G.; Zhu, G.; Moulis, A.; Dearden, S.; Speake, G.; McCormack, R. EGFR Mutation Testing in Lung Cancer: A Review of Available Methods and Their Use for Analysis of Tumour Tissue and Cytology Samples. *J Clin Pathol* **2013**. <https://doi.org/10.1136/jclinpath-2012-201194>.
- (86) Sueoka, N.; Sato, A.; Eguchi, H.; Komiya, K.; Sakuragi, T.; Mitsuoka, M.; Satoh, T.; Hayashi, S.; Nakachi, K.; Sueoka, E. Mutation Profile of EGFR Gene Detected by Denaturing High-Performance Liquid Chromatography in Japanese Lung Cancer Patients. *J. Cancer Res. Clin. Oncol.* **2006**, *133* (2), 93–102. <https://doi.org/10.1007/s00432-006-0144-2>.
- (87) Do, H.; Krypuy, M.; Mitchell, P. L.; Fox, S. B.; Dobrovic, A. High Resolution Melting Analysis for Rapid and Sensitive EGFR and KRAS Mutation Detection in Formalin Fixed Paraffin Embedded Biopsies. *BMC Cancer* **2008**, *8* (1), 142. <https://doi.org/10.1186/1471-2407-8-142>.
- (88) Janne, P. A.; Borras, A. M.; Kuang, Y.; Rogers, A. M.; Joshi, V. A.; Liyanage, H.; Lindeman, N.; Lee, J. C.; Halmos, B.; Maher, E. A.; et al. A Rapid and Sensitive Enzymatic Method for Epidermal Growth Factor Receptor Mutation Screening. *Clin. Cancer Res.* **2006**, *12* (3), 751–758. <https://doi.org/10.1158/1078-0432.CCR-05-2047>.
- (89) Ellison, G.; Donald, E.; McWalter, G.; Knight, L.; Fletcher, L.; Sherwood, J.; Cantarini, M.; Orr, M.; Speake, G. A Comparison of ARMS and DNA Sequencing for Mutation Analysis in Clinical Biopsy Samples. *J. Exp. Clin. Cancer Res.* **2010**, *29* (1), 132. <https://doi.org/10.1186/1756-9966-29-132>.
- (90) Pan, Q.; Pao, W.; Ladanyi, M. Rapid Polymerase Chain Reaction-Based Detection of Epidermal Growth Factor Receptor Gene Mutations in Lung Adenocarcinomas. *J. Mol. Diagnostics* **2005**, *7* (3), 396–403. [https://doi.org/10.1016/S1525-1578\(10\)60569-7](https://doi.org/10.1016/S1525-1578(10)60569-7).
- (91) Dufort, S.; Richard, M.-J.; Lantuejoul, S.; de Fraipont, F. Pyrosequencing, a Method Approved to Detect the Two Major EGFR Mutations for Anti EGFR Therapy in NSCLC. *J. Exp. Clin. Cancer Res.* **2011**, *30* (1), 57. <https://doi.org/10.1186/1756-9966-30-57>.
- (92) Yang, Q.; Qiu, T.; Wu, W.; Zhu, C.; Liu, L.; Ying, J.; Wang, S. Simple and Sensitive Method for Detecting Point Mutations of Epidermal Growth Factor Receptor Using Cationic Conjugated Polymers. *ACS Appl. Mater. Interfaces* **2011**, *3* (11), 4539–4545. <https://doi.org/10.1021/am201248y>.
- (93) Bylicki, O.; Paleiron, N.; Margery, J.; Guisier, F.; Vergnenegre, A.; Robinet, G.; Auliac, J.-B.; Gervais, R.; Chouaid, C. Targeting the PD-1/PD-L1 Immune Checkpoint in EGFR-Mutated or ALK-Translocated Non-Small-Cell Lung Cancer. *Target. Oncol.* **2017**, *12* (5), 563–569. <https://doi.org/10.1007/s11523-017-0510-9>.
- (94) Berghoff, A. S.; Bellosillo, B.; Caux, C.; de Langen, A.; Mazieres, J.; Normanno, N.; Preusser, M.; Provencio, M.; Rojo, F.; Wolf, J.; et al. Immune Checkpoint Inhibitor Treatment in Patients with Oncogene- Addicted Non-Small Cell Lung Cancer (NSCLC): Summary of a Multidisciplinary Round-Table Discussion. *ESMO Open* **2019**, *4* (3), e000498. <https://doi.org/10.1136/esmooopen-2019-000498>.
- (95) Gall, J. G.; Pardue, M. L. Formation and Detection of RNA-DNA Hybrid Molecules in Cytological Preparations. *Proc. Natl. Acad. Sci.*

- U. S. A. **1969**, *63* (2), 378–383.
- (96) RUDKIN, G. T.; STOLLAR, B. D. High Resolution Detection of DNA–RNA Hybrids in Situ by Indirect Immunofluorescence. *Nature* **1977**, *265* (5593), 472–473. <https://doi.org/10.1038/265472a0>.
- (97) Hu, L.; Ru, K.; Zhang, L.; Huang, Y.; Zhu, X.; Liu, H.; Zetterberg, A.; Cheng, T.; Miao, W. Fluorescence in Situ Hybridization (FISH): An Increasingly Demanded Tool for Biomarker Research and Personalized Medicine. *Biomark. Res.* **2014**, *2* (1), 3. <https://doi.org/10.1186/2050-7771-2-3>.
- (98) Espinosa, R.; Le Beau, M. M. Gene Mapping by FISH. *Methods Mol. Biol.* **1997**, *68*, 53–76.
- (99) Theisen, A. Microarray - Based Comparative Genomic Hybridization (ACGH). *Nat. Educ.* **2008**, *1*, 45.
- (100) Chial, H. Cytogenetic Methods and Disease: Flow Cytometry, CGH, and FISH. *Nat. Educ.* **2008**, *1* (1), 76.
- (101) Shayesteh, L.; Lu, Y.; Kuo, W.-L.; Baldocchi, R.; Godfrey, T.; Collins, C.; Pinkel, D.; Powell, B.; Mills, G. B.; Gray, J. W. PIK3CA Is Implicated as an Oncogene in Ovarian Cancer. *Nat. Genet.* **1999**, *21* (1), 99–102. <https://doi.org/10.1038/5042>.
- (102) Anselmo, A. C.; Mitragotri, S. Nanoparticles in the Clinic. *Bioeng. Transl. Med.* **2016**, *1* (1), 10–29. <https://doi.org/10.1002/btm2.10003>.
- (103) Pinkel, D.; Segraves, R.; Sudar, D.; Clark, S.; Poole, I.; Kowbel, D.; Collins, C.; Kuo, W.-L.; Chen, C.; Zhai, Y.; et al. High Resolution Analysis of DNA Copy Number Variation Using Comparative Genomic Hybridization to Microarrays. *Nat. Genet.* **1998**, *20* (2), 207–211. <https://doi.org/10.1038/2524>.
- (104) DeRisi, J. L.; Iyer, V. R.; Brown, P. O. Exploring the Metabolic and Genetic Control of Gene Expression on a Genomic Scale. *Science* **1997**, *278* (5338), 680–686.
- (105) Deng, N.; Zhou, H.; Fan, H.; Yuan, Y. Single Nucleotide Polymorphisms and Cancer Susceptibility. *Oncotarget* **2017**, *8* (66), 110635–110649. <https://doi.org/10.18632/oncotarget.22372>.
- (106) Erichsen, H. C.; Chanock, S. J. SNPs in Cancer Research and Treatment. *Br. J. Cancer* **2004**, *90* (4), 747–751. <https://doi.org/10.1038/sj.bjc.6601574>.
- (107) Stankiewicz, P.; Beaudet, A. L. Use of Array CGH in the Evaluation of Dysmorphology, Malformations, Developmental Delay, and Idiopathic Mental Retardation. *Curr. Opin. Genet. Dev.* **2007**, *17* (3), 182–192. <https://doi.org/10.1016/j.gde.2007.04.009>.
- (108) Lupski, J. R. Brain Copy Number Variants and Neuropsychiatric Traits. *Biol. Psychiatry* **2012**, *72* (8), 617–619. <https://doi.org/10.1016/j.biopsych.2012.08.007>.
- (109) Wiszniewska, J.; Bi, W.; Shaw, C.; Stankiewicz, P.; Kang, S.-H. L.; Pursley, A. N.; Lalani, S.; Hixson, P.; Gambin, T.; Tsai, C.-H.; et al. Combined Array CGH plus SNP Genome Analyses in a Single Assay for Optimized Clinical Testing. *Eur. J. Hum. Genet.* **2014**, *22*, 79–87. <https://doi.org/10.1038/ejhg.2013.77>.
- (110) Rovelet-Lecrux, A.; Hannequin, D.; Raux, G.; Meur, N. Le; Laquerrière, A.; Vital, A.; Dumanchin, C.; Feuillette, S.; Brice, A.; Vercelletto, M.; et al. APP Locus Duplication Causes Autosomal Dominant Early-Onset Alzheimer Disease with Cerebral Amyloid Angiopathy. *Nat. Genet.* **2006**, *38* (1), 24–26. <https://doi.org/10.1038/ng1718>.
- (111) Toft, M.; Ross, O. A. Copy Number Variation in Parkinson's Disease. *Genome Med.* **2010**, *2* (9), 62. <https://doi.org/10.1186/gm183>.
- (112) Fellermann, K.; Stange, D. E.; Schaeffeler, E.; Schmalz, H.; Wehkamp, J.; Bevins, C. L.; Reinisch, W.; Teml, A.; Schwab, M.; Lichter, P.; et al. A Chromosome 8 Gene-Cluster Polymorphism with Low Human Beta-Defensin 2 Gene Copy Number Predisposes to Crohn Disease of the Colon. *Am. J. Hum. Genet.* **2006**, *79* (3), 439–448. <https://doi.org/10.1086/505915>.
- (113) Sebat, J.; Lakshmi, B.; Malhotra, D.; Troge, J.; Lese-Martin, C.; Walsh, T.; Yamrom, B.; Yoon, S.; Krasnitz, A.; Kendall, J.; et al. Strong Association of De Novo Copy Number Mutations with Autism. *Science* (80-.). **2007**, *316* (5823), 445–449. <https://doi.org/10.1126/science.1138659>.
- (114) Rosenblum, D.; Joshi, N.; Tao, W.; Karp, J. M.; Peer, D. Progress and Challenges towards Targeted Delivery of Cancer Therapeutics. *Nat. Commun.* **2018**. <https://doi.org/10.1038/s41467-018-03705-y>.
- (115) Peer, D.; Karp, J. M.; Hong, S.; Farokhzad, O. C.; Margalit, R.; Langer, R. Nanocarriers as an Emerging Platform for Cancer Therapy. *Nat. Nanotechnol.* **2007**, *2* (12), 751–760. <https://doi.org/10.1038/nnano.2007.387>.
- (116) Sadauskas, E.; Wallin, H.; Stoltenberg, M.; Vogel, U.; Doering, P.; Larsen, A.; Danscher, G. Kupffer Cells Are Central in the Removal of Nanoparticles from the Organism. *Part. Fibre Toxicol.* **2007**, *4*, 10. <https://doi.org/10.1186/1743-8977-4-10>.
- (117) Rosenblum, D.; Peer, D. Omics-Based Nanomedicine: The Future of Personalized Oncology. *Cancer Lett.* **2014**, *352* (1), 126–136. <https://doi.org/10.1016/j.canlet.2013.07.029>.
- (118) Villaverde, G.; Baeza, A. Targeting Strategies for Improving the Efficacy of Nanomedicine in Oncology. *Beilstein J. Nanotechnol.* **2019**, *10*, 168–181. <https://doi.org/10.3762/bjnano.10.16>.
- (119) Nichols, J. W.; Bae, Y. H. EPR: Evidence and Fallacy. *J. Control. Release* **2014**, *190*, 451–464. <https://doi.org/10.1016/j.jconrel.2014.03.057>.
- (120) Netti, P. A.; Baxter, L. T.; Boucher, Y.; Skalak, R.; Jain, R. K. Time-Dependent Behavior of Interstitial Fluid Pressure in Solid Tumors: Implications for Drug Delivery. *Cancer Res.* **1995**, *55* (22), 5451–5458.
- (121) Raavé, R.; van Kuppevelt, T. H.; Daamen, W. F. Chemotherapeutic Drug Delivery by Tumoral Extracellular Matrix Targeting. *J. Control. Release* **2018**, *274*, 1–8. <https://doi.org/10.1016/j.jconrel.2018.01.029>.
- (122) Villegas, M. R.; Baeza, A.; Vallet-Regí, M. Hybrid Collagenase Nanocapsules for Enhanced Nanocarrier Penetration in Tumoral Tissues. *ACS Appl. Mater. Interfaces* **2015**, *7* (43), 24075–24081. <https://doi.org/10.1021/acsami.5b07116>.
- (123) Gupta, P. K. Drug Targeting in Cancer Chemotherapy: A Clinical Perspective. *J. Pharm. Sci.* **1990**, *79* (11), 949–962. <https://doi.org/10.1002/jps.2600791102>.
- (124) Kreuter, J. Nanoparticles—a Historical Perspective. *Int. J. Pharm.* **2007**, *331* (1), 1–10. <https://doi.org/10.1016/j.ijpharm.2006.10.021>.
- (125) Hossen, S.; Hossain, M. K.; Basher, M. K.; Mia, M. N. H.; Rahman, M. T.; Uddin, M. J. Smart Nanocarrier-Based Drug Delivery Systems for Cancer Therapy and Toxicity Studies: A Review. *J. Adv. Res.* **2019**, *15*, 1–18. <https://doi.org/10.1016/j.jare.2018.06.005>.
- (126) Sercombe, L.; Veerati, T.; Moheimani, F.; Wu, S. Y.; Sood, A. K.; Hua, S. Advances and Challenges of Liposome Assisted Drug Delivery. *Front. Pharmacol.* **2015**, *6*, 286. <https://doi.org/10.3389/fphar.2015.00286>.
- (127) Szebeni, J.; Moghimi, S. M. Liposome Triggering of Innate Immune Responses: A Perspective on Benefits and Adverse Reactions. *J. Liposome Res.* **2009**, *19* (2), 85–90. <https://doi.org/10.1080/08982100902792855>.
- (128) Gregoriadis, G. Drug Entrapment in Liposomes. *FEBS Lett.* **1973**, *36* (3), 292–296.
- (129) Bangham, A. D. Properties and Uses of Lipid Vesicles: An Overview. *Ann. N. Y. Acad. Sci.* **1978**, *308*, 2–7.
- (130) Szoka, F.; Papahadjopoulos, D.; Papahadjopoulos, D. Procedure for Preparation of Liposomes with Large Internal Aqueous Space

- and High Capture by Reverse-Phase Evaporation. *Proc. Natl. Acad. Sci. U. S. A.* **1978**, *75* (9), 4194–4198.
- (131) Zumbuehl, O.; Weder, H. G. Liposomes of Controllable Size in the Range of 40 to 180 Nm by Defined Dialysis of Lipid/Detergent Mixed Micelles. *Biochim. Biophys. Acta* **1981**, *640* (1), 252–262.
- (132) Lesoin, L.; Crampon, C.; Boutin, O.; Badens, E. The Journal of Supercritical Fluids Preparation of Liposomes Using the Supercritical Anti-Solvent (SAS) Process and Comparison with a Conventional Method. *J. Supercrit. Fluids* **2011**, *57*, 162–174. <https://doi.org/10.1016/j.supflu.2011.01.006>.
- (133) Otake, K.; Shimomura, T.; Goto, T.; Imura, T.; Furuya, T.; Yoda, S.; Takebayashi, Y.; Sakai, H.; Abe, M. Preparation of Liposomes Using an Improved Supercritical Reverse Phase Evaporation Method. *Langmuir* **2006**, *22* (6), 2543–2550. <https://doi.org/10.1021/la051654u>.
- (134) Noble, G. T.; Stefanick, J. F.; Ashley, J. D.; Kiziltepe, T.; Bilgicer, B. Ligand-Targeted Liposome Design: Challenges and Fundamental Considerations. *Trends Biotechnol.* **2014**, *32* (1), 32–45. <https://doi.org/10.1016/j.tibtech.2013.09.007>.
- (135) Ruoslahti, E. Peptides as Targeting Elements and Tissue Penetration Devices for Nanoparticles. *Adv. Mater.* **2012**, *24* (28), 3747–3756. <https://doi.org/10.1002/adma.201200454>.
- (136) Samson, A. A. S.; Park, S.; Kim, S.-Y.; Min, D.-H.; Jeon, N. L.; Song, J. M. Liposomal Co-Delivery-Based Quantitative Evaluation of Chemosensitivity Enhancement in Breast Cancer Stem Cells by Knockdown of GRP78/CLU. *J. Liposome Res.* **2019**, *29* (1), 44–52. <https://doi.org/10.1080/08982104.2017.1420081>.
- (137) Zhang, L.; Ren, Y.; Wang, Y.; He, Y.; Feng, W.; Song, C. Pharmacokinetics, Distribution and Anti-Tumor Efficacy of Liposomal Mitoxantrone Modified with a Luteinizing Hormone-Releasing Hormone Receptor-Specific Peptide. *Int. J. Nanomedicine* **2018**, *Volume 13*, 1097–1105. <https://doi.org/10.2147/IJN.S150512>.
- (138) Sercombe, L.; Veerati, T.; Moheimani, F.; Wu, S. Y.; Sood, A. K.; Hua, S. Advances and Challenges of Liposome Assisted Drug Delivery. *Front. Pharmacol.* **2015**, *6*, 286. <https://doi.org/10.3389/fphar.2015.00286>.
- (139) Choi, S.; Kim, W.; Kim, J. Surface Modification of Functional Nanoparticles for Controlled Drug Delivery. *J. Dispers. Sci. Technol.* **2003**, *24* (3–4), 475–487. <https://doi.org/10.1081/DIS-120021803>.
- (140) Saha, R. N.; Vasanthakumar, S.; Bende, G.; Snehalatha, M. Molecular Membrane Biology Nanoparticulate Drug Delivery Systems for Cancer Chemotherapy Nanoparticulate Drug Delivery Systems for Cancer Chemotherapy. *Mol. Membr. Biol.* **2010**, *27* (7), 215–231. <https://doi.org/10.3109/09687688.2010.510804>.
- (141) Dufès, C.; Al Robaian, M.; Somani, S. Transferrin and the Transferrin Receptor for the Targeted Delivery of Therapeutic Agents to the Brain and Cancer Cells. *Ther. Deliv.* **2013**, *4* (5), 629–640. <https://doi.org/10.4155/tde.13.21>.
- (142) Yin, W.; Rogge, M. Targeting RNA: A Transformative Therapeutic Strategy. *Clin. Transl. Sci.* **2019**, *12* (2), 98–112. <https://doi.org/10.1111/cts.12624>.
- (143) Moss, K. H.; Popova, P.; Hadrup, S. R.; Astakhova, K.; Taskova, M. Lipid Nanoparticles for Delivery of Therapeutic RNA Oligonucleotides. *Mol. Pharm.* **2019**, *16* (6), 2265–2277. <https://doi.org/10.1021/acs.molpharmaceut.8b01290>.
- (144) Hawkins, P. N.; Ando, Y.; Dispenzeri, A.; Gonzalez-Duarte, A.; Adams, D.; Suhr, O. B. Evolving Landscape in the Management of Transthyretin Amyloidosis. *Ann. Med.* **2015**, *47* (8), 625–638. <https://doi.org/10.3109/07853890.2015.1068949>.
- (145) Khalil, I. A.; Yamada, Y.; Harashima, H. Optimization of siRNA Delivery to Target Sites: Issues and Future Directions. *Expert Opin. Drug Deliv.* **2018**, *15* (11), 1053–1065. <https://doi.org/10.1080/17425247.2018.1520836>.
- (146) Adams, D.; Gonzalez-Duarte, A.; O’Riordan, W. D.; Yang, C.-C.; Ueda, M.; Kristen, A. V.; Tourneir, I.; Schmidt, H. H.; Coelho, T.; Berk, J. L.; et al. Patisiran, an RNAi Therapeutic, for Hereditary Transthyretin Amyloidosis. *N. Engl. J. Med.* **2018**, *379* (1), 11–21. <https://doi.org/10.1056/NEJMoa1716153>.
- (147) Hong, V.; Steinmetz, N. F.; Manchester, M.; Finn, M. G. Labeling Live Cells by Copper-Catalyzed Alkyne–Azide Click Chemistry. *Bioconj. Chem.* **2010**, *21* (10), 1912–1916. <https://doi.org/10.1021/bc100272z>.
- (148) Hacker, S. M.; Backus, K. M.; Lazear, M. R.; Forli, S.; Correia, B. E.; Cravatt, B. F.; Author, N. C. Global Profiling of Lysine Reactivity and Ligandability in the Human Proteome HHS Public Access Author Manuscript. *Nat Chem* **2017**, *9* (12), 1181–1190. <https://doi.org/10.1038/nchem.2826>.
- (149) Abello, N.; Kerstjens, H. A. M.; Postma, D. S.; Bischoff, R. Selective Acylation of Primary Amines in Peptides and Proteins. *J. Proteome Res.* **2007**, *6* (12), 4770–4776. <https://doi.org/10.1021/pr070154e>.
- (150) Khushman, M.; Bhardwaj, A.; Patel, G. K.; Laurini, J. A.; Roveda, K.; Tan, M. C.; Patton, M. C.; Singh, S.; Taylor, W.; Singh, A. P. Exosomal Markers (CD63 and CD9) Expression Pattern Using Immunohistochemistry in Resected Malignant and Nonmalignant Pancreatic Specimens. *Pancreas* **2017**, *46* (6), 782–788. <https://doi.org/10.1097/MPA.0000000000000847>.
- (151) Löttsch, B.; Dölle, S.; Vieths, S.; Worm, M. Exploratory Analysis of CD63 and CD203c Expression in Basophils from Hazelnut Sensitized and Allergic Individuals. *Clin. Transl. Allergy* **2016**, *6* (1), 45. <https://doi.org/10.1186/s13601-016-0134-7>.
- (152) Vences-Catalán, F.; Levy, S. Immune Targeting of Tetraspanins Involved in Cell Invasion and Metastasis. *Front. Immunol.* **2018**, *9*, 1277. <https://doi.org/10.3389/fimmu.2018.01277>.
- (153) Zhang, P.; Zhao, N.; Zeng, Z.; Feng, Y.; Tung, C.-H.; Chang, C.-C.; Zu, Y. Using an RNA Aptamer Probe for Flow Cytometry Detection of CD30-Expressing Lymphoma Cells. *Lab. Invest.* **2009**, *89* (12), 1423–1432. <https://doi.org/10.1038/labinvest.2009.113>.
- (154) Miotke, L.; Maity, A.; Ji, H.; Brewer, J.; Astakhova, K. Enzyme-Free Detection of Mutations in Cancer DNA Using Synthetic Oligonucleotide Probes and Fluorescence Microscopy. *PLoS One* **2015**, *10* (8), e0136720. <https://doi.org/10.1371/journal.pone.0136720>.
- (155) Jefferies, W. A.; Brandon, M. R.; Hunt, S. V.; Williams, A. F.; Gatter, K. C.; Mason, D. Y. Transferrin Receptor on Endothelium of Brain Capillaries. *Nature* **1984**, *312* (5990), 162–163. <https://doi.org/10.1038/312162a0>.
- (156) Sharma, G.; Lakkadwala, S.; Modgil, A.; Singh, J. The Role of Cell-Penetrating Peptide and Transferrin on Enhanced Delivery of Drug to Brain. *Int. J. Mol. Sci.* **2016**, *17* (6). <https://doi.org/10.3390/ijms17060806>.
- (157) Lee, J. H.; Engler, J. A.; Collawn, J. F.; Moore, B. A. Receptor Mediated Uptake of Peptides That Bind the Human Transferrin Receptor. *Eur. J. Biochem.* **2001**, *268* (7), 2004–2012. <https://doi.org/10.1046/j.1432-1327.2001.02073.x>.
- (158) Falanga, A.; Melone, P.; Cagliani, R.; Borbone, N.; D’Errico, S.; Piccialli, G.; Netti, P.; Guarnieri, D. Design, Synthesis and Characterization of Novel Co-Polymers Decorated with Peptides for the Selective Nanoparticle Transport across the Cerebral Endothelium. *Molecules* **2018**, *23* (7), 1655. <https://doi.org/10.3390/molecules23071655>.
- (159) Dai, X.; Xiong, Y.; Xu, D.; Li, L.; Su, Z.; Zhang, Q.; Zheng, Q. TFR Binding Peptide Screened by Phage Display Technology-Characterization to Target Cancer Cells. *Trop. J. Pharm. Res.* **2014**, *13* (3), 331–338. <https://doi.org/10.4314/tjpr.v13i3.3>.
- (160) Tan, Y.; Liu, W.; Zhu, Z.; Lang, L.; Wang, J.; Huang, M.; Zhang, M.; Yang, C. Selection and Identification of Transferrin Receptor-

- Specific Peptides as Recognition Probes for Cancer Cells. *Anal. Bioanal. Chem.* **2018**, *410* (3), 1071–1077. <https://doi.org/10.1007/s00216-017-0664-4>.
- (161) Qian, Z.; Rhodes, C. A.; McCroskey, L. C.; Wen, J.; Appiah-Kubi, G.; Wang, D. J.; Guttridge, D. C.; Pei, D. Enhancing the Cell Permeability and Metabolic Stability of Peptidyl Drugs by Reversible Bicyclization. *Angew. Chemie Int. Ed.* **2017**, *56* (6), 1525–1529. <https://doi.org/10.1002/anie.201610888>.
- (162) Lennard, K. R.; Tavassoli, A. Peptides Come Round: Using SICLOPPS Libraries for Early Stage Drug Discovery. *Chem. - A Eur. J.* **2014**, *20* (34), 10608–10614. <https://doi.org/10.1002/chem.201403117>.
- (163) NHS ester labeling of amino biomolecules <https://www.lumiprobe.com/protocols/nhs-ester-labeling> (accessed Jul 24, 2019).
- (164) Protocol: Maleimide labeling of proteins and other thiolated biomolecules <https://www.lumiprobe.com/protocols/protein-maleimide-labeling> (accessed Jul 29, 2019).
- (165) Li, Y.; He, Q.; Hu, X.; Liu, Y.; Cheng, X.; Li, X.; Deng, F. Improved Performance of Collagen Scaffolds Crosslinked by Traut's Reagent and Sulfo-SMCC. *J. Biomater. Sci. Polym. Ed.* **2017**, *28* (7), 629–647. <https://doi.org/10.1080/09205063.2017.1291296>.
- (166) Hermanson, G. T.; Preceded by: Hermanson, G. T. *Bioconjugate Techniques*.
- (167) *Sulfo-SMCC Protocol and Product Information Sheet Sulfo-SMCC Crosslinking Protocol*; 2015.
- (168) Aaberg-Jessen, C.; Sørensen, M. D.; Matos, A. L. S. A.; Moreira, J. M.; Brünner, N.; Knudsen, A.; Kristensen, B. W. Co-Expression of TIMP-1 and Its Cell Surface Binding Partner CD63 in Glioblastomas. <https://doi.org/10.1186/s12885-018-4179-y>.
- (169) Astakhova, I. K.; Hansen, L. H.; Vester, B.; Wengel, J. Peptide–LNA Oligonucleotide Conjugates. *Org. Biomol. Chem.* **2013**, *11* (25), 4240. <https://doi.org/10.1039/c3ob40786a>.
- (170) Wegner, A.; Aktories, K.; Ditsch, A.; Just, I.; Schoepper, B.; Selve, N.; Wille, M. Actin-Gelsolin Interaction; Springer, Boston, MA, 1994; pp 97–104. https://doi.org/10.1007/978-1-4615-2578-3_9.
- (171) Shi, J.; Gao, Y.; Yang, Z.; Xu, B. Exceptionally Small Supramolecular Hydrogelators Based on Aromatic–Aromatic Interactions. *Beilstein J. Org. Chem.* **2011**, *7* (1), 167–172. <https://doi.org/10.3762/bjoc.7.23>.
- (172) Ramachandran, S.; Tseng, Y.; Yu, Y. B. Repeated Rapid Shear-Responsiveness of Peptide Hydrogels with Tunable Shear Modulus. **2005**. <https://doi.org/10.1021/bm049284w>.
- (173) Taskova, M.; Madsen, C. S.; Jensen, K. J.; Hansen, L. H.; Vester, B.; Astakhova, K. Antisense Oligonucleotides Internally Labeled with Peptides Show Improved Target Recognition and Stability to Enzymatic Degradation. *Bioconjug. Chem.* **2017**, *28* (3), 768–774. <https://doi.org/10.1021/acs.bioconjchem.6b00567>.
- (174) Okholm, A.; Kjems, J.; Astakhova, K. Fluorescence Detection of Natural RNA Using Rationally Designed “Clickable” Oligonucleotide Probes. *RSC Adv.* **2014**, *4* (86), 45653–45656. <https://doi.org/10.1039/C4RA07165D>.
- (175) Oh, S.; Kim, B. J.; Singh, N. P.; Lai, H.; Sasaki, T. Synthesis and Anti-Cancer Activity of Covalent Conjugates of Artemisinin and a Transferrin-Receptor Targeting Peptide. *Cancer Lett.* **2009**, *274* (1), 33–39. <https://doi.org/10.1016/J.CANLET.2008.08.031>.
- (176) Tam, J. P.; Wu, C.-R.; Liu, W.; Zhang, J.-W. *Disulfide Bond Formation in Peptides by Dimethyl Sulfoxide. Scope and Applications*; 1991; Vol. 113.
- (177) Jandl, B.; Sedghiniya, S.; Carstens, A.; Astakhova, K. Peptide–Fluorophore Hydrogel as a Signal Boosting Approach in Rapid Detection of Cancer DNA. *ACS Omega* **2019**, *4* (9), 13889–13895. <https://doi.org/10.1021/acsomega.9b01586>.